

AD-A041 530

PURDUE UNIV LAFAYETTE IND THERMAL SCIENCES AND PROPULSION NOZZLE STUDIES. VOLUME II. DESIGN OF MAXIMUM THRUST --ETC(U)  
MAR 77 J G ALLMAN, J D HOFFMAN

F33615-73-C-2010

AFAPL-TR-77-1-VOL-2

NL

UNCLASSIFIED

1 OF 2  
AD  
A041 530



AFAPL-TR-77-1  
Volume II

*no hold*

*J*

*12*

AD A 041 530

## PROPULSION NOZZLE STUDIES

### Volume II DESIGN OF MAXIMUM THRUST NOZZLE-BASE-BOATTAIL CONTOURS

THERMAL SCIENCES AND PROPULSION CENTER  
PURDUE UNIVERSITY  
WEST LAFAYETTE, IND. 47907

MARCH 1977

TECHNICAL REPORT AFAPL-TR-77-1, Volume II  
FINAL REPORT FOR PERIOD SEPTEMBER 1972 - MAY 1976

Approved for public release; distribution unlimited

AD No. —  
DDC FILE COPY.

AIR FORCE AERO PROPULSION LABORATORY  
AIR FORCE WRIGHT AERONAUTICAL LABORATORIES  
AIR FORCE SYSTEMS COMMAND  
WRIGHT-PATTERSON AIR FORCE BASE, OHIO 45433

*DDC*  
*R* RECEIVED  
JUL 11 1977  
*D*

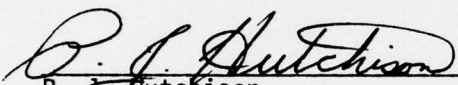


## NOTICE

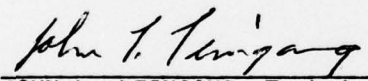
When Government drawings, specifications, or other data are used for any purpose other than in connection with a definitely related Government procurement operation, the United States Government thereby incurs no responsibility nor any obligation whatsoever; and the fact that the government may have formulated, furnished, or in any way supplied the said drawings, specifications, or other data, is not to be regarded by implication or otherwise as in any manner licensing the holder or any other person or corporation, or conveying any rights or permission to manufacture, use, or sell any patented invention that may in any way be related thereto.

This report has been reviewed by the Information Office (ASD/OIP) and is releasable to the National Technical Information Services (NTIS). At NTIS, it will be available to the general public, including foreign nations.

This technical report has been reviewed and is approved for publication.

  
P. J. Hutchison  
Project Engineer

FOR THE COMMANDER

  
JOHN L. LEINGANG, Technical Manager  
Advanced Component Technology  
Ramjet Technology Branch  
Ramjet Engine Division

Copies of this report should not be returned unless return is required by security considerations, contractual obligations, or notice on a specific document.

UNCLASSIFIED

SECURITY CLASSIFICATION OF THIS PAGE (When Data Entered)

REPORT DOCUMENTATION PAGE		READ INSTRUCTIONS BEFORE COMPLETING FORM
1. REPORT NUMBER AFAPL-TR-77-1, Volume II	2. GOVT ACCESSION NO.	3. RECIPIENT'S CATALOG NUMBER
4. TITLE (and Subtitle) PROPULSION NOZZLE STUDIES, VOLUME II. DESIGN OF MAXIMUM THRUST NOZZLE-BASE-BOATTAIL CONTOURS.	5. TYPE OF REPORT & PERIOD COVERED Final Sept 1972 - May 1976	
7. AUTHOR(s) Jeffrey G. Allman and Joe D. Hoffman	8. CONTRACT OR GRANT NUMBER(s) F33615-73-C-2010	
9. PERFORMING ORGANIZATION NAME AND ADDRESS Thermal Sciences and Propulsion Center Purdue University West Lafayette, Indiana 47907	10. PROGRAM ELEMENT, PROJECT, TASK AREA & WORK UNIT NUMBERS 3012/301213	
11. CONTROLLING OFFICE NAME AND ADDRESS Air Force Aero Propulsion Laboratory Air Force Wright Aeronautical Laboratories Air Force Systems Command	12. REPORT DATE March 1977	
14. Wright-Patterson AFB, Ohio 45433	13. NUMBER OF PAGES 122 p.	
15. SECURITY CLASS. (of this report) Unclassified		15a. DECLASSIFICATION/DOWNGRADING SCHEDULE
16. DISTRIBUTION STATEMENT (of this Report)  Approved for public release; distribution unlimited.		
17. DISTRIBUTION STATEMENT (of the abstract entered in Block 20, if different from Report)		
18. SUPPLEMENTARY NOTES		
19. KEY WORDS (Continue on reverse side if necessary and identify by block number)  Gas Dynamics      Nozzle Jet Propulsion      Boattail Optimization		
20. ABSTRACT (Continue on reverse side if necessary and identify by block number)  A production-type computer program has been developed for the design of maximum thrust axisymmetric nozzle-base-boattail contours. The flow field analysis is based on the governing equations for the rotational flow of a frozen or equilibrium gas mixture. The contour optimization is based on the direct optimization of a nonlinear function of several (three or less) geometric variables.  The nozzle and boattail contours are modeled as a second-order polynomial		

DD FORM 1 JAN 73 1473

EDITION OF 1 NOV 65 IS OBSOLETE  
S/N 0102-014-6601

UNCLASSIFIED

SECURITY CLASSIFICATION OF THIS PAGE (When Data Entered)

408142

Jmcc

next page

UNCLASSIFIED

cont. SECURITY CLASSIFICATION OF THIS PAGE (When Data Entered)

and a cone, respectively. For fixed initial expansion contours and nozzle and boattail lengths, the second-order polynomial nozzle contour is uniquely specified by the nozzle throat attachment angle and the nozzle exit lip radius, and the conical boattail is uniquely specified by the boattail exit lip radius. These three independent parameters are varied to determine the unique nozzle-base-boattail configuration that yields maximum thrust.

Three methods are included in the program to determine the maximum thrust contour. Each method requires an initial estimate of the geometry that produces maximum thrust. The methods are derivative methods that perturb the wall geometry parameters to determine approximate local derivatives. This information is used to calculate a search direction and a step length in the optimization variable space. Successive applications of the procedure modify the contour parameters until the maximum thrust configuration is obtained.

The first method is axial iteration. It treats the thrust as a function of up to three independent coordinates, and moves in the direction of each coordinate individually, using first and second partial derivative approximations to determine the step length. The second method is a gradient technique, the method of steepest descent. It computes an approximation to the gradient of the thrust function and steps an arbitrary step length in the direction of the gradient. The third technique is Newton's method, a second-derivative method. Newton's method computes first and second-derivatives of the thrust function, defining both the direction and the step length for the optimization step.

The three methods were first applied to the design of maximum thrust nozzle contours. Each of the methods converges efficiently to the maximum thrust nozzle contour. Newton's method and axial iteration converge very quickly, in approximately twenty nozzle flow field calculations or less. The method of steepest descent requires as much as twice as many flow field calculations as the other methods, but proceeds to the exact maximum by converging to a point whose gradient is zero. The nozzle contours from these methods are shown to yield nearly identical thrusts to those predicted by maximization using the calculus of variations, affirming the validity of the direct optimization approach.

The three methods were also applied to the design of nozzle-base-boattail configurations. The three-dimensional optimizations were found to be practical for finding the maximum thrust attainable for a nozzle-base-boattail assembly. Each of the three methods converged efficiently to the maximum thrust nozzle-base-boattail contour.

UNCLASSIFIED

SECURITY CLASSIFICATION OF THIS PAGE (When Data Entered)

# PREFACE

This final report was submitted by the Thermal Sciences and Propulsion Center of Purdue University, under Contract No. F33615-73-C-2010. The effort was sponsored by the Air Force Aero Propulsion Laboratory, Air Force Wright Aeronautical Laboratories, Air Force Systems Command, Wright-Patterson AFB, Ohio under Project No. 3012, Task 301213, and Work Unit 30121306 with P. J. Hutchison/AFAPL/RJT as Project Engineer. Jeffrey G. Allman and Joe D. Hoffman of Purdue University were technically responsible for the work.

ACCESSION for	
DTIC	White Section <input checked="" type="checkbox"/>
DDC	Diff Section <input type="checkbox"/>
UNANNOUNCED	<input type="checkbox"/>
JUSTIFICATION	
BY	
DISTRIBUTION/AVAILABILITY CODES	
Dist.	AVAIL. and/or SPECIAL
A	

DDC  
 RECEIVED  
 JUL 11 1977  
 REGISTERED  
 D



Preceding Page BLANK - <sup>NOT</sup> FILMED

TABLE OF CONTENTS

	<u>PAGE</u>
I. INTRODUCTION . . . . .	1
II. ANALYSIS . . . . .	4
1. Flow Field Analysis. . . . .	4
2. Optimization Procedures. . . . .	9
A. Axial Iteration. . . . .	12
B. Method of Steepest Descent . . . . .	13
C. Newton's Method. . . . .	13
III. RESULTS. . . . .	16
1. Nozzle Design. . . . .	17
2. Nozzle-Base-Boattail Design. . . . .	19
IV. CONCLUSIONS. . . . .	23
APPENDICES . . . . .	25
A. CHARACTERISTIC AND COMPATIBILITY EQUATIONS . . . . .	25
B. KLIEGEL'S TRANSONIC SOLUTION . . . . .	31
C. NOMINAL CASE AND CORRELATION FACTORS FOR BASE PRESSURE MODEL . . . . .	34
D. PROGRAM DESCRIPTION. . . . .	36
E. INPUT PARAMETERS . . . . .	59
F. SAMPLE CASES . . . . .	68
1. Sample Case 1. . . . .	68
2. Sample Case 2. . . . .	77
3. Sample Case 3. . . . .	82



	<u>PAGE</u>
4. Sample Case 4. . . . .	90
5. Sample Case 5. . . . .	98
REFERENCES . . . . .	111

# LIST OF ILLUSTRATIONS

<u>FIGURE</u>	<u>PAGE</u>
1. Combined Nozzle-Base-Boattail Optimization Model . . .	2
2. Combined Nozzle-Base-Boattail Flow Field Model . . . .	7
3. Nozzle Thrust as a Function of Wall Geometry . . . . .	11
4. Boattail Thrust as a Function of Wall Geometry . . . . .	11
5. Results of Nozzle Optimization Using Various Procedures	18
D-1. Characteristic Coordinate System for the Nozzle Flow Field. . . . .	44
D-2. Characteristic Coordinates for an Inverse Wall Point and an Interior Point . . . . .	46
D-3. Characteristic Coordinate System for the Boattail Flow Field. . . . .	48
D-4. Point Labeling Scheme for an Interior Point. . . . .	50
D-5. Point Labeling Scheme for an Inverse Wall Point. . . .	52
D-6. Point Labeling Scheme for a Direct Wall Point. . . . .	54
D-7. Point Labeling Scheme for an Axis Point. . . . .	56
E-1. Specification of the Nozzle Geometry . . . . .	66
E-2. Specification of the Boattail Geometry . . . . .	67
F-1. Output for Sample Case 1 . . . . .	72
F-2. Output for Sample Case 2 . . . . .	78
F-3. Output for Sample Case 3 . . . . .	83
F-4. Output for Sample Case 4 . . . . .	92
F-5. Output for Sample Case 5 . . . . .	101

# LIST OF TABLES

<u>TABLE</u>	<u>PAGE</u>
1. Comparison of the Performance of Maximum Thrust Nozzle Contours . . . . .	20
2. Results of a Nozzle-Base-Boattail Three-Dimensional Optimization. . . . .	22
D.1. List of Programs, Subroutines, and Function Subprograms	37
D.2. Logical Subroutine Calling Sequences. . . . .	38
E.1. Input Parameters for Nozzle . . . . .	60
E.2. Input Parameters for Boattail . . . . .	62
E.3. Input Parameters for Optimization . . . . .	64

## LIST OF SYMBOLS AND ABBREVIATIONS

a	Speed of sound.
I	Coordinate of right-running Mach line.
J	Coordinate of left-running Mach line.
M	Mach number.
n	Number of independent optimization variables.
p	Static pressure.
P	Stagnation pressure.
R	Gas constant.
t	Static temperature.
T	Stagnation temperature.
u	x-component of velocity.
v	y-component of velocity.
x	Axial coordinate.
y	Radial coordinate.
$\alpha$	Mach angle.
$\gamma$	Specific heat ratio.
$\delta$	Equals 0 for planar flow and 1 for axisymmetric flow.
$\eta$	Correlation factor for base pressure model.
$\theta$	Flow angle.
$\rho$	Density or radius of curvature.

### Subscripts

- ab Boattail attachment point.
- amb Ambient property.
- an Nozzle throat attachment point.
- b Base region property.
- eb Boattail exit lip point property.
- en Nozzle exit lip point property.
- t Throat property.
- td Downstream of the throat.
- tu Upstream of the throat.
- x Partial derivative with respect to x.
- y Partial derivative with respect to y.
- $\pm$  Left- or right-running Mach line, respectively.

### Superscripts

- \* Critical property, or stationary point.



## SECTION I

### INTRODUCTION

Current design techniques for propulsive nozzle contours assume that the nozzle exhausts into a static region having a specified ambient pressure. The design objective is to select that contour which yields maximum thrust for that ambient pressure. As illustrated in Fig. 1, the thrust producing region is much more complex. The nozzle is generally installed in an airframe with an annular base region between the nozzle lip and the airframe lip. Often the aft portion of the airframe, referred to as the boattail, is contoured to lessen the thrust loss associated with the low pressure base region. Consideration of boattail and base thrusts modifies the optimum nozzle contour from that for an isolated nozzle.

A technique for designing conical nozzles in a cylindrical boattail including the effects of the base region was developed by Byington and Hoffman (1), making possible performance increases of up to two percent. No analogous technique is available for designing contoured nozzles including the effects of the base region or for designing contoured nozzles and contoured boattails including the effects of the base region.

The objective of the present investigation is to develop an efficient method for the design of maximum thrust contours for nozzle-base-boattail assemblies, such as illustrated in Fig. 1.

The nozzle and boattail contours must satisfy certain geometric and physical constraints; for example, fixed overall length for both contours, specified throat radius and initial expansion contour for the nozzle, specified outer radius and initial expansion contour for the boattail, and specified initial conditions for the nozzle and boattail flow fields. Substantial effort has been directed to procedures for maximum thrust nozzle design, and several computer programs for nozzle design based on the calculus of variations have been developed. The difficulty with the calculus of variations approach is that if the gas dynamic model is modified or the general geometry of the thrust producing region is changed, the entire optimization analysis and computer program must be reworked, a task requiring several man years of effort.

---

(1) C.M. Byington, Jr. and J.D. Hoffman, "Effects of Base Pressure on Conical Thrust Nozzle Optimization," AIAA Journal, Vol. 7, No. 3, March 1970, pp. 380-382.

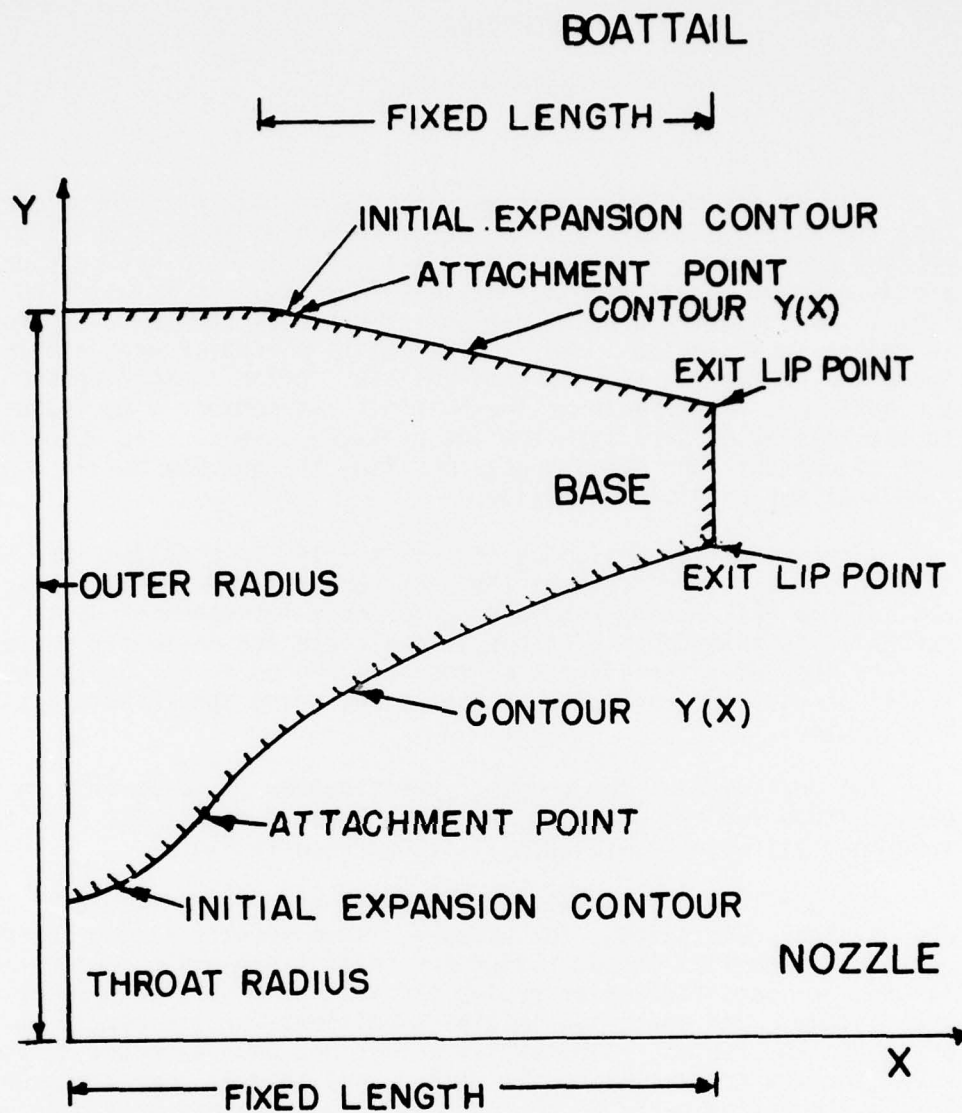


Figure 1. Combined Nozzle-Base-Boattail Optimization Model

The approach taken in this investigation is to develop an optimization procedure that is valid for any gas dynamic model and a variety of geometric configurations. To achieve that goal, the nozzle wall contour was assumed to be a second-order polynomial of the form  $y = a + bx + cx^2$ , and the boattail contour was assumed to be a first-order polynomial of the form  $y = a + bx$ . Nonlinear programming methods (2) are employed to vary the polynomial coefficients  $a$ ,  $b$ , and  $c$ , seeking the nozzle and boattail contours that yield maximum thrust.

Two questions must be answered. First, do wall contours specified by polynomials yield results comparable to those obtained by the calculus of variations? Second, which nonlinear programming methods most efficiently solve the nonlinear programming problem?

The present analysis is limited to applications where the external flow over the boattail is supersonic. Viscous effects are neglected in both the nozzle flow field and the boattail flow field. Consequently, transonic flow effects and flow separation effects on the boattail are both neglected. The resulting computer program is thus limited to supersonic flight speeds at design conditions where separation does not occur. The optimization procedure, however, does not depend on the flow field model, and it should be possible to apply the procedure to any flight speed, including viscous effects, when rapid and accurate numerical methods for determining the corresponding flow field become available.

---

(2) D.M. Himmelblau, Applied Nonlinear Programming, McGraw-Hill Book Co., New York, 1972.

## SECTION II

### ANALYSIS

The design of maximum thrust contours for any thrust producing element requires the ability to analyze the flow field in that particular element, and an optimization method for determining the maximum thrust contour. The flow field analysis procedure and the optimization methods employed in this investigation are discussed in this section.

#### 1. Flow Field Analysis

The nozzle-base-boattail assembly geometry is illustrated in Fig. 1. The initial expansion contours for both the nozzle and the boattail are assumed to be circular arcs. The nozzle contour is assumed to be a second-order polynomial of the form

$$y(x) = a + bx + cx^2 \quad (1)$$

and the boattail contour is assumed to be a first-order polynomial of the form

$$y(x) = a + bx \quad (2)$$

The above choices for the nozzle and boattail contours require the determination of the coefficients  $a$ ,  $b$ , and  $c$  for the nozzle contour and the coefficients  $a$  and  $b$  for the boattail contour. These coefficients are uniquely determined by specifying the nozzle throat attachment angle  $\theta_{an}$ , the nozzle exit radius  $y_{en}$ , the boattail exit radius  $y_{eb}$ , and by requiring that the polynomial contours attach smoothly to the circular arc initial-expansion contours (see Fig. 1). These three parameters uniquely specify a nozzle-base-boattail configuration. The optimization procedure searches through the allowable ranges of these three parameters to determine the particular set of values that yields the maximum total thrust on the nozzle-base-boattail assembly.

The gas dynamic model is that for the steady axisymmetric flow of an inviscid fluid in the absence of work, heat transfer, and body forces. Such a flow is isentropic. The governing partial differential equations are the following (3).

$$\rho u_x + \rho v_y + u \rho_x + v \rho_y + \delta \rho v / y = 0 \quad (3)$$

$$\rho u u_x + \rho v u_y + p_x = 0 \quad (4)$$



$$\rho uv_x + \rho vv_y + p_y = 0 \quad (5)$$

$$u p_x + v p_y - a^2 u \rho_x - a^2 v \rho_y = 0 \quad (6)$$

Equation (3) is the continuity equation, equations (4) and (5) are the x and y Euler momentum equations, and equation (6) is a form of the speed of sound equation for an isentropic flow.

This system of four partial differential equations may be replaced by a system of characteristic and compatibility equations, which are ordinary differential equations (see Appendix A). For isentropic flow, the acoustic speed is a function of the local static pressure and density. The composition is assumed to be a general mixture, either fixed (frozen) in composition, or in chemical equilibrium. The gas dynamic model requires that the entropy, the stagnation pressure, and the stagnation enthalpy remain constant along streamlines, although these properties may vary between streamlines. A conventional predictor-corrector second-order numerical integration procedure (4) is employed to integrate the characteristic and compatibility equations, starting from a supersonic initial-value line.

Several procedures have been developed for analyzing the transonic flow in the throat region of convergent-divergent nozzles. Kliegel's method (5) is employed in the present study because it is accurate and easy to use. Kliegel's method stems from a study by Hall (6). Both solutions involve expansions for the velocity components u and v in inverse powers of R, the ratio of the upstream throat wall radius of curvature  $\rho t_u$  to the throat radius  $y_t$  ( $R = \rho t_u / y_t$ ). Hall used a straight expansion in inverse powers of R. However, the resulting series is divergent for  $R < 1$ . Kliegel modified Hall's approach, developing an expansion in inverse powers of  $(R + 1)$ , which is convergent for  $R < 1$ . The complete third-order axisymmetric solution for the velocity components derived by Hall and Kliegel is presented in Appendix B. Thus, the velocity components along an initial-value line

(3) M.J. Zucrow and J.D. Hoffman, Gas Dynamics, Vol. I, John Wiley and Sons, New York, 1976, pp. 549.

(4) M.J. Zucrow and J.D. Hoffman, Gas Dynamics, Vol. I, John Wiley and Sons, New York, 1976, Chapter 12.

(5) J.R. Kliegel and J.N. Levine, "Transonic Flow in Small Radius of Curvature Nozzles," AIAA Journal, Vol. 7, No. 7, July 1969, pp. 1375-1378.

(6) I.M. Hall, "Transonic Flow in Two-Dimensional and Axially-Symmetric Nozzles," Quarterly Journal of Mechanics and Applied Mathematics, Vol. XV, Pt. 4, 1962, pp. 487-508.



may be calculated, defining a starting line for the numerical solution of the supersonic portion of the nozzle flow field by the method of characteristics.

The nozzle flow field is illustrated in Fig. 2. Contour AA' is the circular arc initial expansion contour. Point D is the nozzle throat attachment point where the maximum thrust contour DF attaches smoothly to the initial expansion contour. The maximum thrust nozzle contour is obtained by varying both the location of point D along the initial expansion contour and the contour between points D and F. The initial-value line AB is obtained by applying Kliegel's method, or by defining the line point by point from any transonic flow analysis. Starting from the initial-value line, the method of characteristics is applied to calculate the flow field in region ABCFA. Region ABCEDA is termed the kernel, and is affected solely by the initial-value line properties and the nozzle initial-expansion contour. Region DEFD, which is influenced by the nozzle wall contour, is the flow field region bounded by the right-running Mach line DE originating on the wall contour at the attachment point D and the left-running Mach line EF passing through the nozzle exit lip point F.

The analysis program employed in the study is a modification of the program developed by Pasley and Hoffman (7). That program was modified to minimize the computational effort during optimization, where many similar flow fields are computed. This is particularly pertinent in the nozzle, where much computational effort is spent calculating the flow field in the kernel. In general, the nozzle throat attachment angle  $\theta_{an}$  corresponding to point D has some minimum value below which the optimization search will never proceed. The portion of the kernel upstream of that point is fixed and need not be recalculated as point D and the contour DF are varied during the optimization search. That minimum nozzle throat attachment point is indicated as point G on Fig. 2. Consequently, right-running Mach line GH may be stored and employed as the initial-value line for subsequent nozzle flow field calculations. The secondary-start line, as this new initial-value line is called, may save as much as 50 percent of the computational effort required for a nozzle flow field analysis. Care must be exercised, however, not to compute the secondary start line at too large an angle, since subsequent nozzle flow field calculations must have throat attachment angles greater than that of the secondary-start line. The program is not capable of restarting at any nozzle throat attachment angle less than or equal to that of the secondary-start line.

The left-running Mach line IJ is the initial-value line for the boattail flow field analysis. All of the flow properties along the initial-value line must be known from a prior analysis of the flow

---

(7) S.A. Pasley and J.D. Hoffman, "Flow Field Analysis of a Nozzle-Boattail System," Air Force Aero Propulsion Laboratory, AFAPL-TR-74-38, 1974.

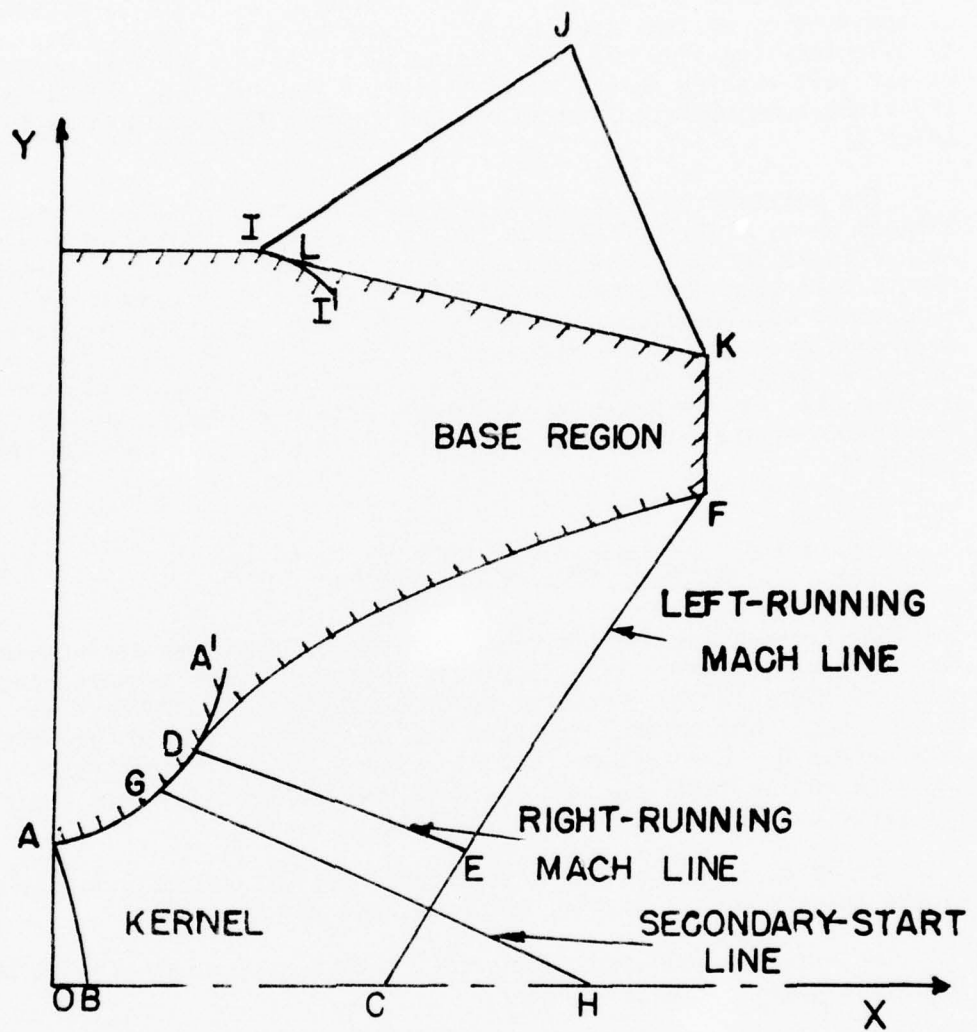


Figure 2. Combined Nozzle-Base-Boattail Flow Field Model

around the forward section of the vehicle. If such information is unavailable, a uniform flow initial-value line may be employed. Contour II' is the circular arc initial expansion contour, and point L is the point where the conical boattail contour KL attaches to the initial expansion contour II'. The external flow field is assumed to be supersonic, so that the method of characteristics may be employed to calculate the flow field in region IJKI. That region is bounded by the left-running Mach line IJ, which is the initial-value line, and the right-running Mach line JK passing through the boattail exit lip point K.

The boattail contour and nozzle contour may have a base region between them, as illustrated in Fig. 2. The total thrust on the vehicle must account for the base pressure in this annular region. Several models have been developed for predicting the base pressure aft of a supersonic nozzle-boattail assembly. The empirical base pressure model developed by Addy (8) was employed in the present investigation. A curve fit of Addy's data, similar to that employed by Byington and Hoffman (1), was employed to relate the base pressure  $p_b$  to the exit conditions of the nozzle and boattail. This curve fit has the following form.

$$\frac{p_b}{p_{eb}} = f(p_{en}/p_{eb})\eta(M_{eb})\eta(M_{en})\eta(T_{eb}/T_{en})\eta(\theta_{en}) \quad (7)$$

The four  $\eta$  functions are correlation factors, which are applied to the nominal case for which  $f(p_{en}/p_{eb})$  was obtained. Each factor accounts for variations in the parameter denoted within the corresponding parentheses. The nominal case and the correlation factors are discussed in Appendix C. Correlation factors based on specific heat ratio  $\gamma$  and the base region radii  $y_{en}$  and  $y_{eb}$  have been neglected, since their influence on the base pressure is slight.

The total thrust of the nozzle-base-boattail assembly is the sum of the thrusts of the nozzle, the base, and the boattail.

The program developed during this investigation can perform the following types of calculations.

1. Analysis of a specified nozzle-base-boattail assembly.
2. Design of a maximum thrust nozzle contour.
3. Design of a maximum thrust boattail contour.
4. Design of a maximum thrust nozzle-base-boattail contour.

(8) A.L. Addy, "Analysis of the Axisymmetric Base-Pressure and Base-Temperature Problem with Supersonic Interacting Freestream-Nozzle Flows Based on the Flow Model of Korst, et al., Part I: A Computer Program and Representative Results for Cylindrical Afterbodies," Advanced Systems Laboratory, Redstone Arsenal, Alabama, Report No. RD-TR-69-12, July 1969.

## 2. Optimization Procedures

The nozzle and boattail flow fields are entirely independent, and are calculated separately. Thus, the nozzle and boattail contour parameters are related only when considering a nozzle-base-boattail assembly, because they influence base pressure and hence total thrust on the assembly.

The nozzle typically provides the greatest thrust contribution to the vehicle. The boattail and base regions are normally contoured in such a way as to minimize the low pressure base region and boattail divergence loss effects.

The approach taken in this investigation is to model the wall contour geometry as a second-order polynomial for the nozzle contour and a first-order polynomial for the boattail contour (three independent parameters). These parameters are systematically varied to find the maximum thrust nozzle-base-boattail contour.

The nozzle-base-boattail assembly is first modeled as a two independent variable problem by fixing the width of the base region to be the minimum allowed width acceptable in the final design (which may be zero if a sharp trailing edge is permissible). Consequently, specification of the nozzle exit lip radius  $y_{en}$  fixes the value of the boattail exit radius  $y_{eb}$ , so that the boattail contour is completely specified. The nozzle throat attachment angle  $\theta_{an}$  and exit lip radius  $y_{en}$  remain free to vary. This constitutes an optimization in two independent parameters, which is carried out until convergence is attained. This two-dimensional optimization yields a good initial estimate for the final nozzle-base-boattail maximum thrust contour.

The problem is then redefined to be an optimization in three independent variables, with the nozzle and boattail exit radii no longer related. The three-dimensional optimization is then carried out until the maximum thrust producing contour is obtained.

Two special cases may arise that reduce the optimization problem from a three-dimensional problem to either a two-dimensional problem or a one-dimensional problem. The first case arises when an optimization step requires the boattail exit radius  $y_{eb}$  to become less than the nozzle exit radius  $y_{en}$  (or less than  $y_{en} + \Delta y_b$ , where  $\Delta y_b$  is the minimum allowable base width). In that case, the boattail exit radius  $y_{eb}$  is specified as  $y_{eb} = y_{en} + \Delta y_b$ , and the solution continues as a two-dimensional optimization problem with  $\theta_{an}$  and  $y_{en}$  as the independent variables. The second case arises when an optimization step requires a nozzle exit radius  $y_{en}$  greater than the maximum radius of the boattail. In that case,  $y_{en}$  (or  $y_{en} + \Delta y_b$ ) and  $y_{eb}$  are set equal to the maximum boattail radius, and the solution continues as a one-dimensional optimization problem with  $\theta_{an}$  as the single independent variable. The program can efficiently perform an axial iteration optimization in one-dimension, as encountered in a nozzle optimization with fixed exit radius, boattail



optimization with fixed exit radius, or nozzle-base-boattail assembly optimization with fixed boattail contour and nozzle exit radius.

The analysis program is capable of calculating the thrust for nozzle-base-boattail assemblies that have crossing exit radii. That situation can not occur physically, but may occur during the calculation of the function derivatives required to compute an optimization step.

A parametric study of the thrust as a function of the wall geometry for a nozzle-base-boattail assembly was conducted to gain insight into the design of maximum thrust nozzle-base-boattail contours.

The study was conducted for a nozzle having an upstream radius of curvature  $\rho_{tu} = 3.0$  in., a downstream radius of curvature  $\rho_{td} = 0.5$  in., a throat radius  $y_{tn} = 1.0$  in., and a length  $x_{en} = 10.0$  in. The properties of the gas flowing in the nozzle were specific heat ratio  $\gamma = 1.2$ , gas constant  $R = 60.0$  (ft-lbf)/(lbm-R), stagnation temperature  $T = 6000$  R, stagnation pressure  $P = 1000$  psia, and ambient pressure  $p_{amb} = 0.0$ . The boattail had a length  $x_{eb} = 10.0$  in., an initial radius  $y_{tb} = 9.0$  in., and an initial expansion contour radius  $\rho_{td} = 5.0$  in. The properties of the air flowing around the boattail were specific heat ratio  $\gamma = 1.4$ , gas constant  $R = 53.3$  (ft-lbf)/(lbm-R), stagnation temperature  $T = 600$  R, and stagnation pressure  $P = 12.0$  psia. Lines of constant thrust were determined for the nozzles and the boattails (see Figs. 3 and 4). It is seen that the thrust varies smoothly, and that there is one clearly defined global maximum thrust for the nozzle. A difference table reduction of the data showed that locally both the nozzle thrust and the boattail thrust varied approximately quadratically.

Nonlinear programming optimization techniques may be divided into two broad categories; derivative-free methods and derivative methods. Derivative-free methods employ systematic searches through the domain of the objective function, in this case the total thrust of the nozzle-base-boattail assembly. These methods seek the extremum by comparing several function values (i.e., the thrust) for various combinations of the independent variables ( $\theta_{an}$ ,  $y_{en}$ ,  $y_{eb}$ ), moving to the point having the greater thrust. The idea is to step to the absolute extremum in an organized fashion, without recalculating the objective function at the same point more than once, and without sampling the objective function prohibitively often. This class of methods is most useful when the objective function is a function of many variables.

Derivative methods employ more information about the function than a simple comparison of the function value at two points. They use derivative information about the objective function, and are most effectively employed where the objective function is smooth and depends on a few variables. This class of methods was the more successful in the present investigation.

The general procedure of any optimization method is to begin with a starting point (base point). The algorithm then selects a direction



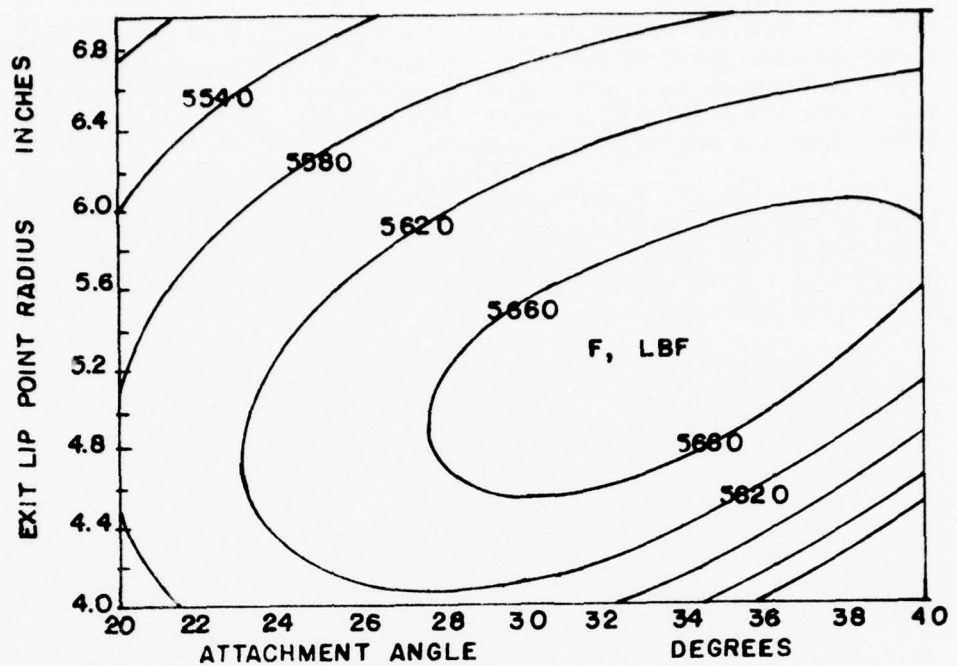


Figure 3. Nozzle Thrust as a Function of Wall Geometry

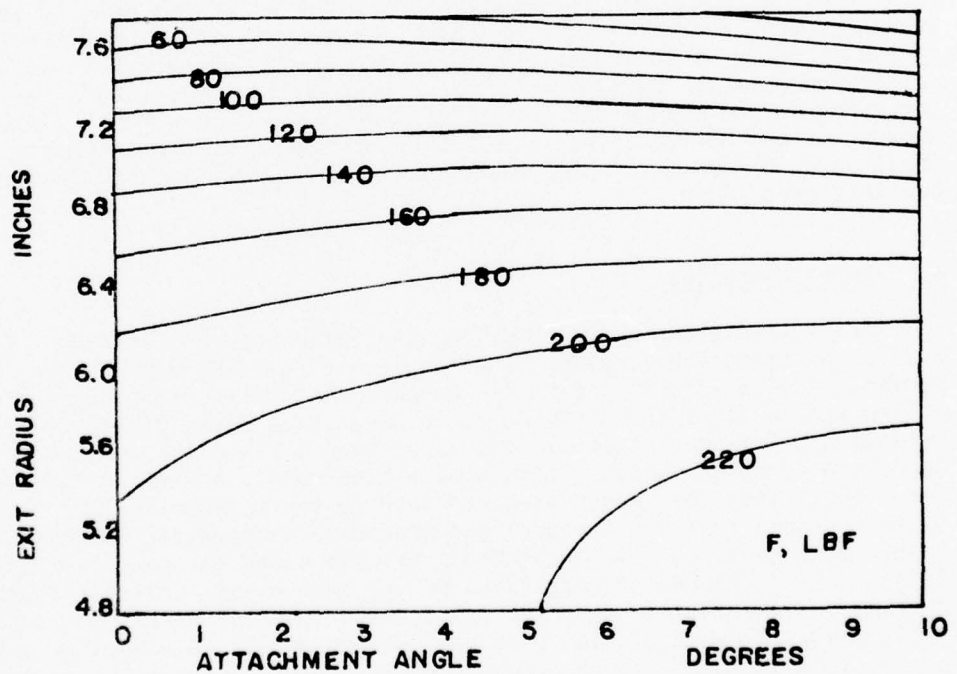


Figure 4. Boattail Thrust as a Function of Wall Geometry

and a distance for moving the base point toward the extremum. The number of base point moves and the number of function evaluations required for each base point move determines the efficiency of the algorithm, since a function evaluation requires much more computational effort than the optimization logic.

Inherent in all optimization procedures is a weakness at abrupt folds of the objective function surface and along ridges and plateaus. Fortunately, the objective function considered in the present investigation (i.e., the thrust) does not have any of these features, thus simplifying the algorithms.

Each optimization method requires an initial estimate of the maximum thrust contour. The method then systematically revises the estimate, moving to the extremum of the objective function. This initial estimate should be reasonably close to the final solution, so that the optimization does not require a prohibitive number of steps, or the analysis does not encounter flow separation or strong internal oblique shock waves. One-dimensional gas dynamic relations for the area ratio required to expand the nozzle flow to the freestream pressure are sufficient to estimate the nozzle exit radius. Some suitably small annular base width specifies the initial boattail exit radius.

Finite perturbations for each of the independent parameters are used in forming the finite-difference derivative approximations used in each of the optimization methods. These perturbations must be large enough so that the corresponding thrust increments are not influenced by the accuracy of the numerical algorithm, yet small enough to accurately approximate local derivatives of the thrust. Also, each perturbation should change the thrust by roughly the same amount. Typical values for the perturbations are 2.0 deg for the nozzle attachment angle, and 20 percent of the nozzle throat radius for the nozzle and boattail exit radii.

#### A. Axial Iteration

Axial iteration is a multidimensional line search algorithm. It treats the objective function as a function of several coordinates, then performs a line search in each of the coordinate directions successively. A line search finds the distance for a base point move, given a search direction. This may be envisioned as passing a plane through the objective function surface, through the base point, and along the search direction. The line search seeks to move to the maximum on this slice. Given a priori that the surface is approximately quadratic locally, the line search perturbs the independent variable along the search direction by an equal increment on both sides of the base point. First and second-derivative information is formed using these function values for base point moves in one-dimension (see Newton's method), the dimension successively being each of the independent parameters. The new base point estimate is then found, and the objective function is evaluated at that

point. The base point moves to the maximum of the points thus far evaluated, and proceeds to the next independent variable. Convergence is attained when a base point move changes the objective function less than a specified relative tolerance.

Axial iteration requires  $3n$  (where  $n$  is the number of independent parameters) function evaluations per pass through the algorithm, and does not have difficulty with poor initial estimates for the maximum thrust contour. Further, this method has one of the good features of the nonderivative methods, in that it steps to the maximum of the points evaluated, not necessarily the predicted point. It is a very simple method, and converges very rapidly.

#### B. Method of Steepest Descent

Method of steepest descent, or hill climbing, is a first derivative method. By perturbing the objective function  $n$  times (where  $n$  is the number of independent variables) about the base point ( $n + 1$  function evaluations), a finite difference approximation to the gradient may be calculated. The search direction is then specified along the gradient direction. The algorithm marches stepwise in that direction, seeking the extremum, and moves the base point to that extremum.

If the first step after computing an approximation to the gradient does not increase the objective function, which normally occurs near the maximum, the perturbation sizes and the step size are halved. A new approximation to the gradient is then computed. The procedure is repeated from successive base points until convergence is achieved. This method is relatively simple, and convergence is monotonic.

The principal drawback to the method of steepest descent is that the search can sometimes zig-zag back and forth in a so-called "hem-stitching pattern" (9). This is especially true along ridges in the objective function surface. Consequently, the method may be very inefficient and require a large number of steps. However, the algorithm will eventually converge to the extremum.

This method is recommended primarily in cases where a good initial estimate of the wall geometry is not available or to check the result obtained by any other method to ensure that the absolute maximum is attained. After several base point moves, one of the other, faster converging, methods may be employed to complete the solution.

#### C. Newton's Method

Newton's method is a second-derivative method. The objective function is approximated by a Taylor series expansion about the base

---

(9) Y. Bard, Nonlinear Parameter Estimation, Academic Press, New York, 1974.

point which is truncated after the second-derivative terms. In one-dimension, the following equation is obtained.

$$f(x) = f(a) + f_x(a)(x-a) + \frac{1}{2!} f_{xx}(a)(x-a)^2 \quad (8)$$

where  $f$  is the objective function,  $a$  is the base point, and the derivatives are evaluated at the base point,  $a$ . Taking the derivative of equation (8) with respect to  $x$  and noting that  $f(a)$ ,  $f_x(a)$ , and  $f_{xx}(a)$  are constant yields

$$f_x(x) = f_x(a) + f_{xx}(a)(x-a) \quad (9)$$

At a stationary point  $x = x^*$  (maximum, minimum, or saddle point),  $f_x(x^*)$  is identically zero. Consequently, at a stationary point, equation (9) becomes

$$0 = f_x(a) + f_{xx}(a)(x^*-a) \quad (10)$$

Solving equation (10) for  $x^*$  yields

$$x^* = a - f_x(a)/f_{xx}(a) \quad (11)$$

If  $f(x)$  is not quadratic,  $x^*$  is not exactly the extremum. Usually, however, it is an improvement, and convergence is approached iteratively.

In the case of more than one dimension,  $x^*$ ,  $a$ , and  $f_x(a)$  are replaced by column vectors, and  $f_{xx}(a)$  is an  $n \times n$  matrix of second derivatives, termed the Hessian. Thus, equation (11) becomes

$$\vec{x}^* = \vec{a} - \vec{f}_{xx}(\vec{a})^{-1} \vec{f}_x(\vec{a}) \quad (12)$$

Solving for  $\vec{x}^*$  in equation (12) requires inversion of the Hessian, which, in general, may present a numerical accuracy problem. In the present problem, where  $n \leq 3$ , the Hessian has proven to be nonsingular and well conditioned, and no problem arises.

Newton's method converges very rapidly. In fact, it converges in exactly one pass for a quadratic function. However, it does require a relatively large number of function evaluations for each base point move  $[(n^2 + 3n + 2)/2 \text{ evaluations/move}]$ .

When applying Newton's method, it may be possible to employ the Hessian computed for a given base point for several base point moves before recomputing second derivatives. In the case of a nearly quadratic function, the second derivatives are approximately constant, and the procedure may be useful. The thrust function considered in the present study was not close enough to a quadratic function globally, and the method did not converge unless second derivatives were computed at each step.



Further, when the objective function is not globally quadratic, Newton's method may predict bad base point moves, particularly if the initial estimate is far from the extremum. Hence, there is special incentive for a good first guess.

Newton's method performs quite well in the present problem. Bard (9) states that it is relatively common to find cases where Newton's method may be 25,000 times more efficient than the method of steepest descent! Though not outperforming the other methods nearly so dramatically in the present study, it is clearly an efficient method.

## SECTION III

### RESULTS

The optimization methods presented in Section II have been applied to the design of maximum thrust nozzle contours, boattail contours, and nozzle-base-boattail contours. These contours are modeled as first- and second-order polynomials. The nozzle thrust predicted by the maximum thrust-producing second-order polynomial is comparable to that predicted by the calculus of variations, which places no restrictions on the functional form of the wall contour. A study comparing the results of the two approaches was conducted for different length nozzles operating at two ambient pressures.

A method of nozzle optimization employing the calculus of variations is based on forming a functional consisting of the following terms:

- (1) the term to be maximized (the axial pressure forces along the contour  $y = y_w(x)$ ),
- (2) the design constraint along the nozzle wall  $y = y_w(x)$  (such as constant nozzle length or surface area),
- (3) the constraint that the contour  $y = y_w(x)$  is a streamline, and
- (4) the constraint that the governing partial differential equations must be satisfied in the region of the flow field influenced by the nozzle contour.

Each of the constraints is multiplied by a Lagrange multiplier, and a sum of terms (1) through (4) is formed. No constraint is placed on the form of  $y = y_w(x)$ .

Following the formalism of the calculus of variations, the first variation of the functional is determined and set equal to zero. A set of conditions, known as Euler equations, transversality equations, and corner conditions, results from setting the first variation equal to zero. These design equations guarantee a maximum thrust contour for the assumed constraints. Because the design equations are nonlinear, an iterative solution is performed. A trial contour,  $y = y_w(x)$ , is assumed, the flow field is determined by the method of characteristics, and the design equations are solved for the Lagrange multipliers. During the above procedure, one transversality equation along the nozzle wall is not employed. That design equation, expressed in terms of the flow field properties, the nozzle contour  $y = y_w(x)$ , and the Lagrange multi-

pliers, is then checked to see if it is satisfied. If it is satisfied, the assumed contour is the maximum thrust nozzle contour. If it is not satisfied, the contour is modified and the entire procedure is repeated for the modified contour. This relaxation of the nozzle contour is repeated until the design condition is satisfied within a specified tolerance. Typically five to ten modifications of the nozzle contour are required. For each modification, the nozzle flow field and Lagrange multiplier field must be calculated; the Lagrange multiplier field calculation requiring approximately 60 percent as much computation time as that required for the nozzle flow field calculation. Thus, the indirect approach requires from eight to sixteen times the computation time required for one nozzle flow field calculation.

The calculus of variations is an indirect approach to finding maximum thrust nozzle, boattail, and nozzle-base-boattail contours. The advantage of the indirect approach is that no restrictions are placed on the general forms of the contours  $y = y_w(x)$ . The contours are free to assume any shape required to yield maximum thrust. The disadvantages are that a tremendous amount of time is required to formulate and solve the variational problem to obtain the design equations, and to develop a computer program to solve for the Lagrange multiplier field for a maximum thrust nozzle. This problem is further complicated by consideration of base and boattail effects. Even if these could be accounted for, a subject of some speculation, the entire problem would need to be entirely reworked if changes were made to the gas dynamic model, such as the inclusion of boundary layer drag or nonequilibrium chemistry effects. In spite of these disadvantages, the indirect method is of great value in that it yields absolutely the best solution to the specified problem.

The concept of modeling the contours of a complete nozzle-base-boattail assembly as polynomials, and performing a direct optimization to find maximum thrust has proven to be practical, and an example is presented to demonstrate the application of the optimization techniques.

## 1. Nozzle Design

Sample nozzle optimizations were carried out using the three methods outlined in Section II for the nozzle illustrated in Fig. 3. Their paths to the extremum is shown in Fig. 5, which illustrates that each of the techniques has the following properties.

- a. Each converges.
- b. Each converges to the same stationary point.
- c. The stationary point converged upon is the global maximum.
- d. Each method converges to the global maximum efficiently, without an excessive number of base point moves.

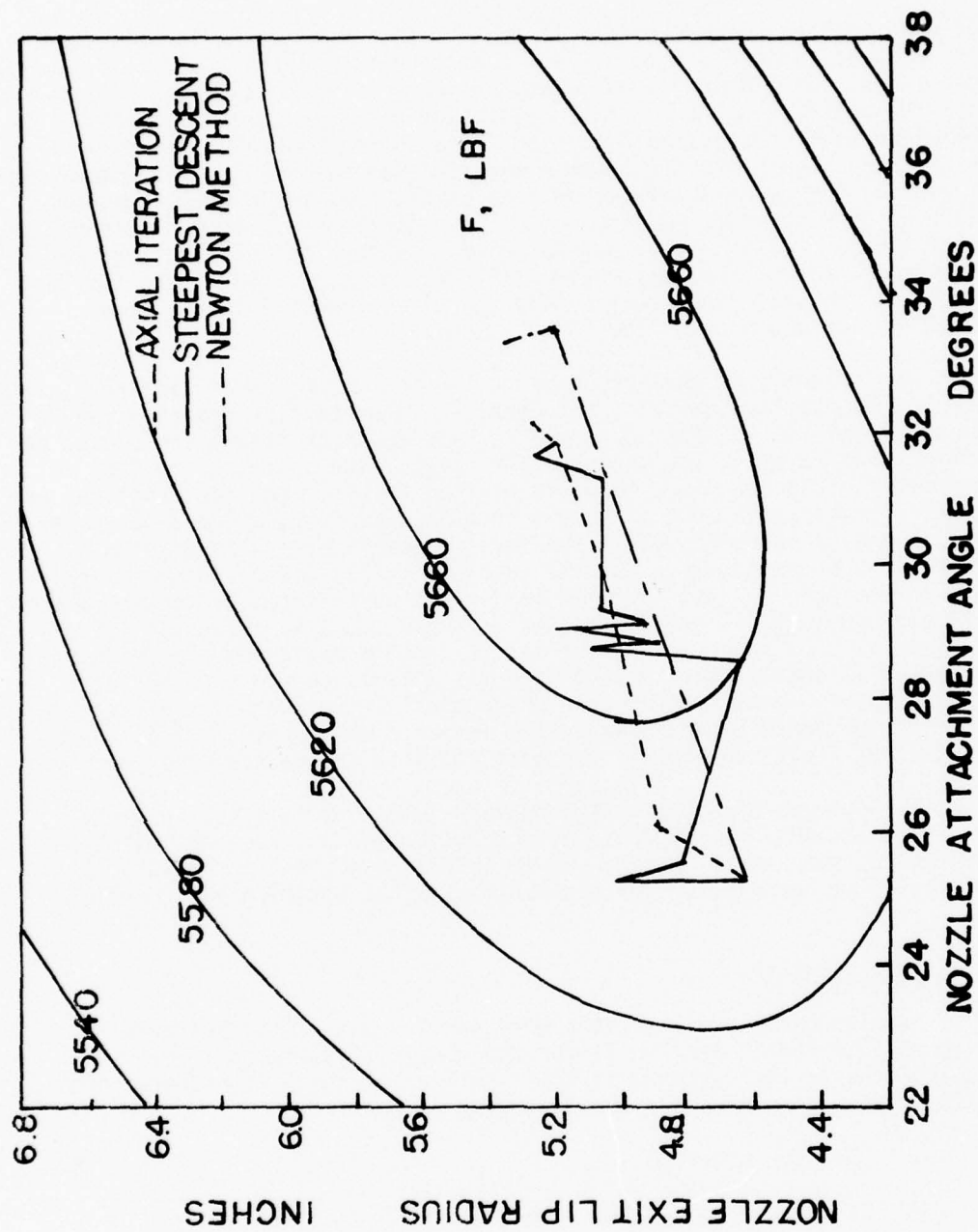


Figure 5. Results of Nozzle Optimization Using Various Procedures



Thus, several practical optimization techniques are available to find the nozzle wall geometry that yields maximum thrust.

To demonstrate that the quadratic wall contours develop thrust comparable to that developed by the calculus of variations contours, a parametric study was performed for a variety of nozzle lengths and two ambient pressures. The results of this study are presented in Table 1. The calculus of variations procedure employed in the comparison is that developed by Rao (10).

The nozzle parameters for the study are upstream radius of curvature  $r_{tu} = 3.0$  in., downstream radius of curvature  $r_{td} = 0.5$  in., throat radius  $r_t = 1.0$  in., specific heat ratio  $\gamma = 1.2$ , gas constant  $R = 60$  (ft-lbf)/(lbm-R), stagnation temperature  $T = 6000$  R, and stagnation pressure  $P = 1000$  psia.

The thrusts delivered by the contours designed by the calculus of variations are compared with the thrusts delivered by the contours designed by the direct optimization of the second-order polynomial nozzle wall. Both methods predicted essentially the same maximum obtainable thrust, with the direct optimization method not having the analytical difficulties of the calculus of variations approach. Slight variations of the maximum thrust predicted by the two approaches are acceptable because they use different, although similar, flow field analysis programs, and the direct optimizations were terminated by nonzero relative tolerances.

Overall agreement between the two approaches, that is, the calculus of variations and the direct optimization of a second-order polynomial wall nozzle, is very good. For the case of zero ambient pressure, agreement for all cases is within 0.2 percent, which is the approximate numerical resolution of the method of characteristic flow field calculation algorithm. The results for an ambient pressure of 5.0 psia are less compatible, in most part due to the second-order polynomial nozzle wall approximation becoming less good. Thus second-order polynomials effectively approximate maximum thrust nozzle contours, justifying this approach.

## 2. Nozzle-Base-Boattail Design

The program is capable of computing the design of a nozzle-base-boattail assembly which yields maximum thrust. This is of great practical value in that it dictates the geometry which can produce maximum performance, without necessitating excessive experience or experimental testing. The optimization models the assembly as having a second-order polynomial nozzle contour, a first-order polynomial (conical) boattail contour, and an annular base. This geometry is uniquely specified

(10) G.V.R. Rao, "Exhaust Nozzle Contour For Optimum Thrust," Jet Propulsion, Vol. 28, 1958, pp. 377-382.

TABLE 1. COMPARISON OF THE PERFORMANCE OF MAXIMUM THRUST  
NOZZLE CONTOURS

Nozzle Length (in.)	Ambient Pressure (psia)	Thrust, lbf		$\Delta F$ , percent
		Calculus of Variations Prediction	Second-Order Polynomial Wall	
1.5475	0.0	4556.0	4555.7	0.01
2.3215	0.0	4802.7	4798.1	0.10
3.0706	0.0	4981.4	4979.0	0.05
3.8205	0.0	5124.5	5120.9	0.07
4.5731	0.0	5241.7	5234.9	0.13
6.2965	0.0	5433.1	5428.7	0.08
7.9759	0.0	5569.6	5561.2	0.15
9.6527	0.0	5669.4	5662.5	0.12
12.746	0.0	5806.7	5801.2	0.09
16.9164	0.0	5935.7	5926.6	0.15
20.5326	0.0	6014.4	6003.2	0.19
24.4965	0.0	6081.4	6068.2	0.21
1.4139	5.0	4468.4	4453.1	0.34
2.8861	5.0	4880.4	4848.3	0.66
7.9850	5.0	5311.8	5300.1	0.22
11.836	5.0	5379.0	5367.4	0.22
16.060	5.0	5394.9	5377.6	0.32

knowing nozzle and boattail lengths, initial expansion contours, nozzle attachment angle  $\theta_{an}$ , nozzle exit radius  $y_{en}$ , and boattail exit radius  $y_{eb}$ . The last three parameters are varied in such a way as to find that unique combination ( $\theta_{an}$ ,  $y_{en}$ ,  $y_{eb}$ ) which yields maximum thrust.

There are several constraints on these variables, besides the minimum and maximum values for each necessary to bracket the extremum. The nozzle and boattail exits must not cross, a physical impossibility. This has been taken one step further in that they can be specified to be at least some specified minimum base width ( $\Delta y_b$ ) away from each other. If the optimization violates this, the two exit radii become a fixed distance apart, and the optimization proceeds with one less independent variable ( $n = 2$ ). The nozzle exit radius may also be constrained to be less than some maximum value. This could be encountered if the nozzle exit radius became larger than that of the airframe. This causes the nozzle exit radius to become fixed and the optimization proceeds with one less independent variable ( $n = 1$ ).

A nozzle-base-boattail optimization is presented in Table 2 to illustrate the application of the program. Each of the three methods in Section II is applied to the same case. The nozzle is the same as illustrated in Fig. 3. The boattail is the same as illustrated in Fig. 4 except that it has an outer radius  $y_{tb} = 5.3$  in. Note that axial iteration and Newton's method converge comparably, while the method of steepest descent converges to a larger tolerance much more slowly. Newton's method is more prone to failure than axial iteration, because it requires a better estimate of the partial derivatives to take a successful step.

Thus, maximum thrust nozzle-base-boattail contours may be approximated as polynomials and may be directly optimized efficiently using several techniques. The order of the approximating polynomials seems to be effective. The nozzle contour has been shown conclusively to be well approximated by a second-order polynomial. Since the boattail typically contributes an order of magnitude less thrust than does the nozzle, it was modeled as conical. Thus, there are as many as three independent parameters, since the attachment angle may be inferred from the exit lip point for a conical boattail.

TABLE 2. RESULTS OF A NOZZLE-BASE-BOATTAIL THREE-DIMENSIONAL OPTIMIZATION

Method	Step	n	Function Evaluations	$\theta_{an}$ , deg	$y_{en}$ , in.	$\theta_{ab}$ , deg	$y_{eb}$ , in.	F, lbf
Axial iteration	0	2	1	30.000	4.00	7.059	4.100	5710.71
	1	2	7	27.223	4.296	5.344	4.396	5734.72
	2	2	13	29.365	4.377	4.906	4.477	5737.39
	3	2	19	29.579	4.391	4.722	4.491	5737.46
	0	3	20	29.578	4.391	4.130	4.591	5737.65
	1	3	29	28.700	4.369	3.780	4.650	5737.74
Steepest descent	0	2	1	30.000	4.000	7.059	4.100	5710.71
	1	2	9	29.947	4.497	4.094	4.597	5735.93
	2	2	12	29.947	4.497	4.094	4.597	5735.93
	3	2	16	29.938	4.448	4.385	4.548	5736.09
	4	2	19	29.932	4.448	4.395	4.548	5736.09
	5	2	24	29.888	4.443	4.413	4.543	5736.70
	0	3	25	29.888	4.443	3.923	4.643	5736.27
	1	3	30	29.888	4.443	3.823	4.643	5736.27
	2	3	34	29.888	4.443	3.823	4.643	5736.27
	3	3	39	29.973	4.427	3.889	4.632	5736.29
Newton's method	0	2	1	30.000	4.0	7.059	4.100	5710.71
	1	2	7	29.597	4.235	5.653	4.335	5734.89
	2	2	13	29.552	4.349	4.974	4.449	5737.30
	3	2	19	28.710	4.399	4.674	4.499	5737.47
	0	3	20	28.710	4.399	4.082	4.599	5737.64
	1	3	30	28.551	4.347	3.661	4.670	5737.76



## SECTION IV

### CONCLUSIONS

A method has been developed for the design of maximum thrust nozzles, boattails, and nozzle-base-boattail contours. These contours may be quickly and efficiently found using any of several direct optimization techniques, providing a practical and dependable basis for design.

Nozzle and boattail optimizations select second-order polynomial wall contours. Nozzle-base-boattail optimizations assume a first-order polynomial (conical) boattail contour and a second-order polynomial nozzle contour. Better approximations for both nozzle and boattail maximum thrust contours may be obtained using higher-order polynomial walls, and hence degrees of freedom. Each additional degree of freedom allows a better fit of the general surface which yields maximum thrust. However, each additional degree of freedom also increases the number of independent contour parameters required to uniquely specify the contour geometry, geometrically increasing the number of function evaluations necessary to perform an optimization. The second-order polynomial wall nozzle and conical wall boattail were selected as an effective compromise. The polynomials are shown to yield substantially identical thrust to that produced by maximum thrust contours designed by the calculus of variations for unconstrained wall geometry.

Three techniques were developed for determining the wall polynomial coefficients. The first method is an axial iteration. It is a fast converging method, and has the least difficulty with a poor initial estimate for the solutions of the methods studied. This method also can take steps from simple sampling, if terms of higher than second order dominate the objective function and second and first derivative information yields a poor step.

The second technique is the method of steepest descent. This method converges monotonically to the extremum and cannot overstep it. It may, however, require an exorbitant number of steps to attain the maximum. It can step directly away from a poor initial estimate of the maximum, or converge to the extremum from an approximate solution obtained from one of the other methods. This algorithm is primarily intended as a classical reference.

The third method is Newton's method. This, too, is one of the classical optimization methods, and worked very well in the present study. Newton's method does require accurate derivative approximations, and care must be taken to be sure finite-difference increments are large enough to be beyond the numerical resolution of the analysis, yet small enough to detect local functional trends.

All three optimization techniques efficiently select the wall geometry that produces maximum thrust in a nozzle-base-boattail assembly. This makes for a simple and practical approach to the design of maximum thrust nozzle-base-boattail contours.

## APPENDICES

### APPENDIX A. CHARACTERISTIC AND COMPATIBILITY EQUATIONS

The following equations govern steady two-dimensional isentropic (i.e., rotational) flow,

$$\rho u_x + \rho v_y + \rho u_x + \rho v_y + \delta \rho v/y = 0 \quad (\text{A-1})$$

$$\rho u u_x + \rho v u_y + p_x = 0 \quad (\text{A-2})$$

$$\rho u v_x + \rho v v_y + p_y = 0 \quad (\text{A-3})$$

$$\rho u_x + \rho v_y - a^2 \rho u_x - a^2 \rho v_y = 0 \quad (\text{A-4})$$

where  $\delta = 0$  for planar flows and  $\delta = 1$  for axisymmetric flows. For isentropic flow, the speed of sound,  $a$ , is a known function of the static pressure  $p$  and the density  $\rho$ . Thus,

$$a = a(p, \rho) \quad (\text{A-5})$$

Equations A-1 through A-4 comprise a system of four quasi-linear nonhomogeneous first-order partial differential equations for the four variables  $u$ ,  $v$ ,  $p$ , and  $\rho$ .

This system of partial differential equations may be replaced by an equivalent system of four compatibility equations which are valid along three distinct characteristic curves: the streamline and the two Mach lines. The compatibility equations are total differential equations, as are the equations defining the characteristic curves. Thus, a much simpler numerical method can be employed to solve the system of total differential equations.

The characteristic and compatibility equations for the above system of equations are found by multiplying equations A-1 through A-4 by the unknown parameters  $\sigma_1$  through  $\sigma_4$ , respectively, and summing. Thus,

$$\sigma_1(\text{A-1}) + \sigma_2(\text{A-2}) + \sigma_3(\text{A-3}) + \sigma_4(\text{A-4}) = 0 \quad (\text{A-6})$$

After this sum is formed, the coefficients of the x derivatives of u, v, p, and  $\rho$  are factored out to yield

$$\begin{aligned}
 & (\rho\sigma_1 + \rho u\sigma_2) \left[ u_x + \frac{\rho v\sigma_2}{\rho\sigma_1 + \rho u\sigma_2} u_y \right] + (\rho u\sigma_3) \left[ v_x + \frac{\rho\sigma_1 + \rho v\sigma_3}{\rho u\sigma_3} v_y \right] + \\
 & (\sigma_2 + u\sigma_4) \left[ p_x + \frac{\sigma_3 + v\sigma_4}{\sigma_2 + u\sigma_4} p_y \right] + \\
 & (u\sigma_1 - a^2 u\sigma_4) \left[ \rho_x + \frac{v\sigma_1 - a^2 v\sigma_4}{u\sigma_1 - a^2 u\sigma_4} \rho_y \right] + \sigma_1 \delta\sigma v/y = 0 \quad (A-7)
 \end{aligned}$$

The slopes of the characteristic curves,  $dy/dx = \lambda$ , are then the coefficients of the y derivatives of u, v, p, and  $\rho$  in equation A-7. Thus,

$$\lambda = \frac{v\sigma_2}{\sigma_1 + u\sigma_2} = \frac{\sigma_1 + v\sigma_3}{u\sigma_3} = \frac{\sigma_3 + v\sigma_4}{\sigma_2 + u\sigma_4} = \frac{v\sigma_1 - a^2 v\sigma_4}{u\sigma_1 - a^2 u\sigma_4} \quad (A-8)$$

If u, v, p, and  $\rho$  are assumed to be continuous functions, then  $du/dx = u_x + \lambda u_y$ , etc., and the terms in brackets in equation A-7 may be replaced by their equivalent values,  $du/dx$ , etc. Thus, equation A-7 becomes

$$\begin{aligned}
 & \rho(\sigma_1 + u\sigma_2)du + \rho u\sigma_3 dv + (\sigma_2 + u\sigma_4)dp + \\
 & u(\sigma_1 - a^2 \sigma_4)d\rho + \sigma_1(\delta\rho v/y)dx = 0 \quad (A-9)
 \end{aligned}$$

Equation A-9 is the compatibility equation, which is valid along the characteristics defined by Equation A-8. It remains to eliminate  $\sigma_1$  to  $\sigma_4$  from equation A-8 and A-9.

Equation A-8, when written as a system of equations considering  $\sigma_1$  through  $\sigma_4$  as the unknowns, becomes

$$\sigma_1(\lambda) + \sigma_2(u\lambda - v) + \sigma_3(0) + \sigma_4(0) = 0 \quad (A-10)$$

$$\sigma_1(-1) + \sigma_2(0) + \sigma_3(u\lambda - v) + \sigma_4(0) = 0 \quad (A-11)$$

$$\sigma_1(0) + \sigma_2(\lambda) + \sigma_3(-1) + \sigma_4(u\lambda - v) = 0 \quad (A-12)$$



$$\sigma_1(u\lambda - v) + \sigma_2(0) + \sigma_3(0) + \sigma_4[-a^2(u\lambda - v)] = 0 \quad (\text{A-13})$$

For equations A-10 through A-13 to have any solution for the  $\sigma$ 's other than the trivial solution of zero, the determinant of the coefficient matrix of equations A-10 to A-13 must be zero. Defining  $S = (u\lambda - v)$ , that condition yields

$$\begin{vmatrix} \lambda & S & 0 & 0 \\ -1 & 0 & S & 0 \\ 0 & \lambda & -1 & S \\ S & 0 & 0 & -a^2 S \end{vmatrix} = 0 \quad (\text{A-14})$$

Expanding the determinant gives

$$S^2[S^2 - a^2(1 + \lambda^2)] = 0 \quad (\text{A-15})$$

Equation A-15 is a fourth-order polynomial equation in terms of  $\lambda$ ; hence four roots, and thus four characteristic directions, should be found. Two roots are obtained by setting the leading term,  $S^2$ , equal to zero. Thus,

$$\lambda_0 = \left(\frac{dy}{dx}\right)_0 = \frac{v}{u} \text{ (repeated twice)} \quad (\text{A-16})$$

which is a repeated root, and is the differential equation for the streamline. The subscript 0 is used to denote the streamline. Hence, the streamline is a dual characteristic in rotational flow. The remaining two roots are obtained from the quadratic term in equation A-15, which, when substituting  $S = (u\lambda - v)$ , becomes

$$(u^2 - a^2)\lambda^2 - 2uv\lambda + (v^2 - a^2) = 0 \quad (\text{A-17})$$

Solving equation A-17 for  $\lambda$  gives

$$\lambda_{\pm} = \left(\frac{dy}{dx}\right)_{\pm} = \frac{uv \pm a^2 \sqrt{M^2 - 1}}{u^2 - a^2} \quad (\text{A-18})$$

where the subscripts  $\pm$  correspond to the  $\pm$  root of the quadratic equation. Equation A-18 can be simplified by making the substitution  $u = V \cos \theta$ ,  $v = V \sin \theta$ ,  $\theta = \tan^{-1}(v/u)$  and  $\alpha = \sin^{-1}(1/M)$ . The result is

$$\lambda_{\pm} = \left(\frac{dy}{dx}\right)_{\pm} = \tan(\theta \pm \alpha) \quad (\text{A-19})$$

Equation A-19 is the differential equation of the Mach lines for supersonic flow; hence, the remaining two characteristics for rotational flow are the Mach lines. The + denotes the left-running Mach line and the - denotes the right-running Mach line.

Thus, three distinct characteristics exist through each point in a rotational flow: the streamline and the two Mach lines.

The compatibility equation valid on each characteristic is obtained from Equation A-9 by solving equations A-10 through A-13 for  $\sigma_1$  through  $\sigma_4$ . Equations A-10 through A-13 may be rewritten as follows.

$$\sigma_2 = -(\lambda/S)\sigma_1 \quad (A-20)$$

$$\sigma_1 = S\sigma_3 \quad (A-21)$$

$$S\sigma_4 = \sigma_3 - \lambda\sigma_2 \quad (A-22)$$

$$a^2 S\sigma_4 = S\sigma_1 \quad (A-23)$$

Along streamlines,  $S = (u\lambda - v) = 0$ , and equations A-20 through A-23 become

$$\sigma_1 \lambda = 0 \quad (A-24)$$

$$\sigma_1 = 0 \quad (A-25)$$

$$\sigma_2 \lambda - \sigma_3 = 0 \quad (A-26)$$

$$0 = 0 \quad (A-27)$$

Thus, along streamlines,

$$\sigma_1 = 0 \quad \text{and} \quad \sigma_3 = \lambda\sigma_2 \quad (A-28)$$

and  $\sigma_2$  and  $\sigma_4$  are unspecified, and hence arbitrary. Substituting equation A-28 into equation A-9 yields

$$\sigma_2[\rho u du + \rho v dv + dp] + \sigma_4[u dp - a^2 u d\rho] = 0 \quad (A-29)$$

Since  $\sigma_2$  and  $\sigma_4$  are both arbitrary, their coefficients must be identically zero. Thus, along streamlines

$$\rho u du + \rho v dv + dp = 0 \quad (A-30)$$

$$dp - a^2 d\rho = 0 \quad (A-31)$$

On the Mach lines, the quadratic factor in equation A-15 is zero, which gives

$$S^2 - a^2(1 + \lambda^2) = 0 \quad (A-32)$$

Solving for  $(S/a^2)$  from equation A-32 and substituting the result into equation A-23 yields equation A-22, which shows that only one of these equations is independent on Mach lines. Thus, along Mach lines,

$$\sigma_1 = S\sigma_3, \quad \sigma_2 = -\lambda\sigma_3, \quad \text{and} \quad \sigma_4 = (S/a^2)\sigma_3 \quad (A-33)$$

and  $\sigma_3$  remains arbitrary. Substituting equation A-33 into equation A-9 and dividing by  $\sigma_3$ , which is nonzero and arbitrary, yields the compatibility equation valid on Mach lines. Thus,

$$\begin{aligned} (\rho v) du_{\pm} - (\rho u) dv_{\pm} + [\lambda_{\pm} - u(u\lambda_{\pm} - v)/a^2] dp_{\pm} - \\ [v(u\lambda_{\pm} - v)/y] dx_{\pm} = 0 \end{aligned} \quad (A-34)$$

The subscript + indicates that equation A-34 is valid on left-running Mach lines, and the subscript - denotes that equation A-34 is valid on right-running Mach lines.

An alternate and more useful form of equation A-34 is obtained by making the substitutions  $u = V\cos\theta$ ,  $v = V\sin\theta$ ,  $\theta = \tan^{-1}(v/u)$ , and  $\alpha = \sin^{-1}(1/M)$ . Thus,

$$\frac{\sqrt{M^2-1}}{\rho V^2} dp_{\pm} \mp d\theta_{\pm} + \frac{v}{yVM\cos(\theta \pm \alpha)} dx_{\pm} = 0 \quad (A-35)$$

where the upper subscripts on  $dp$ ,  $d\theta$ , and  $dx$  correspond to the upper signs in the terms  $\mp d\theta$  and  $\cos(\theta \pm \alpha)$ , and vice versa. Equation A-30 along a streamline becomes

$$\rho V dV + dp = 0 \quad (A-36)$$

which is Bernoulli's equation.

Thus, three distinct characteristics are obtained, the streamline and the two Mach lines, with two compatibility equations valid on the streamline and one compatibility equation valid on each Mach line, a total of four compatibility equations. This system of characteristic and compatibility equations is sufficient to replace the original system of four partial differential equations.

In the numerical implementation of equation A-35 along the Mach lines, left-running Mach lines can become essentially vertical. In that

case, the term  $dx_{\pm}/\cos(\theta \pm \alpha)$  becomes indeterminate. However, from equation A-19,

$$\frac{dx_{\pm}}{\cos(\theta \pm \alpha)} = \frac{dy_{\pm}}{\sin(\theta \pm \alpha)} \quad (\text{A-37})$$

Substituting equation A-37 into equation A-35 yields

$$\frac{\sqrt{M^2-1}}{\rho V^2} dp_{\pm} \mp d\theta_{\pm} + \delta \frac{v}{yVM\sin(\theta \pm \alpha)} dy_{\pm} = 0 \quad (\text{A-38})$$

In the numerical algorithms developed during this investigation, equation A-35 is employed along right-running Mach lines [that is,  $dy/dx = \tan(\theta - \alpha)$ ], and equation A-37 is employed along left-running Mach lines [that is,  $dy/dx = \tan(\theta + \alpha)$ ].



## APPENDIX B. KLIEGEL'S TRANSONIC SOLUTION

Various techniques have been developed to handle the transonic flow region in convergent-divergent nozzles, from which the method developed by Kliegel (8) was selected. Kliegel employs an expansion in inverse powers of the normalized throat wall radius of curvature  $R(R = \rho_u/y_t)$ . His method differs from that developed by Hall (9) by the use of a toroidal coordinate system instead of a cylindrical coordinate system. A toroidal coordinate system results in an expansion in  $1/(R + 1)$  instead of  $1/R$  for the axial and radial velocity components. This expansion allows for the analysis of nozzles having small normalized throat wall radii of curvature,  $R < 1$ . The solution derived by Kliegel is expressed in the following form.

$$u = 1 + \frac{u_1(r, z)}{(R + 1)} + \frac{1}{(R + 1)^2} [u_1(r, z) + u_2(r, z)] + \frac{1}{(R + 1)^3} [u_1(r, z) + u_2(r, z) + u_3(r, z)] + \dots \quad (B-1)$$

$$v = \left[ \frac{\gamma + 1}{2(R + 1)} \right]^{1/2} \left\{ \frac{v_1(r, z)}{R + 1} + \frac{1}{(R + 1)^2} \times \left[ \frac{3}{2} v_1(r, z) + v_2(r, z) \right] + \frac{1}{(R + 1)^3} \times \left[ \frac{15}{8} v_1(r, z) + \frac{5}{2} v_2(r, z) + v_3(r, z) \right] + \dots \right\} \quad (B-2)$$

where

$$z = \left[ \frac{2(R + 1)}{\gamma + 1} \right]^{1/2} x/y_t \quad (B-3)$$

$$r = y/y_t \quad (B-4)$$

In Eq. B-3  $z$  is the transformed normalized axial coordinate. In Eq. B-4  $r$  is the normalized radial coordinate. The complete third-order axisymmetric solution derived by Hall and modified by Kliegel is as follows.

$$u_1 = \frac{1}{2} r^2 - \frac{1}{4} + z \quad (B-5)$$

$$v_1 = \frac{1}{4} r^3 - \frac{1}{4} r + rz \quad (B-6)$$

$$u_2 = \frac{2\gamma + 9}{24} r^4 - \frac{4\gamma + 15}{24} r^2 + \frac{10\gamma + 57}{288} + z\left(r^2 - \frac{5}{8}\right) - \frac{2\gamma - 3}{6} z^2 \quad (B-7)$$

$$v_2 = \frac{\gamma + 3}{9} r^5 - \frac{20\gamma + 63}{96} r^3 + \frac{28\gamma + 93}{288} r + z\left[\frac{2\gamma + 9}{6} r^3 - \frac{4\gamma + 15}{12} r\right] + rz^2 \quad (B-8)$$

$$u_3 = \frac{556}{10368} r^6 - \frac{388\gamma^2 + 1161\gamma + 1881}{2304} r^4 + \frac{304\gamma^2 + 831\gamma + 1242}{1728} r^2 - \frac{2708\gamma^2 + 7839\gamma + 14211}{82944} + z\left[\frac{52\gamma^2 + 518\gamma + 327}{384} r^4 - \frac{52\gamma^2 + 75\gamma + 279}{192} r^2 + \frac{92\gamma^2 + 1808\gamma + 639}{1152}\right] + z^2\left[-\frac{7\gamma - 3}{8} r^2 + \frac{13\gamma - 27}{48}\right] + \frac{4\gamma^2 - 57\gamma + 27}{144} z^3 \quad (B-9)$$

$$v_3 = \frac{6836\gamma^2 + 23031\gamma + 3027}{82944} r^7 - \frac{3380\gamma^2 + 11391\gamma + 15291}{13824} r^5 + \frac{3424\gamma^2 + 11271\gamma + 15228}{13824} r^3 - \frac{7100\gamma^2 + 22311\gamma + 30249}{82944} r + z\left[\frac{556\gamma^2 + 1737\gamma + 3069}{1728} r^5 - \frac{388\gamma^2 + 1161\gamma + 1181}{576} r^3 + \right.$$

$$\frac{304\gamma^2 + 831\gamma + 1242}{864} r \Big] + z^2 \left[ \frac{52\gamma^2 + 51\gamma + 327}{192} r^3 - \right. \\ \left. \frac{52\gamma^2 + 75\gamma + 279}{192} r \right] - z^3 \left[ \frac{7\gamma - 3}{12} r \right] \quad (B-10)$$

Kliegel's analysis is valid for irrotational flow of a perfect gas in an axisymmetric circular arc throat.

## APPENDIX C. NOMINAL CASE AND CORRELATION

### FACTORS FOR BASE PRESSURE MODEL

The pressure,  $p_b$ , acting on an annular base area depends on the boattail Mach number and static pressure, the nozzle exit Mach number, exit angle and static pressure, the specific heat ratios of the gases, the stagnation temperatures of the two streams, and the ratio of nozzle exit radius to boattail exit radius. A model which accurately predicts the base pressure as a function of all these parameters has not been developed yet, but the model by Addy (12) does include the effects of each of these parameters and gives a reasonable approximation to the base pressure. Byington and Hoffman (1) correlated his data by a curve fit of the form

$$\frac{p_b}{p_{eb}} = f(p_{en}/p_{eb})\eta(M_{eb})\eta(M_{en})\eta(T_{eb}/T_{en})\eta(\theta_{en}) \quad (C-1)$$

The nominal case used for  $f(p_{en}/p_{eb})$  was:  $M_{eb} = 2.0$ ,  $\gamma = 1.2$ ,  $M_{en} = 2.0$ ,  $\theta_{en} = 0$  deg,  $(T_{eb}/T_{en}) = 1.0$ , and  $(y_{eb}/y_{en}) = 0.6$ . This resulted in the following third-order polynomial curve fit.

$$f(p_{en}/p_{eb}) = 0.27435080 + 0.13825822 \times (p_{en}/p_{eb}) - 0.01754651 \times (p_{en}/p_{eb})^2 + 0.00097156 \times (p_{en}/p_{eb})^3 \quad (C-2)$$

The four  $\eta$  functions are correlation factors which are applied to the nominal case. Each factor accounts for variations in the parameter denoted by its argument and was obtained by a curve fit of the data presented by Addy (12). Correlation factors based on the specific heat ratios and exit lip point coordinates have been neglected since their influence on the base pressure is slight. The four  $\eta$  correlation factors are

$$\eta(M_{eb}) = \frac{2.0}{M_{eb}} \quad (C-3)$$

$$\eta(M_{en}) = \frac{3.5 - 2.5/M_{en}}{M_{en}} \quad (C-4)$$



$$\eta(T_{eb}/T_{en}) = 0.978 + 0.022(T_{en}/T_{eb}) \quad (C-5)$$

$$\eta(\theta_{en}) = 1.0 + \theta_{en}/45.0 \quad (C-6)$$

The correlation factors  $\eta(M_{en})$  and  $\eta(\theta_{en})$  are not accurate near  $\rho_{en}/\rho_{eb} = 1.0$ .

#### APPENDIX D. PROGRAM DESCRIPTION

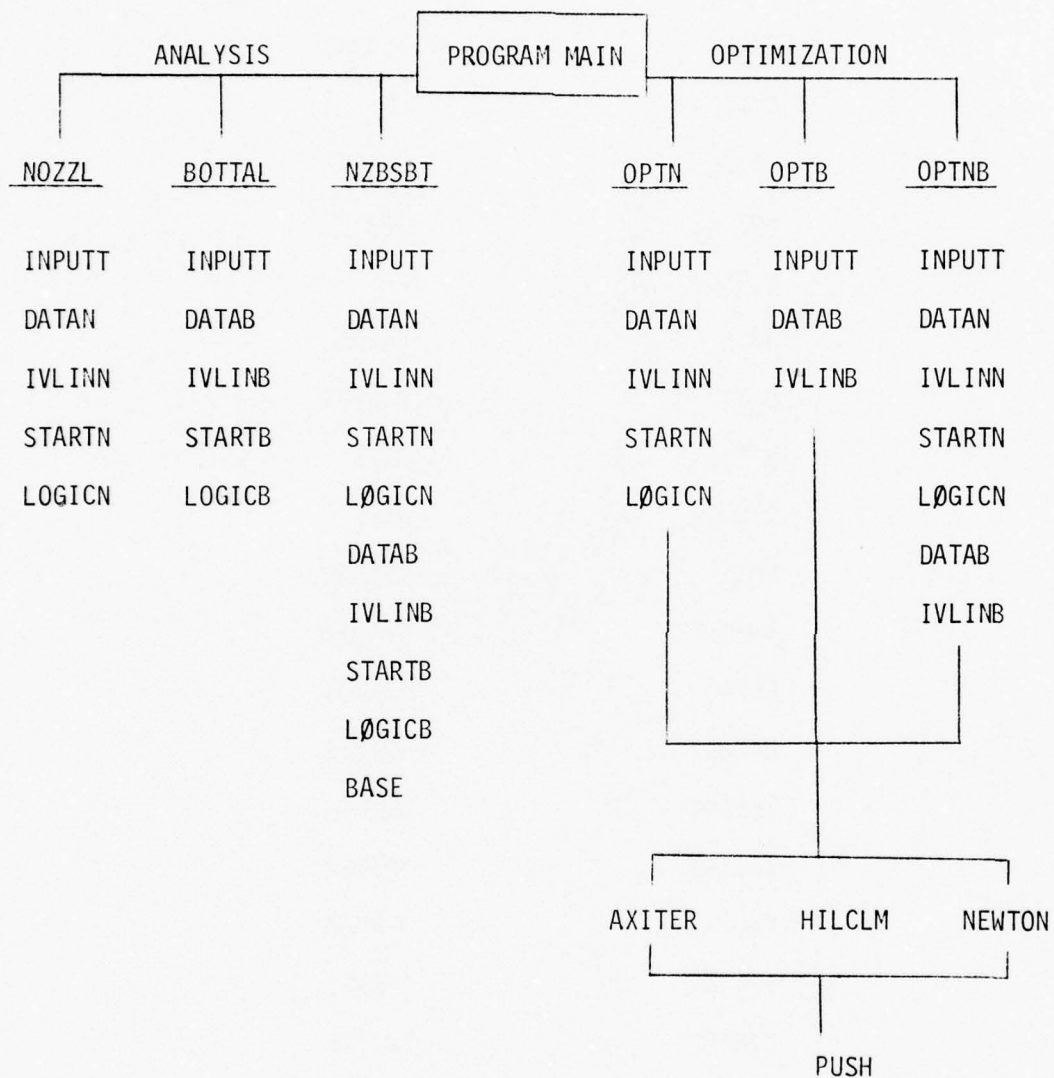
A brief description of the computer program is presented here to supplement the comments in the code. Where appropriate, the logic of each subroutine is discussed. A list of the programs, subroutines, and functions subprograms is presented in Table D-1. A diagram of the control logic followed by the program is shown in Table D-2.

The computer program consists of approximately 4000 cards. It requires 30 second of central processor time for compilation on the CDC 6500 computer. Nozzle flow field analyses typically require 8 to 10 seconds of computation time, although that time is reduced to 4 to 6 seconds when the secondary-start line option is utilized effectively. Boattail flow field analyses are substantially faster than nozzle flow field analyses, requiring only 4 to 6 seconds of computation time.

TABLE D.1. LIST OF PROGRAMS, SUBROUTINES, AND FUNCTION SUBPROGRAMS

MAIN	THERMO
TITLE	EM
NOZZL	PPOINT
BOTTAL	INWALL
NZBSBT	F
OPTN	DRWALL
OPTB	WALLPT
OPTNB	AXIS
CONBOT	BASE
PUSH	TRAN2D
INPUTT	TRAN1D
DATAN	TRAN4
DATAB	TRAN12
IVLINN	TRAN14
IVLINB	TRAN24
XYLINE	TRAN3D
STARTN	TRANSL
STARTB	AXITER
LOGICN	HILCLM
LOGICB	NEWTON
WRITE	GAUSS
THRST	

TABLE D.2. LOGICAL SUBROUTINE CALLING SEQUENCES





MAIN. Program MAIN reads the first data card, which specifies whether an analysis or an optimization is to be performed, and the type of geometry. The parameter IOPT specifies either an analysis (IOPT = 1) or an optimization (IOPT = 2). ITYPE specifies the type of geometry: a complete nozzle-base-boattail system (ITYPE = 1), a nozzle only (ITYPE = 2), or a boattail only (ITYPE = 3). The first card also contains an alphanumeric job title for the run. When successive runs are being made, this data card must be specified for each run. Program MAIN then calls the appropriate analysis or optimization master control subroutine.

TITLE. Subroutine TITLE writes out the standard comments and job title on the first page of the output.

NØZZL. Subroutine NØZZL contains the overall logic for the nozzle flow field analysis. All of the input data for the nozzle are read in by calling subroutine INPUTT. Then subroutine IVLINN is called to generate the initial-value line, and subroutine STARTN is called to determine the wall contour parameters. Subroutine LØGICN, which contains the logic for determining the nozzle flow field by the method of characteristics, is then called.

BØTTAL. Subroutine BØTTAL contains the overall logic for the boattail flow field analysis. All of the input data for the boattail are read in by calling subroutine INPUTT. The subroutine IVLINB is called to generate the initial-value line, and subroutine STARTB is called to determine the wall contour parameters. Subroutine LØGICB, which contains the logic for determining the boattail flow field by the method of characteristics, is then called.

NZBSBT. Subroutine NZBSBT contains the overall logic for the analysis of the nozzle-base-boattail combination. There is a section for the nozzle flow field analysis, a section for the boattail flow field analysis, and a section for the base region analysis. The analyses are performed in the order stated. The same logic pattern is followed for the flow field analyses for both the nozzle (see subroutine NØZZL) and the boattail (see subroutine BØTTAL). The logic pattern reads in all of the input data, generates an initial-value line, calculates wall contour parameters, and employs the method of characteristics to analyze the flow field. After the flow fields for both the nozzle and boattail have been computed, subroutine BASE calculates the base pressure and the base thrust.

ØPTN. Subroutine ØPTN is the master logic program for nozzle contour optimization. All of the input data are read in and the initial-value line is generated. Then LØGICN is called to compute the secondary-start line, which is a right-running Mach line attached to the minimum allowed throat angle [ANMIN(1)] and extending either to the axis of symmetry or to

the exit plane of the nozzle. LOGICN then restarts from this line, thus increasing the efficiency of multiple nozzle flow field calculations in a nozzle or a nozzle-base-boattail optimization (see discussion in Section II). The parameter IMETH specifies which optimization algorithm is to be employed (IMETH = 1, Axial Iteration; IMETH = 2, Method of Steepest Descent; IMETH = 3, Newton's Method). The appropriate subroutine is then called to perform the nozzle contour optimization.

OPTB. Subroutine OPTB is the master logic program for boattail contour optimization. All of the input data are read in and the initial-value line is generated. The optimization method specified by the parameter IMETH (see subroutine OPTN) is called to perform the boattail contour optimization.

OPTNB. Subroutine OPTNB is the master logic program for a complete nozzle-base-boattail contour optimization. All of the input data are read in and the initial-value line for the nozzle is generated. LOGICN is called to compute the nozzle secondary-start line (see discussion in Section II). The optimization method to be employed is specified by the parameter IMETH (see subroutine OPTN). The appropriate subroutine is called to perform the combined nozzle-base-boattail optimization.

CØNBØT. Subroutine CØNBØT calculates the attachment angle corresponding to a conical boattail, given the boattail exit radius and initial expansion contour. This subroutine employs a Newton's method zero finding algorithm to iteratively solve for the attachment angle.

PUSH. Function PUSH calls the appropriate subroutines to compute the thrust for the specified geometry using the previously specified start lines for the nozzle and/or the boattail. The wall geometry for a nozzle-base-boattail configuration is specified by the following three independent parameters: (1) the nozzle throat attachment angle  $\theta_{an}$ , (2) the nozzle exit radius  $y_{en}$ , and (3) the boattail exit radius  $y_{eb}$  (see Figures E-1 and E-2). Subroutine PUSH sets the variable PUSH equal to the value of the thrust for the specified geometry, and returns to the calling program. This function subprogram serves as the objective function for the optimization algorithms.

INPUTT. Subroutine INPUTT reads in all of the input data through NAMELIST INFO. If an input variable is not specified on the data cards, then that variable is set equal to its default value given in subroutine INPUTT. A discussion of the input is given in Appendix E.

DATAN. Subroutine DATAN defines all of the variables employed in the method of characteristics calculations to be those corresponding to the nozzle. All of the nozzle input variables are printed out at the beginning of the analysis.

DATAB. Subroutine DATAB defines all of the variables employed in the method of characteristics calculations to be those corresponding to the boattail. All of the boattail input variables are printed out at the beginning of the analysis.

IVLINN. Subroutine IVLINN generates an initial-value line for the nozzle flow field analysis. When the input parameter IVLN = 1, the points on the initial-value line are read in. Each data card must contain the location, velocity magnitude, pressure, flow angle, and density at a point on the initial-value line. The number of data cards must be equal to the parameter NPN. If the parameter IVLN = 0, Kliegel's initial-value line is generated. This line begins on the wall at the minimum cross section of the throat and ends downstream a distance EPSLON along the axis. EPSLON is computed in subroutine IVLINN and is a function of the specific heat ratio, throat radius, and throat upstream radius of curvature. All of the properties for each point on the initial-value line are stored in the data storage array SL(K,I) and SLN(K,I).

IVLINB. Subroutine IVLINB determines the initial-value line for the boattail. If the input parameter IVLB = 1, the points on the initial-value line are read in. Each data card must contain the location, velocity magnitude, pressure, flow angle, and density at a point on the initial-value line. The number of data cards must be equal to the parameter NPB. If the parameter IVLB = 0, a uniform flow initial-value line is generated. This uniform line is computed from the free-stream Mach number and the stagnation properties which are specified in the input data. All of the properties for each point on the initial-value line are stored in the data storage arrays SL(K,I) and SLB(K,I).

Each point on the initial-value line is the beginning of a new right-running Mach line. The initial-value line must be specified long enough to insure that the last point on the initial-value line will generate a right-running Mach line beyond the exit lip point of the boattail. For the uniform flow initial-value line, the x-coordinate spacing of the points is determined by the input parameter SPACE. If SPACE = 1.0, the x-coordinate of the last point on the initial-value line will be equal to the boattail length  $x_{en}$ , and the last right-running Mach line will always go beyond the wall exit lip point of the boattail. To keep from generating unnecessary points on the initial-value line, SPACE should be specified between 0.3 and 0.6, depending on the freestream Mach number.

XYLINE. Subroutine XYLINE generates geometrically progressively spaced y-coordinates and the corresponding x-coordinates for points along the nozzle initial-value line. These points may be closely spaced next to the nozzle wall and spread apart as they approach the nozzle axis. The geometric progression is determined by the input parameter RATIØI. For example, if RATIØI = 5.0, then the y distance between the last two points on the initial-value line at the axis will be 5.0 times greater than the y distance between the first two points at the wall. This type of



point spacing permits a closer spacing of points near the wall where the flow property gradients are larger. If  $RATIO1 = 1.0$ , the y-coordinates will be uniformly spaced along the initial-value line.

STARTN. Subroutine STARTN determines the geometric parameters that specify the nozzle contour. The type of wall contour and the parameters that specify the wall contour are printed out. A conical wall, a second-order polynomial wall, or a tabular wall contour may be selected. The input parameter IWALLN determines which type of wall contour is selected. IWALLN = 1 specifies a conical nozzle, IWALLN = 2 specifies a second-order polynomial nozzle, and IWALLN = 5 specifies a tabular nozzle. The half-angle of the conical nozzle is specified by the throat expansion angle  $\theta_{an}$ . For a second-order polynomial wall, the wall exit lip point is determined by specifying either the exit radius  $y_{en}$  or the exit angle  $\theta_{en}$  (see Figure E-1). Subroutine STARTN computes the coefficients for the conical and second-order polynomial wall contours for the following equation.

$$y(x) = a + bx + cx^2 \quad (D-1)$$

The number of points in a tabular wall is specified by the parameter NWALLN, and the arrays XWN(100) and YWN(100) contain the respective x- and y-coordinates of the NWALLN points. The conical wall option and the tabular wall option may be employed only with the flow field analysis option. For the optimization option, the second-order polynomial wall contour option must be specified.

STARTB. Subroutine STARTB determines the geometric parameters that specify the boattail contour. The type of wall contour and the corresponding parameters are printed out. Four types of boattail contours may be selected: conical, cylindrical, second-order polynomial, or tabular contour. The parameter IWALLB determines which type of wall contour is selected. IWALLB = 1 specifies a conical boattail, IWALLB = 2 specifies a second-order polynomial boattail, IWALLB = 3 specifies a cylindrical boattail, and IWALLB = 5 specifies a tabular boattail. The half-angle of the conical boattail is specified by the initial expansion angle  $\theta_{ab}$ . For a second-order polynomial wall, the wall exit lip point is determined by specifying either the exit radius  $y_{eb}$  or the exit angle  $\theta_{eb}$ . Subroutine STARTB computes the coefficients for the boattail wall contours employing the following equation.

$$y(x) = a + bx + cx^2 \quad (D-2)$$

The number of points in a tabular wall is specified by NWALLB, and the arrays XWB(100) and YWB(100) contain the respective x- and y-coordinates of the NWALLB points. The tabular wall option may be employed only with the flow field analysis option. For the optimization option, the conical wall contour option must be specified for a complete nozzle-base-boattail configuration. For the optimization of a boattail contour



by itself, the second-order quadratic wall contour option is employed. When a complete nozzle-base-boattail analysis is being conducted, the base pressure model is restricted to boattails which have the same x-coordinate for the wall exit lip point and the nozzle exit lip point. However, if another base pressure model is inserted which includes the effects of different x-coordinates for the exit lip points of the nozzle and boattail, this will in no way affect any other part of the analysis.

LØGICN. Subroutine LØGICN contains the logic which generates the solution network for the nozzle flow field. Left-running Mach lines are followed to produce the characteristic mesh which constitutes the solution network. These left-running Mach lines originate from either the initial-value line or the nozzle axis. LØGICN determines which of these starting points is to be used for each left-running Mach line. In addition to determining the starting point, LØGICN monitors how many interior points are to be calculated, whether an indirect or direct wall point is to be computed, and when to stop the calculations. The following paragraphs give a more detailed description of the mechanics of subroutine LØGICN.

A thorough knowledge of the I-J characteristics coordinate system shown in Fig. D-1 is required to understand the overall solution logic. Each I-J point represents a calculated point in the characteristic network. The I-coordinate lines represent right-running Mach lines, and the J-coordinate lines represent left-running Mach lines. The point (NPN,1) is the first point of the solution network.

After initiating various control variables, the first point in the characteristic network is obtained. As shown in Figure D-1, this point (NPN,1) is located at the wall on the initial-value line.

When the main loop is entered, a decision must be made immediately as to which type of starting point is to be used. The first NPN - 1 times through the loop an initial-value line point is selected. Thereafter, an axis point is selected. This axis point is located at the intersection of the nozzle axis and the right-running Mach line from the second point on the previous left-running Mach line. After obtaining the starting point for the next left-running Mach line, interior points are calculated along the line, and the variable I is incremented by one after each point is calculated. This procedure continues until the I-coordinate of the interior point is equal to ILIMIT, when a wall point must be computed. After the wall point is computed, the nozzle thrust is computed by subroutine THRST.

Two different methods are used to compute a wall point. Along the circular arc initial expansion region of the throat, where property gradients are high, points are specified along the wall through which the left-running Mach lines must pass. Beyond the initial expansion region of the circular arc throat, the left-running Mach lines are ex-

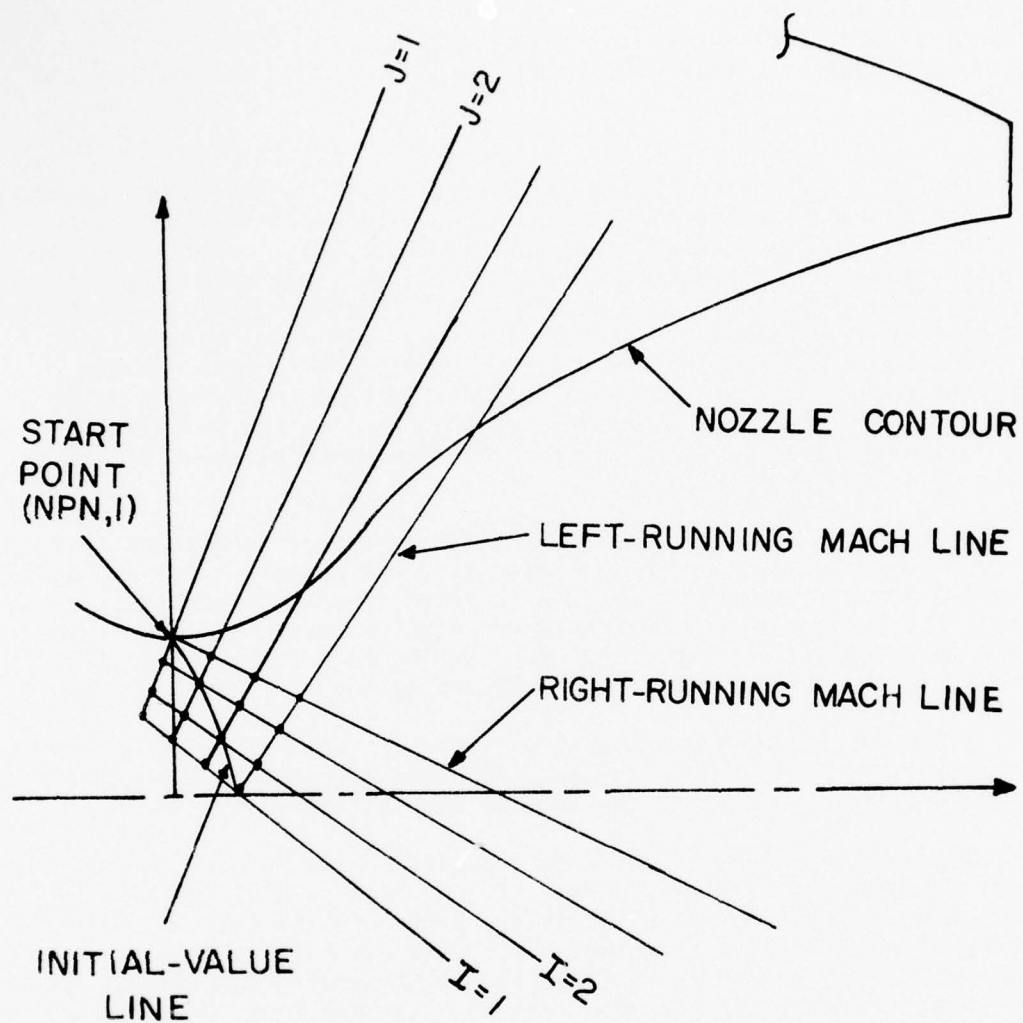


Figure D-1. Characteristic Coordinate System for the Nozzle Flow Field

tended directly to intersect the wall. This latter technique does not require any special modification of the logic, but the former technique does. To handle that situation, the special numbering system shown in Fig. D-2 has been devised. The specified points along the wall are spaced geometrically to increase the accuracy of the solution. The parameter  $RATIO_W$  specifies the ratio of the angular increment spanned by the last two points on the initial expansion contour adjacent to the throat attachment angle  $\theta_{an}$  to the angular increment spanned by the first two points at the throat. Knowing the throat attachment  $\theta_{an}$ ,  $RATIO_W$ , the location of the throat, and the nozzle downstream radius of curvature, the wall point locations may be computed. The interpolated points labeled by  $l$ 's on Figure D-2 are not stored. The calculated wall point  $(I + 1, J - 1)$  illustrated in Figure D-2(a) is stored in the previous left-running Mach line array at the  $(I + 1)$  location. After storing and printing the wall point, the interior point  $(I + 1, J)$  illustrated in Figure D-2(b) is calculated. This entire procedure, which is referred to as the inverse wall point scheme, is repeated until a specified wall point requires the  $x$ -value of the interpolated point  $l$  to exceed that of the last interior point. When this occurs, the parameter  $ITER$  is set equal to 99 in subroutine  $INWALL$ , and the next left-running Mach line is started from either the initial-value line or the axis. The last inverse wall point is computed at the maximum throat angle  $\theta_{an}$ .

The main loop continues to generate left-running Mach lines by the direct wall point method until the  $x$ -coordinate of the wall point exceeds the specified nozzle length  $x_{en}$ . Then the inverse wall point routine is called, using the nozzle exit lip point as the specified wall point. This completes the nozzle flow field analysis.

After the calculation of each interior point, a check is made to see if the Mach lines crossed. If the right-running Mach lines crossed, then the point just calculated is dropped from the flow field and a message is printed indicating this has been done. The properties at the next interior point are then based on the next point along the previous left-running Mach line. If the left-running Mach lines cross, the calculation of points along the new left-running Mach line is terminated. The remaining points up to the wall are defined to be those of the previous left-running Mach line which was just crossed. A message is printed indicating that the left-running Mach lines crossed.

Two important storage procedures are carried out in subroutine  $LØGICN$ . A secondary-start line, which is employed during the optimization procedure, is stored when the parameter  $ISSL$  is non-zero (see Section II). The secondary-start line attaches to the nozzle wall at the minimum allowed throat attachment angle. It is stored in the same location as the initial-value line. Subroutine  $LØGICN$  restarts the analysis from this secondary-start line. The value for  $ISSL = NPN + NPW$  when the secondary-start line is being stored. When the complete secondary-start line has been determined, the value of  $ISSL$  is 0. Note that subsequent restarts must have greater throat attachment angles than the minimum angle which determined the secondary-start line. If the

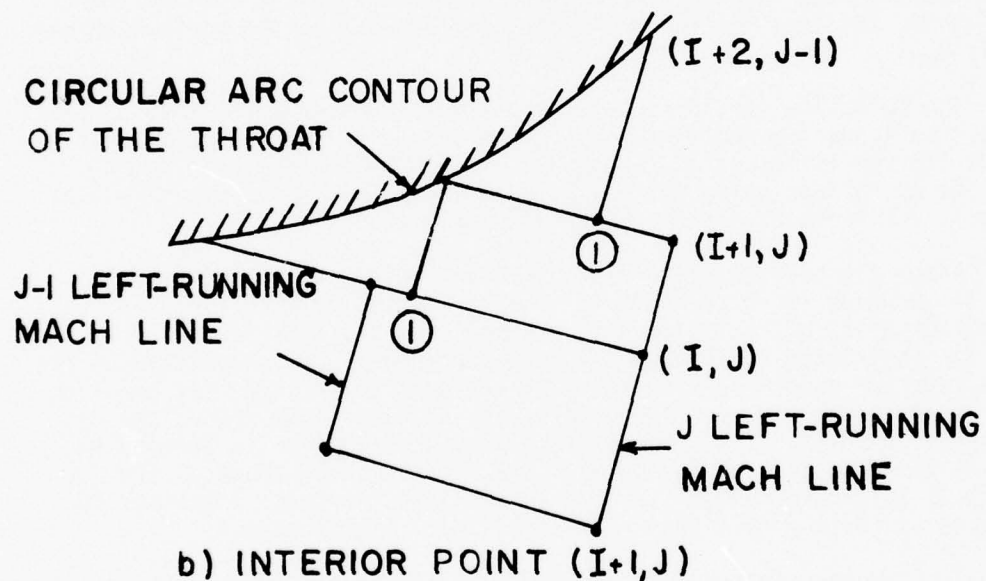
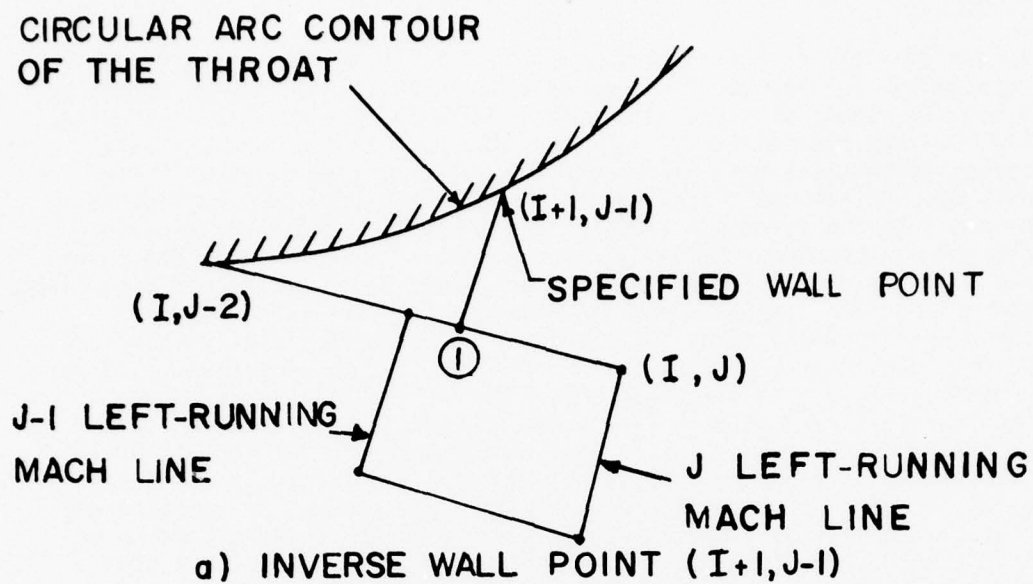


Figure D-2. Characteristic Coordinates for an Inverse Wall Point and an Interior Point



analysis option is utilized, ISSL is set equal to a large number and a secondary-start line is not stored. The flow properties at the final wall point of the flow field are stored in the array DFINAL.

LØGICB. Subroutine LØGICB contains the logic that generates the solution network for the boattail flow field. Right-running Mach lines are followed from the initial-value line to produce the characteristic mesh. Subroutine LØGICB determines how many interior points are to be calculated, when a wall point is to be computed, and when to stop the calculations. The following paragraphs give a detailed description of the mechanics of subroutine LØGICB.

As in the nozzle flow field analysis, an I-J characteristic coordinate system is employed to perform the tracking and storage of the computed points in the boattail flow field. The I-J coordinate system is shown in Fig. D-3. The I-coordinate lines represent right-running Mach lines, and the J-coordinate lines represent left-running Mach lines. The point (1,1) is the first point of the solution network.

The main loop of subroutine LØGICB is exceptionally straightforward since each right-running Mach line must originate from the initial-value line and terminate at the wall. Thus, the first step in the loop is to obtain a point from the initial-value line. Interior point calculations are then performed until the J-coordinate equals JLIMIT. Then a direct wall point is determined, and the thrust associated with that point is computed. The parameter JLIMIT is set equal to  $J + 1$ , and the entire loop is repeated. When the x-coordinate of the wall point exceeds the boattail length  $x_{eb}$ , the inverse wall point routine is called to determine the flow properties at the boattail exit lip point. The thrust is then computed. The final point on the last Mach line is stored in the array DFINAL. This completes the flow field analysis for the boattail.

If the initial-value line for the boattail flow field analysis has been specified too short, the analysis will be continued until the last point on the initial-value line has been used, at which time the last wall point still does not exceed the specified boattail length  $x_{en}$ . When this occurs, an error message will be printed and the program stops.

WRITE. Subroutine WRITE prints out the results of the characteristic calculations and the secondary-start line. It also determines the proper headings and carriage controls necessary for the various print options.

THRST. Subroutine THRST calculates the thrust at a wall point for the nozzle. For comparison, the one-dimensional flow thrust is also computed. This one-dimensional thrust appears on the last line of output for each left-running Mach line in the nozzle. Subroutine THRST also computes the fraction of the thrust and the mass flow rate between an interior point and the axis.

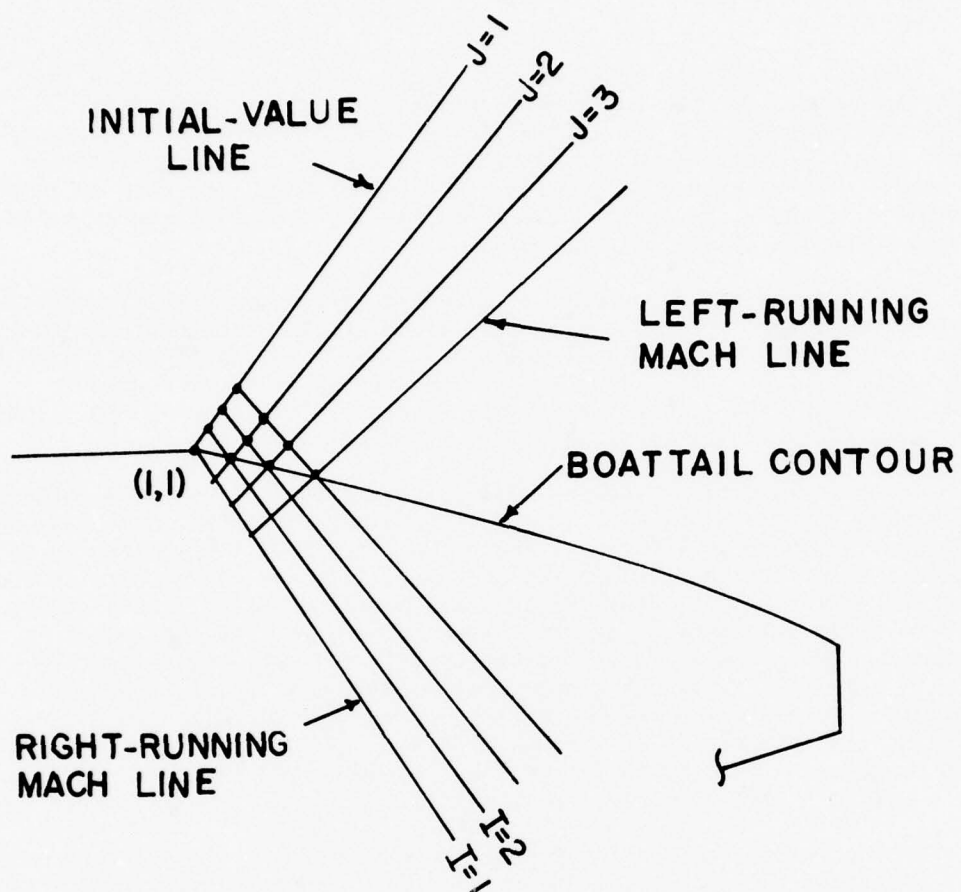


Figure D-3. Characteristic Coordinate System for the Boattail Flow Field

THERMØ. Subroutine THERMØ calculates the thermodynamic properties of the gas which are required by the characteristic and compatibility equations. The Mach number,  $M$ , temperature,  $t$ , and the speed of sound,  $a$ , are computed as a function of the density,  $\rho$ , pressure  $p$ , and velocity  $V$ . The subroutine built into the program is based on the properties of a thermally and calorically perfect gas. Other gas thermodynamic models may be considered by appropriate modifications to subroutine THERMØ.

EM. Function EM determines the Mach number as a function of the area ratio for the one-dimensional flow of a perfect gas. That information is required in subroutine THRST for the one-dimensional thrust comparison. If a gas thermodynamic model other than a perfect gas is specified in subroutine THERMØ, function EM must be modified accordingly.

PØINT. Subroutine PØINT evaluates the solution at an interior point in the flow field using the method of characteristics for rotational flow. The solution process employs the modified Euler predictor-corrector technique for solving the flow field characteristic and compatibility equations. An average property scheme is used to compute the coefficient of each differential. The point labeling scheme for this subroutine is shown in Fig. D-4. The location and flow properties are known at points 1 and 2. Point 4 is located at the intersection of the right-running and left-running Mach lines. The location of point 3 is obtained by extending a streamline back from point 4 until it intersects the line between points 1 and 2. Flow properties at point 3 are obtained by linear interpolation between points 1 and 2. The flow properties  $p$ ,  $\rho$ ,  $V$ , and  $\theta$  at point 4 are then obtained by solving the characteristic and compatibility equations. The equations programmed are as follows. Along the right-running Mach line,

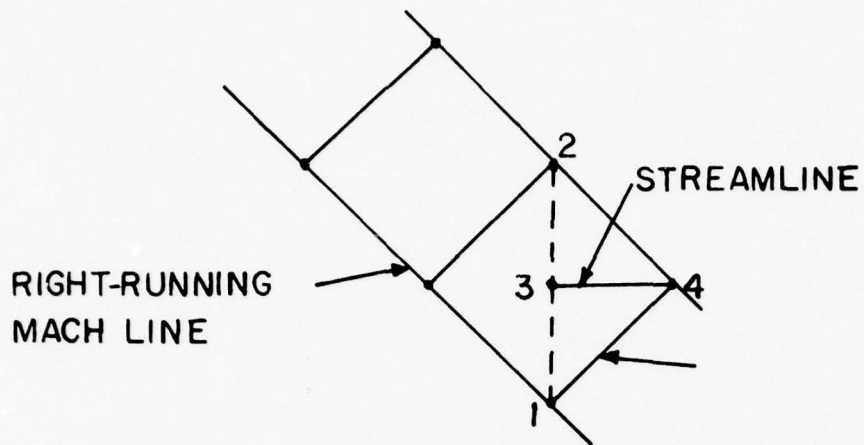
$$\frac{dy}{dx} = \tan (\theta - \alpha) \quad (D-3)$$

$$\frac{\sqrt{M^2 - 1}}{\rho V^2} dp + d\theta + \delta \left[ \frac{V}{yMV \cos (\theta - \alpha)} \right] dx = 0 \quad (D-4)$$

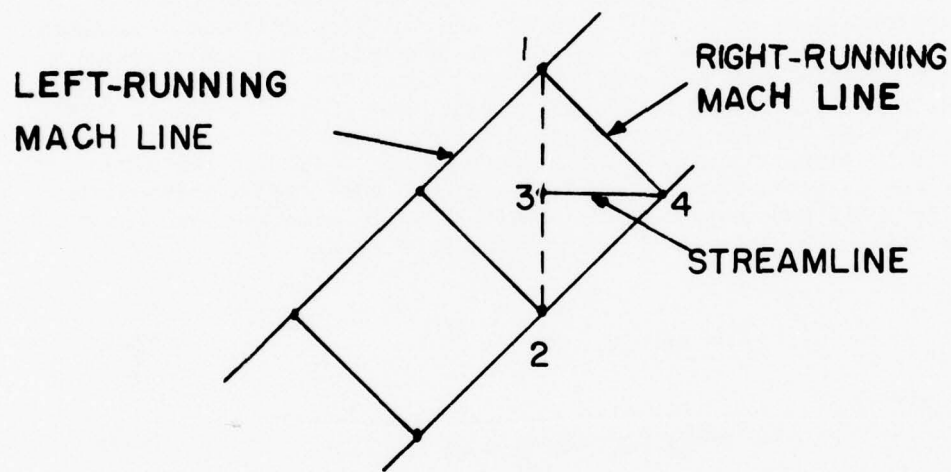
Along the left-running Mach line,

$$\frac{dy}{dx} = \tan (\theta + \alpha) \quad (D-5)$$

$$\frac{\sqrt{M^2 - 1}}{\rho V^2} dp - d\theta + \delta \left[ \frac{V}{yMV \sin (\theta + \alpha)} \right] dy = 0 \quad (D-6)$$



a) BOAT TAIL



b) NOZZLE

Figure D-4. Point Labeling Scheme for an Interior Point



Along the streamline,

$$\frac{dy}{dx} = \frac{v}{u} \quad (D-7)$$

$$\rho V dV + dp = 0 \quad (D-8)$$

$$dp - a^2 d\rho = 0 \quad (D-9)$$

The modified Euler predictor-corrector technique with average properties is used in the numerical analysis. The remaining flow properties are obtained by calling subroutine THERMØ.

INWALL. Subroutine INWALL evaluates the solution at a specified wall point in the circular arc throat region using an inverse method of characteristics for rotational flow. The location and flow properties are known at points 2, 3, and 5 in Fig. D-5. The solution is sought at point 4 where the location ( $x_4, y_4$ ) and slope  $\theta_4$  are already known. A left-running Mach line is extended rearward from point 4 to point 1, where the flow properties are obtained by linear interpolation between points 2 and 3. The compatibility equations are then solved for the flow properties  $p$ ,  $\rho$ ,  $V$ , and  $\theta$  at point 4. The equations programmed are as follows. Along the left-running Mach line,

$$\frac{dy}{dx} = \tan (\theta + \alpha) \quad (D-10)$$

$$\frac{\sqrt{M^2 - 1}}{\rho V^2} dp - d\theta + \delta \left[ \frac{v}{y M V \sin (\theta + \alpha)} \right] dy = 0 \quad (D-11)$$

Along the nozzle wall,

$$\frac{dy}{dx} = \frac{v}{u} \quad (D-12)$$

$$\rho V dV + dp = 0 \quad (D-13)$$

$$dp - a^2 d\rho = 0 \quad (D-14)$$

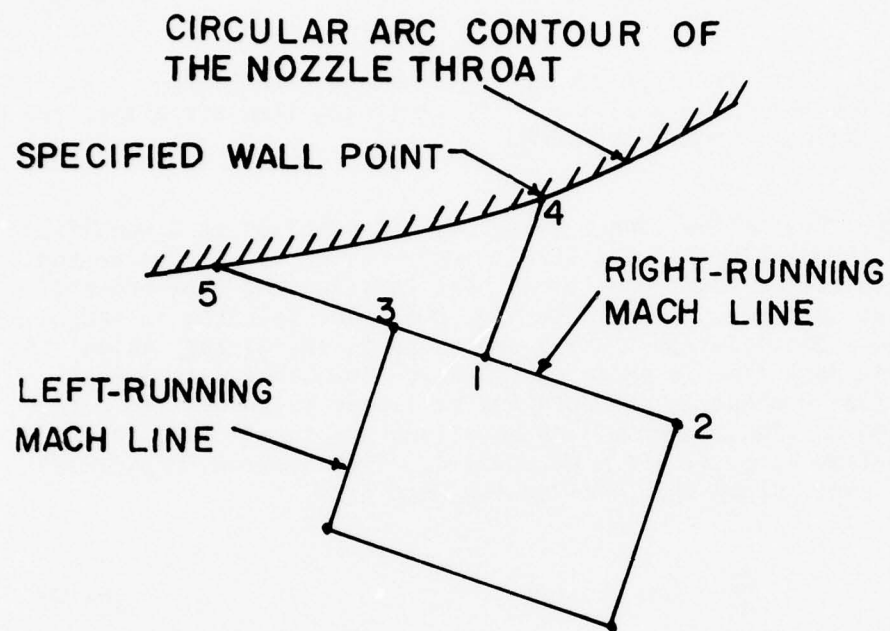


Figure D-5. Point Labeling Scheme for an Inverse Wall Point

The modified Euler predictor-corrector technique with average properties is used in the numerical analysis. The remaining flow properties are obtained by calling subroutine THERMØ.

F. Function F calculates the nozzle wall point spacing required for the portion of the circular arc throat between the secondary-start line attachment point and the circular arc throat attachment point. The objective is to maintain consistent spacing for those points upstream of the secondary-start line attachment point and those downstream of that point.

First, function F computes the number of wall points from the minimum throat attachment point to the specified throat attachment point using the original wall point spacing between the nozzle throat and the minimum throat attachment point. Then an iteration is performed to find the exact spacing which allows the last point to lie at the specified throat attachment point. Thus, the inverse wall points located downstream of the secondary start line point are spaced consistently with those upstream of that point, and the last inverse wall point is the specified throat attachment point.

DRWALL. Subroutine DRWALL determines the solution at a direct wall point using the method of characteristics for rotational flow. The location and flow properties are known at points 2 and 3 in Fig. D-6. Since the wall contour  $y(x)$  and the wall slope  $dy(x)/dx = \tan\theta$  are known, it is only necessary to locate point 4 on the wall and to calculate the flow properties  $p$ ,  $\rho$ , and  $V$  at that point. Left-running characteristics and compatibility equations are used for the nozzle wall, and right-running characteristic and compatibility equations are used for the boattail wall. The equations programmed are as follows. Along the Mach lines,

$$\frac{dy}{dx} = \tan(\theta \pm \alpha) \quad (D-15)$$

$$\frac{\sqrt{M^2 - 1}}{\rho V^2} dp_{\pm} \mp d\theta_{\pm} + \delta \left[ \frac{v}{yMV \sin(\theta \pm \alpha)} \right] dy_{\pm} = 0 \quad (D-16)$$

The upper signs are used for the nozzle analysis, and the lower signs are used for the boattail analysis. Along the walls,

$$\frac{dy}{dx} = \frac{v}{u} \quad (D-17)$$

$$\rho V dV + dp = 0 \quad (D-18)$$

$$dp - a^2 dp = 0 \quad (D-19)$$

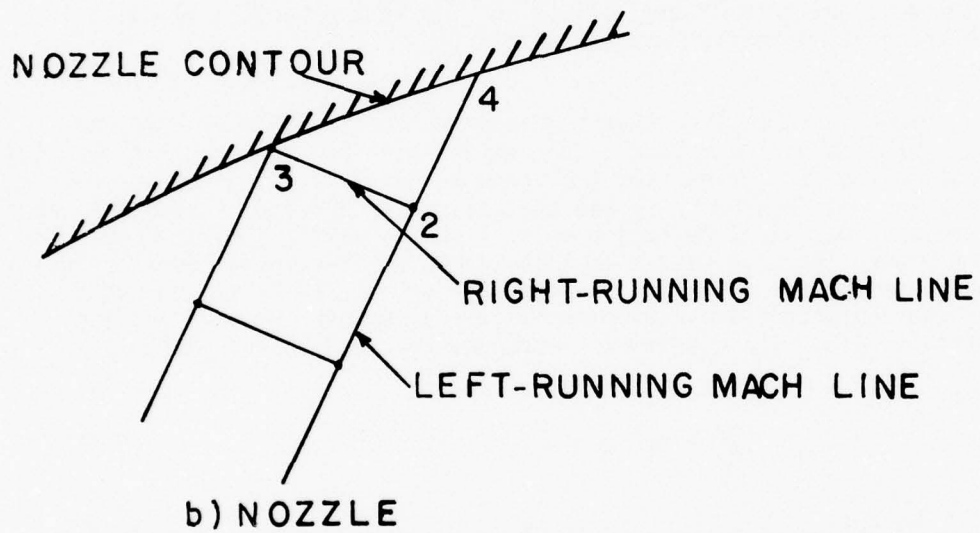
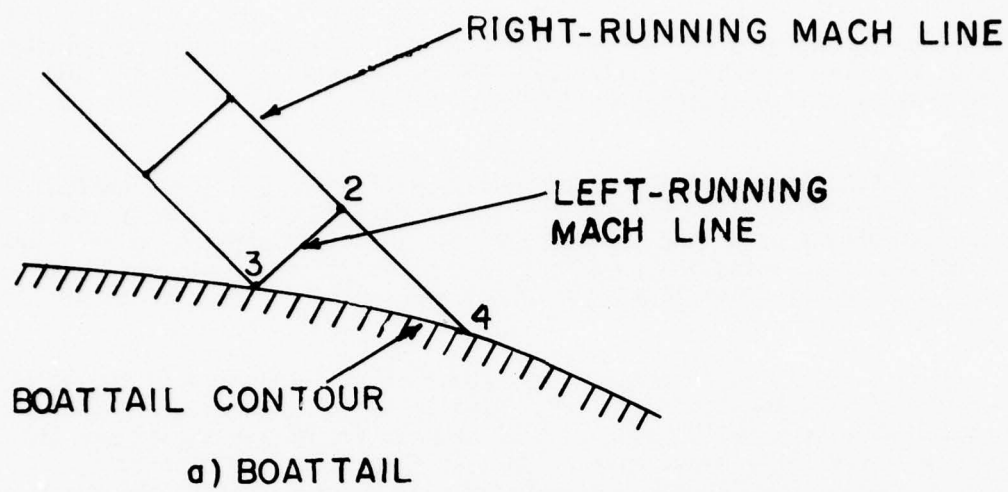


Figure D-6. Point Labeling Scheme for a Direct Wall Point



The modified Euler predictor-corrector technique with average properties is employed in the numerical analysis. The remaining flow properties are obtained by calling subroutine THERM.

WALLPT. Subroutine WALLPT locates the intersection of a Mach line with the wall contour. The x-coordinate, y-coordinate, and wall slope are computed for the solution point and returned to subroutine DRWALL. If a tabular wall has been specified, then conical wall segments are fit between each two data points on the wall.

AXIS. Subroutine AXIS determines the solution at an axis point using the method of characteristics for rotational flow. The location and flow properties are known at points 1 and 3 in Fig. D-7. Since the flow is axisymmetric, the flow angle  $\theta$  and y-coordinate at the axis must be zero. The compatibility equations along the right-running Mach line and the axis are solved to obtain the flow properties,  $p$ ,  $\rho$ , and  $V$ . The equations programmed are as follows. Along the Mach line,

$$\frac{dy}{dx} = \tan (\theta - \alpha) \quad (D-20)$$

$$\frac{\sqrt{M^2 - 1}}{\rho V^2} dp + d\theta + \delta \left[ \frac{V}{yMV \cos (\theta - \alpha)} \right] dx = 0 \quad (D-21)$$

Along the axis,

$$\rho V dV + dp = 0 \quad (D-22)$$

$$dp - a^2 d\rho = 0 \quad (D-23)$$

The modified Euler predictor-corrector technique, based on employing average properties for the corrector, is used in the numerical analysis. The remaining flow properties are obtained by calling subroutine THERM.

BASE. Subroutine BASE calculates the base pressure, the base thrust, and the total nozzle-base-boattail thrust. The exit lip point properties for the nozzle and the boattail are known from the nozzle and boattail flow field calculations. Using the known exit lip point properties in the base pressure model derived from the curve fit of Addy's (3) data, the base pressure and the base thrust are calculated. The total thrust is summed and printed out. Subroutine BASE also notes if the boattail exit radius is less than the nozzle exit radius, a physical impossibility. A message to this effect is printed out, and the program continues.

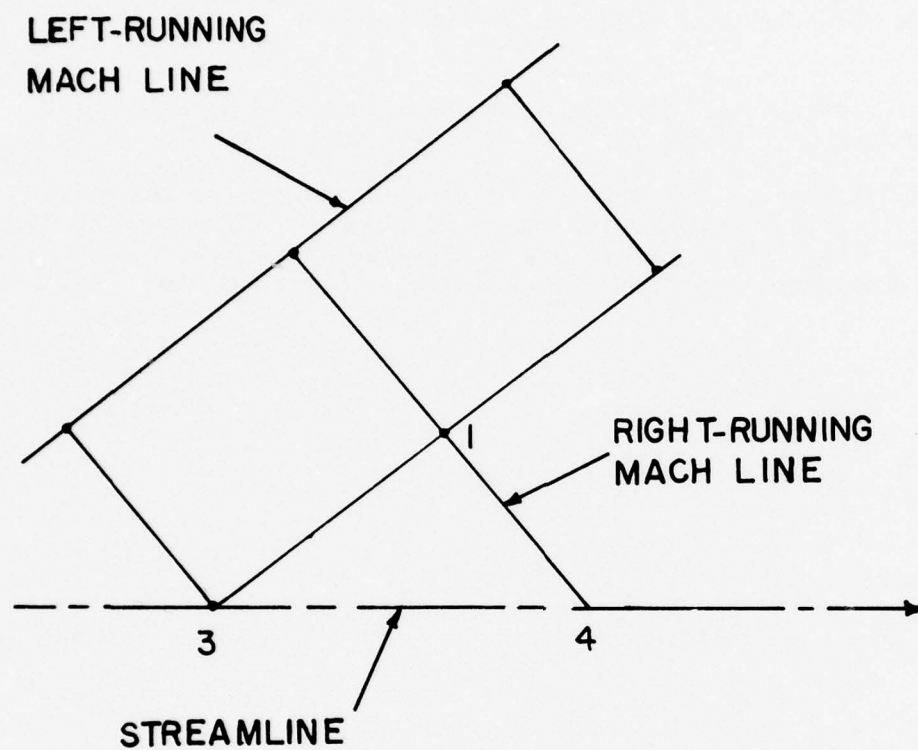


Figure D-7. Point Labeling Scheme for an Axis Point

TRAN2D. Subroutine TRAN2D transfers the properties stored at location D (I,J,N) in the D array to point 2.

TRAN1D. Subroutine TRAN1D transfers the properties stored at location D (I,J,N) in the D array to point 1.

TRAN4. Subroutine TRAN4 transfers the properties stored at point 4 to the D array at location D (I,J,N).

TRAN12. Subroutine TRAN12 transfers the properties stored at point 2 to point 1.

TRAN14. Subroutine TRAN14 transfers the properties stored at point 4 to point 1.

TRAN24. Subroutine TRAN24 transfers the properties stored at point 4 to point 2.

TRAN3D. Subroutine TRAN3D transfers the properties stored at location D (I,J,N) in the D array to point 3.

TRANSL. Subroutine TRANSL transfers the properties stored at point 4 to the secondary-start line array SL (K,JJP).

AXITER. Subroutine AXITER performs an axial iteration optimization of the objective function, thrust (PUSH). The subroutine requires an initial estimate (ANGA, RADB, ANGC, RADD) and increments (DA, DB, DC, DD) for each of the independent variables. The variables ANGC and DC are employed only when optimizing a boattail contour by itself. It then perturbs each of the variables in turn, fitting a quadratic polynomial of the form  $y = a + bx + cx^2$  along the variable direction. The algorithm then finds the maximum point of the quadratic polynomial, calculates the objective function there, and steps to the maximum of the points on this line. The algorithm then proceeds to the next independent variable. Note that since all of the variables are independent, the search directions are orthogonal. If the algorithm encounters a prespecified boundary in any of the variables, this is noted and the variable is set equal to the boundary value. If the algorithm encounters an inequality constraint, such as the nozzle and boattail exit lip points coming closer than some previously specified value  $\Delta y_b$ , the variables become dependent ( $y_{eb} = y_{en} + \Delta y_b$ ) and the variable space is diminished by one dimension.

The optimization may then proceed until convergence, when the function changes less than some specified relative tolerance. This algorithm stops in some (ITERØ) number of base point moves with an error message.

HILCLM. Subroutine HILCLM performs an optimization using the method of steepest descent (hill climbing). Beginning with an initial estimate (ANGA, RADB, ANGC, RADD) and increments (DA, DB, DC, DD), a first-order approximation to the unit gradient is calculated. The base point is then successively moved along the direction of the gradient until the objective function decreases. Then, the algorithm recalculates the gradient and begins again. This continues until the first step along a gradient no longer increases the objective function. Then the finite difference increments and step length are halved and the algorithm continues. Convergence is attained when the magnitude of the gradient becomes less than some specified relative tolerance. Some maximum number of gradient evaluations (ITERØ) stops the algorithm with an error message.

NEWTON. Subroutine NEWTON performs an optimization employing Newton's method. The algorithm requires a starting point (ANGA, RADB, ANGC, RADD) and increments (DA, DB, DC, DD) to form a matrix of second derivative approximations (Hessian) and a column vector along the negative gradient (see discussion in Section II). Subroutine GAUSS is employed to invert the Hessian and solve for the base point move, both in distance and direction. If this move exceeds the specified optimization boundaries (ANMAX, ANMIN), or the step does not increase the objective function, then some relaxation factor is employed which forces the step to remain in bounds. This then becomes the new base point, and the process repeats. Convergence is attained when the function changes less than some relative tolerance. If the algorithm does not converge within ITERØ base point moves, an error message is printed and the program stops.

GAUSS. Subroutine GAUSS is a simultaneous linear equation solver. A system of N linear equations, with coefficient matrix C and right hand side vector B is solved. The solution is the column vector V. The algorithm employs Gauss reduction, requiring only N - 1 passes to complete the reduction. Back substitution then fills the V vector before it returns to subroutine NEWTON, the calling program.



## APPENDIX E. INPUT PARAMETERS

The first data card in each run specifies the type of computation. The variable `IØPT` contained in column 1 selects whether an analysis (`IØPT` = 1) or an optimization (`IØPT` = 2) is performed. The variable `ITYPE` specified in column 2 determines the type of geometry being considered: `ITYPE` = 1 for a complete nozzle-base-boattail assembly, `ITYPE` = 2 for a nozzle only, and `ITYPE` = 3 for a boattail only. The remaining 78 spaces are available for any alphanumeric job title, which is printed at the beginning of each run.

All other input parameters are read in by subroutine `INPUTT` through a `NAMELIST` file called `INFØ`. Each of the parameters has a default value defined within the program. All of the input parameters necessary to perform nozzle, boattail, or nozzle-base-boattail analyses and optimizations are included in `NAMELIST INFØ`.

The code has the capability of using tabular values for gas properties, wall contours, and initial-value lines. If tabular gas properties are not input, the program uses a constant specific heat ratio and gas constant (table of 1 row). However, to use the tabular gas property option, the number of rows in the gas table `NGASN` or `NGASB`, respectively, (up to 20) must be specified. Each row includes a velocity magnitude, a specific heat ratio, and a gas constant.

Normally, the tabular wall contour option is not employed and the wall contour is internally computed as either a conical contour or a quadratic polynomial contour. When the tabular wall option is employed, the number of points on the tabular wall is given by `NWALLN` and `NWALLB` for the nozzle and boattail, respectively. Each point must have an x- and y-coordinate, up to a maximum of 100 wall points.

When the tabular initial-value line option is not utilized, an initial-value line is internally generated, using Kliegel's transonic analysis for the nozzle and a uniform flow for the boattail. The procedure for specifying tabular initial-value lines is discussed in the descriptions of subroutines `IVLINN` and `IVLINB` in Appendix D.

Tables E-1 through E-3 list the program input variables, a description of each variable, the engineering symbol for each variable, and the units and default value of each variable. When no units are specified, the variable is dimensionless. Figures E-1 and E-2 illustrate the nozzle and boattail geometries.

TABLE E.1. INPUT PARAMETERS FOR NOZZLE

Variable	Description	Units	Default Value
NPN	Number of points on the initial-value line.		11
IVLN	Type of initial-value line: 0 Kliegel, 1 read in points.		0
RATIOI	Geometric ratio of point spacing along the initial-value line.		5.0
IVLSN	Terminate analysis after nozzle initial-value line calculation; 0 no, 1 yes.		0
NPW	Number of points along throat initial expansion contour.		22
RATIOW	Geometric ratio of point spacing along throat expansion contour.		5.0
ICN	Number of applications of the corrector.		2
TOLN	Fractional convergence tolerance of the corrector.		0.001
KWRITN	Output option: 0 every point, 1 initial-value, axis, and wall points, 2 wall points, 3 exit lip point.		0
IDN	Dump flag: 0 no, 1 yes.		0
YTN	Throat radius, $y_t$ .	in.	1.0
THETTN	Throat attachment angle, $\theta_{an}$ .	deg	30.0
RUN	Nozzle throat upstream radius of curvature, $\rho_{tu}$ .	in.	3.0
RDN	Nozzle throat downstream radius of curvature, $\rho_{td}$ .	in.	0.5
XEN	Nozzle exit length, $x_{en}$ .	in.	10.0
YEN	Nozzle exit radius, $y_{eb}$ .	in.	5.0
THETEN	Nozzle exit angle, $\theta_{an}$ .	deg	0.0
IWALLN	Wall contour: 1 cone, 2 second-order polynomial, 5 tabular.		2

TABLE E.1. CONTINUED

Variable	Description	Units	Default Value
DTHETN	Incremental angle change in Prandtl-Meyer expansion.	deg	1.0
DELTAN	1.0 axisymmetric nozzle, 0.0 planar nozzle.		1.0
P0N	Stagnation pressure, $P_0$ .	psia	1000.0
T0N	Stagnation temperature, $T_0$ .	R	6000.0
PAMB	Ambient pressure, $p_{amb}$ .	psia	0.0
NGASN	Number of rows in gas property table, if 1, then constant $\gamma$ and R.		1
VELN	Tabular values of velocity magnitude, V, NGASN values.	$\frac{ft}{sec}$	none
GAMN	Tabular values of specific heat ratio, $\gamma$ , NGASN values.		1.2
RGASN	Tabular values of gas constant, R, NGASN values.	$\frac{ft-lbf}{lbm-R}$	60.0
NWALLN	Number of points on tabular wall.		none
XWN	x-coordinates of points on tabular wall, NWALLN values.	in.	none
YWN	y-coordinates of points on tabular wall, NWALLN values.	in.	none

TABLE E.2. INPUT PARAMETERS FOR BOATTAIL

Variable	Description	Units	Default Value
NPB	Number of points on the initial-value line.		30
IVLB	Type of initial-value line: 0 uniform, 1 read in points.		0
IVLSB	Terminate boattail analysis after boat-tail initial-value line calculation: 0 no, 1 yes.		0
ICB	Number of applications of the corrector.		2
TOLB	Fractional convergence tolerance of the corrector.		0.001
KWRITB	Output option: 0 every point, 1 initial-value, axis and wall points, 2 wall points, 3 exit lip point.		0
IDB	Dump flag: 0 no, 1 yes.		0
MS	Freestream Mach number.		1.4
SPACE	Spacing factor for points along the initial-value line.		0.5
YTB	Initial boattail radius, $y_t$ .	in.	8.0
THETTB	Boattail attachment angle, $\theta_t$ .	deg	2.0
RDB	Boattail downstream radius of curvature, $\rho_{td}$ .	in.	5.0
XEB	Boattail exit length, $x_{eb}$ .	in.	10.0
YEB	Boattail exit radius, $y_{eb}$ .	in.	7.0
THETEB	Boattail exit angle, $\theta_{eb}$ .	deg	0.0
IWALLB	Wall contour: 1 cone, 2 second-order polynomial, 3 cylindrical, 5 tabular		2
DTHETB	Incremental angle change in Prandtl-Meyer expansion.	deg	1.0

TABLE E.2. CONTINUED

Variable	Description	Units	Default Value
DELTAB	1.0 axisymmetric boattail, 0.0 planar boattail.		1.0
P0B	Stagnation pressure, $P_0$ .	psia	12.0
T0B	Stagnation temperature, $T_0$ .	R	600.0
NGASB	Number of rows in gas property table, if 1, then constant $\gamma$ and R.		1
VELB	Tabular values of velocity magnitude, V, NGASB values.	$\frac{\text{ft}}{\text{sec}}$	none
GAMB	Tabular values of specific heat ratio $\gamma$ , NGASB values.		1.4
RGASB	Tabular values of gas constant, R, NGASB values.	$\frac{\text{ft-lbf}}{\text{lbm-R}}$	53.3
NWALLB	Number of points on tabular wall.		none
XWB	x-coordinates of points on tabular wall, NWALLB values.	in.	none
YWB	y-coordinates of points on tabular wall, NWALLB values.	in.	none



TABLE E.3. INPUT PARAMETERS FOR OPTIMIZATION

Variable	Description	Units	Default Value
ANSTRT(1)	Initial estimate of nozzle throat attachment angle, $\theta_{an}$ .	deg	30.0
ANSTRT(2)	Initial estimate of the nozzle exit radius, $y_{en}$ .	in.	5.0
ANSTRT(3)	Initial estimate of the boattail attachment angle, $\theta_{ab}$ . Only employed when designing a boattail alone.	deg	15.0
ANSTRT(4)	Initial estimate of the boattail exit radius, $y_{eb}$ . Only employed when designing a boattail alone.	in.	4.0
ANMAX(1)	Maximum allowed nozzle throat attachment angle.	deg	45.0
ANMAX(2)	Maximum allowed nozzle exit radius.	in.	7.0
ANMAX(3)	Maximum allowed boattail attachment angle.	deg	20.0
ANMAX(4)	Maximum allowed boattail exit radius.	in.	8.0
ANMIN(1)	Minimum allowed nozzle throat attachment angle.	deg	20.0
ANMIN(2)	Minimum allowed nozzle exit radius.	in.	4.0
ANMIN(3)	Minimum allowed boattail attachment angle.	deg	0.0
ANMIN(4)	Minimum allowed boattail exit radius.	in.	4.0
IMETH	Optimization method: 1 axial iteration, 2 method of steepest descent, 3 Newton's method.		3
ITERØ	Maximum number of passes through the optimization algorithm.		10
TØLØ	Relative convergence tolerance for optimization		0.001

TABLE E.3. CONTINUED

Variable	Description	Units	Default Value
KWRITØ	Output option: 0 every point, 1 initial-value, axis, and wall points, 2 wall points, 3 exit lip point.		3
IØP	Specifies type of geometry for optimization: 1 nozzle, 2 boattail, 3 nozzle-base-boattail combination.		1
N	Specifies the dimension of the optimization space (i.e., the number of unconstrained parameters).		2
DA	Nozzle attachment angle perturbation.	deg	1.0
DB	Nozzle exit lip radius perturbation.	in.	$0.2y_{tn}$
DC	Boattail attachment angle perturbation.	deg	0.5
DD	Boattail exit lip radius perturbation.	in.	$0.2y_{tn}$
DBAS	Minimum annular base width, $\Delta y_b$ .	in.	0.0

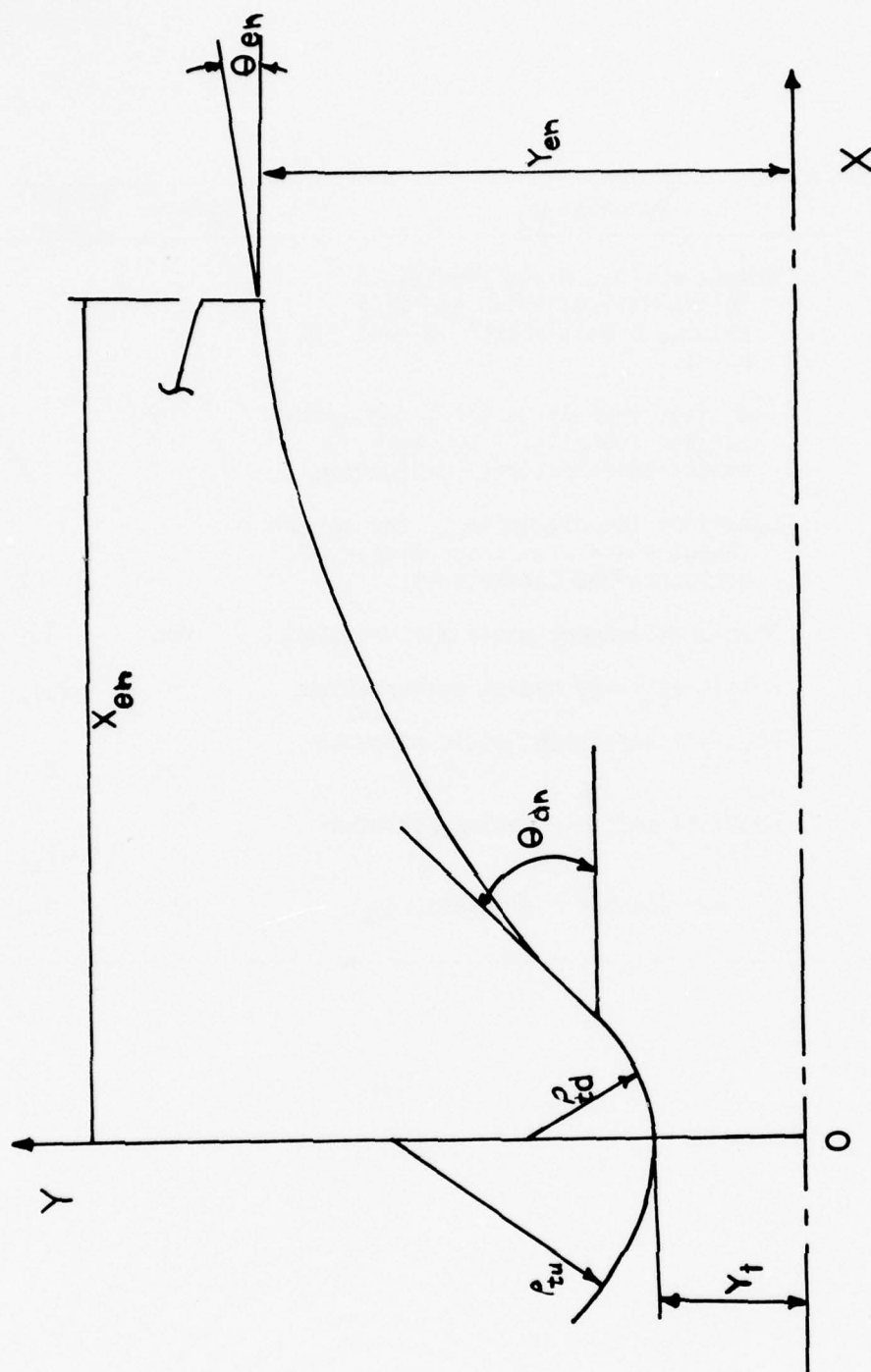


Figure E-1. Specification of the Nozzle Geometry

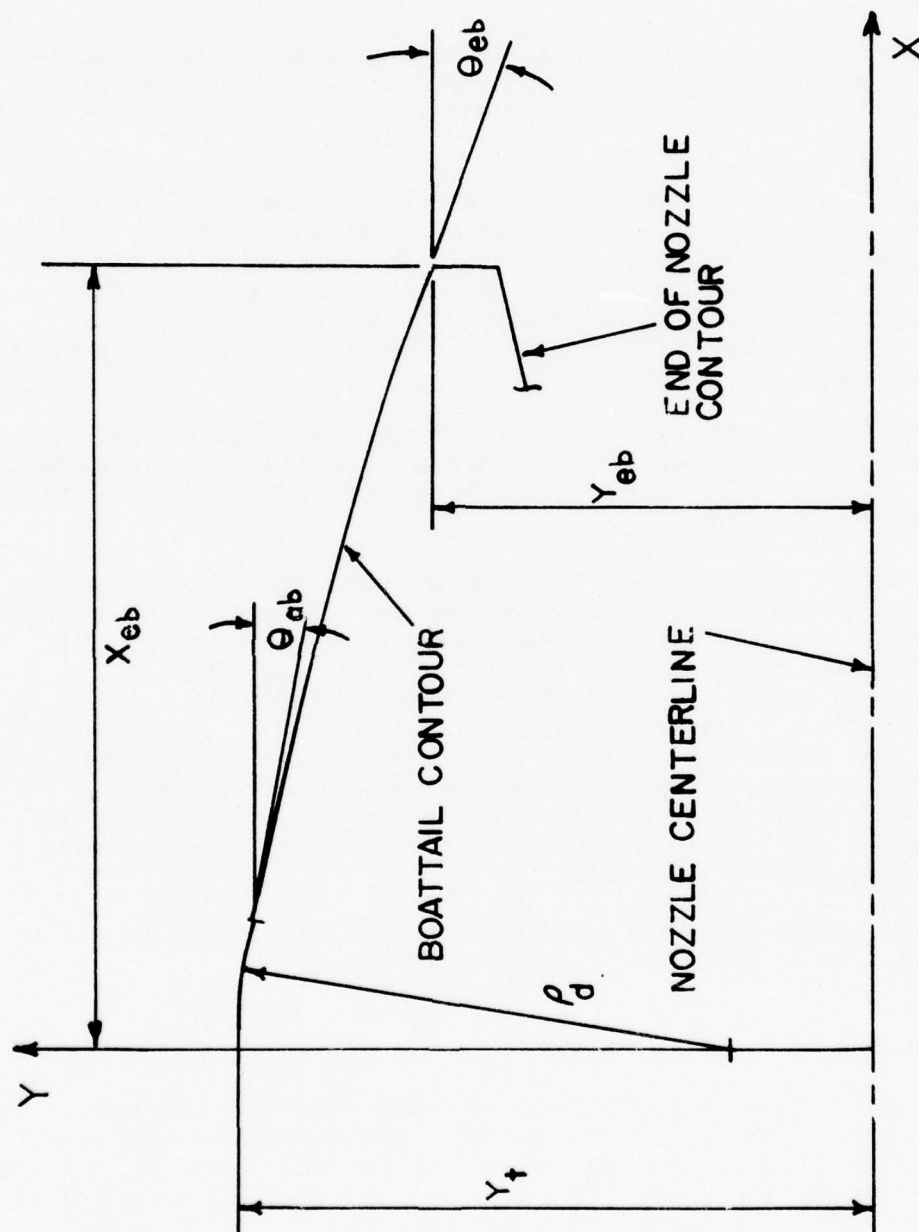


Figure E-2. Specification of the Boattail Geometry

## APPENDIX F. SAMPLE CASES

Five sample cases are presented in this section to illustrate the application of the computer program. These cases exercise most of the options available for analysis or optimization.

Each data deck begins with a TITLE CARD. That card identifies the type of geometry (nozzle, boattail, or nozzle-base-boattail assembly) and whether an analysis or an optimization is desired. Column 1 contains the parameter IOPT which is 1 for an analysis and 2 for an optimization. Column 2 contains the parameter ITYPE, which is 1 for a complete nozzle-base-boattail assembly, 2 for a nozzle, or 3 for a boattail. The remainder of the card (78 columns) may contain any alphanumeric job identification data.

The following cards specify the remaining input data in free format form, read in through NAMELIST INFO. Not all variables need to be defined for each run, as default values are specified in subroutine INPUTT for most of the variables.

Each sample case considers the same thermodynamic model, which is specified by the default values in the program. The gas in the nozzle is a thermally and calorically perfect gas with  $\gamma = 1.2$  and  $R = 60.0$  (ft-lbf)/(lbm-R). Thus, NGASN = 1, GAMN(1) = 1.2, and RGASN(1) = 60.0. The gas flowing around the boattail is also a thermally and calorically perfect gas with  $\gamma = 1.4$  and  $R = 53.3$  (ft-lbf)/(lbm-R). Thus, NGASB = 1, GAMB(1) = 1.4, and RGASB(1) = 53.3. The nozzle gas properties are typical of high temperature exhaust jet gases, and the boattail gas properties are those of air. The stagnation properties are specified: in the nozzle,  $T_0N = 6000.0$  R and  $P_0N = 1000$  psia, and for the boattail  $T_0B = 600.0$  R and  $P_0B = 12.0$  psia.

In each sample case, the geometry to be analyzed is discussed, and the running time on the CDC 6500 computer is given.

### 1. Sample Case 1

The first sample case illustrates a nozzle flow field analysis. It considers a nozzle exhausting into a static region having a pressure of 5.0 psia ( $P_{AMB} = 5.0$ ). Thus, in column 1 of the title card IOPT = 1 and in column 2 of the title card ITYPE = 2. The job identification statement "SAMPLE CASE 1" is contained in the remainder of the title card.



A Kliegel type initial-value line is specified by default (IVLN = 0). The nozzle geometry is specified with the nozzle upstream radius of curvature RUN = 3.0 in., the nozzle downstream radius of curvature RDN = 0.5 in., the nozzle throat radius YTN = 1.0 in., the throat attachment angle THETN = 30.0 deg, the nozzle exit radius YEN = 5.0 in., and the nozzle length XEN = 10.0 in. The nozzle wall is a second-order polynomial contour (IWALLN = 2). All of the parameters are the program default values.

The accuracy of the analysis depends on the number and spacing of the initial-value line points. In this sample case, 11 points are specified spanning the nozzle throat radius (NPN = 11).

The best accuracy is obtained when these points are spaced geometrically across the throat with the ratio of the distance between the two points at the centerline to the distance between the two points at the wall having a value larger than unity. For this sample case, RATIOI = 5.0. That spacing makes the change in property values between points of the computational mesh roughly comparable, because property gradients are greatest near the wall. A similar procedure is employed for points along the nozzle wall on the initial expansion contour. A wall point spacing compatible with the initial-value line spacing is obtained with NPW = 22 and RATIOW = 5.0. It should be noted that the number of points in the flow field solution mesh, and hence the computation time, is proportional to the square of NPN. Large amounts of computation time may be saved by reducing NPN, although a corresponding decrease in accuracy results. The above parameters are all specified by the program default values.

The parameters TOLN and ICN are the fractional convergence tolerance and the maximum number of applications of the corrector, respectively, in the method of characteristics unit processes. Those parameters are specified by their default values (TOLN = 0.001 and ICN = 2).

Output is kept brief by setting KWRITN = 1. This option prints only initial-value line points, axis points, wall points, and the one-dimensional approximation to the solution at the wall points.

The following list presents the data deck for sample case 1. Note that only KWRITN and PAMB are specified, because default values are employed for all of the other parameters.

```
12  SAMPLE CASE 1  NOZZLE ANALYSIS
    $INFO          KWRITN = 1, PAMB = 5.0 $
```

A complete listing of the output from sample case 1 is presented in Fig. F-1. The first page contains the program abstract and the job title. The nozzle flow field analysis data and initial-value line are listed on the second page. Column headings for the initial-value line data are as follows.

X	downstream distance from the nozzle throat, in.
Y	radial distance from the nozzle axis, in.
M	Mach number
P	pressure, psia
Q	velocity magnitude, ft/sec
TH	flow angle, deg.
U	x-component of velocity, ft/sec
V	y-component of velocity, ft/sec
R	density, lbm/ft <sup>3</sup>
T	temperature, R
WDOT	mass flow rate between the axis of symmetry and the given point, lbm/sec
THRUST	thrust between the axis of symmetry and the given point, lbf
ISP	specific impulse for the flow between the axis of symmetry and the given point, lbf-sec/lbm

The initial-value line performance parameters are also listed.

The next three pages of output presented in Fig. F-1 contain the results of the method of characteristics flow field analysis. The first of these three pages presents the wall contour specification and the column headings for the method of characteristics calculations. J and I are the characteristic coordinates, and the next ten columns are the same as described above for the initial-value line output. Columns 13 and 14, headed by MDT/LRC and F/LRC, respectively, refer to the integrated values of the mass flow rate and the thrust along the left-running Mach line from the axis of symmetry to the given point. These two columns represent checks on the accuracy of the program. The mass flow rate at any wall point should be close to the mass flow rate at the throat. The thrust obtained along the wall, THRUST, should be close to the value obtained along the left-running characteristic, F/LRC. The specific impulse, ISP, is printed in the next column, and the number of applications of the corrector, IC, or the specific impulse efficiency, EFF, is printed in the last column. IC is printed when the point is a flow field point computed by any of the method of characteristics unit process, and EFF is printed when the point is the one-dimensional approximation to the wall point solution. When 0 is printed in the last column, the point is on the initial-value line. A -2 in the last column indicates that the point is the nozzle exit lip.

Wall points are located at the end of every left-running Mach line. However, in the throat region of the nozzle, the inverse wall point method is employed. That procedure arbitrarily specifies the wall point locations, thus controlling the spacing and enhancing the accuracy of the flow field analysis. In this region there may be several wall points along the same left-running characteristic. After a wall point is printed, the one-dimensional flow approximation to the solution at the wall point is computed and printed for reference.

The last line of the output gives the total number of characteristics that crossed inside of the nozzle. The formation of oblique shock waves is indicated when this is nonzero.

Sample case 1 required 5 seconds of central processor time on the CDC 6500 computer.

## ANALYSIS AND DESIGN OF SUPERSONIC NOZZLE-BASE-ROCKET COMBINATIONS

## ABSTRACT

THIS PROGRAM WAS PRODUCED AT THE PURDUE UNIVERSITY THERMAL SCIENCE AND PROPULSION CENTER BY J. G. ALLMAN AS A PART OF THE RESEARCH PROGRAM OF THE PURDUE UNIVERSITY THERMAL SCIENCE AND PROPULSION CENTER. THE CONTRACT WAS FOR THE DESIGN AND ANALYSIS OF THE ROCKET-BASED NOZZLE COMBINATIONS OF THE PURDUE UNIVERSITY THERMAL SCIENCE AND PROPULSION CENTER. THE PRINCIPAL INVESTIGATOR FOR PURDUE UNIVERSITY WAS PROFESSOR JOE W. HOFFMAN.

THE EQUATIONS OF MOTION FOR AN INCOMPRESSIBLE SUPERSONIC FLOW ARE SOLVED USING A NUMERICAL METHOD OF CHARACTERISTICS HAVING SECOND-ORDER ACCURACY. THE INITIAL FLOW VARIABLES FOR THE NOZZLE FLOW FIELD CAN BE SPECIFIED OR COMPUTED FROM FLIGHT TEST DATA. THE INITIAL FLOW VARIABLES FOR THE ROCKET FLOW FIELD CAN BE SPECIFIED OR COMPUTED FROM FLIGHT TEST DATA. THE INITIAL FLOW VARIABLES FOR THE NOZZLE AND ROCKET GEOMETRIES CAN BE SPECIFIED AS COMICAL, SECTOR-ORBITAL, OR TABULAR. THE ANALYSIS WAS BASED ON THE GOVERNING GAS DYNAMIC RELATIONS FOR A ROTATIONAL FLOW OF A FROZEN OR EQUILIBRIUM GAS MIXTURE.

## JOB TITLE

SAMPLE CASE 1

NOZZLE ANALYSIS

Figure F-1. Output for Sample Case 1.

## NOZZLE FLOW FIELD ANALYSIS

NP = 11  
 TO = 4000.00 M  
 P0 = 1000.00 PSIA  
 PA0 = 5.00 PSIA  
 I = 0  
 I\*ALL = 22  
 NP\* = 22  
 K\*RTI = 21

VE = 10.000 IN  
 VE\* = 5.000 IN  
 VE\* = 5.000 IN  
 VE\* = 5.000 IN  
 VE\* = 5.000 IN

G = 1.20  
 G\* = 6.00 (FT-LBF)/(LBM-HR)  
 G\* = 1  
 RATIO1 = 5.00  
 RATIO2 = 5.00  
 TOL = .0010

## INITIAL-VALUE LINE

THE INITIAL-VALUE LINE IS A \*LIEGFL VED LINE

I	X	Y	M	P	G	Th	U	V	R	T	*LDT	THRUST	ISP
1	0.000	1.000	1.000	514.66	4816.6	-0.000	3816.6	-0.0	2.2997E-01	5371.2	19.221	3881.137	201.916
2	.012	.988	1.007	513.70	4788.7	.000	3788.7	.7	2.3335E-01	5368.9	19.154	3881.137	201.916
3	.040	.940	1.058	528.90	4741.6	.019	3741.6	1.3	2.3726E-01	5405.7	19.143	3881.137	201.916
4	.097	.870	1.049	534.53	4715.0	.031	3715.0	2.0	2.3726E-01	5404.9	12.014	3881.137	201.916
5	.076	.710	1.040	539.92	4683.6	.043	3683.6	2.6	2.3335E-01	5414.3	9.696	3881.137	201.916
6	.094	.614	1.031	542.49	4654.3	.054	3654.3	3.4	2.4139E-01	5423.5	7.248	3881.137	201.916
7	.114	.499	1.022	550.76	4626.6	.059	3626.6	3.7	2.4333E-01	5432.2	4.786	3881.137	201.916
8	.132	.361	1.015	550.59	4602.4	.054	3602.4	3.4	2.4503E-01	5439.8	2.511	3881.137	201.916
9	.146	.197	1.009	556.52	4574.3	.034	3574.3	2.1	2.4623E-01	5443.4	.740	3881.137	201.916
10	.151	0.000	1.007	560.73	4577.0	0.000	3577.0	0.0	2.4663E-01	5447.7	0.000	3881.137	201.916

## INITIAL-VALUE LINE PERFORMANCE PARAMETERS

THE NOZZLE MASS FLOW RATE IS 19.221 (LBM/SEC)

THE START LINE THRUST IS 3881.1 LBF, AND THE START LINE ISP IS 201.916 (LBF-SEC/LBM)

THE ONE-DIMENSIONAL MASS FLOW RATE IS 19.263 (LBM/SEC), AND THE DISCHARGE COEFFICIENT IS .9974

THE ONE-DIMENSIONAL THRUST IS 3886.9 LBF, AND THE ONE-DIMENSIONAL SPECIFIC IMPULSE IS 202.318 (LBF-SEC/LBM)

THE SPECIFIC IMPULSE EFFICIENCY IS .9940

Figure F-1. Output for Sample Case 1 (Continued).



THE SUPPSONIC WALL CONTOUR IS A SECOND-ORDER POLYNOMIAL WITH THETA = 30.000 DEGREES AND YE = 5.000 IN

J	I	X	Y	M	P	Q	TH	U	V	R	T	ROT/LOC	F/LHC	THRUST	ISP	IC/EF
1	11	0.000	1.000	1.000	514.663	3616.6	-0.000	3616.6	-0.0	2.2997E-01	5371.2	19.221	3681.1			0
2	10	.012	.961	1.075	518.998	3793.7	.004	3793.7	.3	2.3158E-01	5378.7	17.744	3582.4	3665.5	201.102	0
1	12	.006	1.000	1.007	520.191	3845.2	.543	3845.0	36.9	2.2441E-01	5343.0	19.784	3582.4	3665.7	201.740	.9968
1	13	.006	1.000	1.007	520.191	3845.2	.543	3845.0	36.9	2.2441E-01	5343.0	19.784	3582.4	3665.7	201.740	.9968
1	14	.010	1.000	1.015	525.457	3602.0	1.130	3971.3	78.3	2.4508E-01	519.9	19.261	3623.4	3666.0	201.753	.9968
1	15	.015	1.000	1.023	530.395	3625.2	1.763	4047.1	124.6	2.4356E-01	520.3	18.242	3683.5	3666.1	201.156	.9968
1	16	.021	1.000	1.032	536.838	3657.3	2.447	4123.4	176.2	2.4105E-01	524.7	18.591	3734.4	3667.5	201.177	.9968
1	17	.028	1.001	1.042	539.017	3686.3	3.185	4201.2	233.8	2.4023E-01	525.7	18.713	3780.0	3667.6	201.215	.9967
3	9	.025	.914	1.067	523.758	3768.6	.010	3768.6	.7	2.3335E-01	5366.9	16.054	3240.8	3668.4	201.276	0
2	17	.035	1.001	1.036	532.883	3751.9	3.702	4281.1	298.0	1.9552E-01	524.9	17.736	3596.4	3668.7	201.286	.9967
2	18	.042	1.002	1.064	537.744	3768.1	4.843	4361.0	369.5	1.9058E-01	5173.1	18.040	3646.9	3669.1	201.304	.9966
2	19	.042	1.003	1.094	539.677	3768.1	5.772	4442.8	449.1	1.8448E-01	5150.3	18.249	3694.9	3672.2	201.451	.9964
2	20	.059	1.003	1.076	518.308	3797.3	6.775	4527.1	537.8	2.3187E-01	512.7	18.261	3740.8	3674.5	201.571	.9962
2	21	.068	1.003	1.089	510.288	3839.7	7.858	4614.3	636.8	2.2120E-01	504.3	18.598	3765.2	3677.3	201.715	.9960
4	8	.860	.857	1.058	528.895	3741.6	.019	3741.6	1.3	2.3529E-01	5365.7	17.143	2854.6	3680.5	201.484	0
3	22	.076	1.006	1.120	542.335	3934.8	9.027	4704.5	747.4	1.6407E-01	5201.4	19.261	3625.9	3680.5	201.772	.9956
3	23	.084	1.008	1.143	525.482	4670.3	10.249	4792.0	869.9	2.1766E-01	513.4	19.261	3676.7	3684.4	202.066	.9952
3	24	.101	1.010	1.174	506.916	4983.6	11.652	4880.9	1006.5	1.4948E-01	4997.7	18.345	3726.2	3686.8	202.319	.9942
3	25	.114	1.013	1.195	471.258	5040.5	13.123	4971.2	1159.0	1.4167E-01	4875.0	18.584	3774.2	3694.1	202.416	.9939
3	26	.127	1.016	1.197	467.651	4174.4	14.712	5063.0	1329.4	1.3342E-01	4819.8	19.261	3820.9	3695.8	202.647	.9929
5	7	.057	.790	1.049	534.326	3713.0	.031	3713.0	2.0	2.3726E-01	5404.9	12.014	2424.7	3696.3	201.225	0
4	27	.141	1.020	1.619	297.435	4571.3	16.427	5152.6	1519.2	1.2494E-01	4759.0	18.006	3686.5	3696.3	201.225	.9916
4	28	.157	1.023	1.271	227.484	5513.7	18.279	5234.8	1729.1	1.1647E-01	4647.6	18.261	3741.7	3696.9	201.599	.9913
4	29	.173	1.031	1.273	207.096	5663.8	20.278	5312.7	1943.0	1.0427E-01	4593.9	18.591	3793.1	3697.9	201.910	.9905
4	30	.191	1.038	1.274	405.367	4406.8	22.437	5384.5	2223.4	9.6648E-02	4534.3	18.729	3842.3	3697.9	201.455	.9893
6	6	.078	.710	1.040	539.919	3683.6	.043	3683.6	2.6	2.3933E-01	5418.3	9.494	1956.6	3698.0	201.427	0
5	31	.260	1.046	1.337	372.748	4591.3	24.767	5446.7	2415.0	1.7575E-01	5080.0	18.037	4012.6	3698.0	201.427	.9837

Figure F-1. Output for Sample Case 1 (Continued).

J	I	X	Y	M	P	Q	TH	U	V	R	T	MDT/HC	F/LRC	THRUST	ISP	IC/EFF
5	32	.229	1.056	1.946	145.657	6177.7	27.283	5490.4	2831.8	6.0439E-02	4351.3	18.329	3790.3	3948.6	205.426	2
		.229	1.056	1.946	145.657	6177.7	27.283	5490.4	2831.8	6.0439E-02	4351.3	18.329	3790.3	3948.6	205.426	.96J5
5	33	.250	1.067	2.030	126.088	4683.2	30.000	5515.1	3184.2	1.6461E-01	5249.2	19.261	3847.1	4055.4	204.511	2
		.250	1.067	2.030	126.088	4683.2	30.000	5515.1	3184.2	1.6461E-01	5249.2	19.261	3847.1	4055.4	204.511	.9761
6	34	.254	1.067	1.410	336.766	4801.9	29.933	5549.6	3195.4	1.6150E-01	5004.6	19.261	4006.1	4093.0	210.822	2
		.254	1.067	1.410	336.766	4801.9	29.933	5549.6	3195.4	1.6150E-01	5004.6	19.261	4006.1	4093.0	210.822	.9669
7	5	.094	1.031	1.485	302.404	5011.9	.094	3654.3	3.4	1.6760E-01	4955.7	19.261	1462.5	4115.1	211.436	0
		.094	1.031	1.485	302.404	5011.9	.094	3654.3	3.4	1.6760E-01	4955.7	19.261	1462.5	4115.1	211.436	.9544
7	35	.000	1.153	1.632	240.306	5408.1	29.769	5627.2	3216.7	1.2275E-01	4717.5	19.261	4059.5	4028.0	209.577	2
		.000	1.153	1.632	240.306	5408.1	29.769	5627.2	3216.7	1.2275E-01	4717.5	19.261	4059.5	4028.0	209.577	.9544
8	4	.114	.499	1.022	550.763	3626.6	.059	3526.6	3.7	2.4333E-01	5432.2	4.786	965.7	4082.6	212.197	0
		.114	.499	1.022	550.763	3626.6	.059	3526.6	3.7	2.4333E-01	5432.2	4.786	965.7	4082.6	212.197	.9430
8	36	.021	1.222	1.767	195.613	5711.1	29.503	5715.4	3344.0	1.0278E-01	4572.2	19.261	4118.9	4338.2	225.233	2
		.021	1.222	1.767	195.613	5711.1	29.503	5715.4	3344.0	1.0278E-01	4572.2	19.261	4118.9	4338.2	225.233	.9430
9	3	.132	.361	1.015	555.385	3602.4	.054	3602.4	3.4	2.4503E-01	5439.8	2.511	506.5	4182.3	215.503	0
		.132	.361	1.015	555.385	3602.4	.054	3602.4	3.4	2.4503E-01	5439.8	2.511	506.5	4182.3	215.503	.9344
9	37	.057	1.299	1.494	158.915	6087.9	29.572	5811.1	3370.6	6.8370E-02	4415.8	19.261	4183.7	4442.5	220.643	2
		.057	1.299	1.494	158.915	6087.9	29.572	5811.1	3370.6	6.8370E-02	4415.8	19.261	4183.7	4442.5	220.643	.9344
10	2	.146	.137	1.029	558.817	3584.3	.034	3584.3	2.1	2.4429E-01	5445.4	7.45	150.2	4205.6	218.404	0
		.146	.137	1.029	558.817	3584.3	.034	3584.3	2.1	2.4429E-01	5445.4	7.45	150.2	4205.6	218.404	.9282
10	36	.007	1.383	2.020	96.367	6772.6	29.138	5915.5	3397.7	5.5975E-02	4016.0	19.261	4252.4	4540.5	215.733	2
		.007	1.383	2.020	96.367	6772.6	29.138	5915.5	3397.7	5.5975E-02	4016.0	19.261	4252.4	4540.5	215.733	.9282
11	1	.151	0.000	1.007	560.226	3577.0	0.000	3577.0	0.0	2.4601E-01	5447.7	0.000	4322.7	4271.2	222.210	0
		.151	0.000	1.007	560.226	3577.0	0.000	3577.0	0.0	2.4601E-01	5447.7	0.000	4322.7	4271.2	222.210	.9242
11	39	.069	1.473	2.274	82.084	6861.2	28.585	6025.1	3324.0	4.5813E-02	3915.4	19.261	4322.7	4631.0	240.632	2
		.069	1.473	2.274	82.084	6861.2	28.585	6025.1	3324.0	4.5813E-02	3915.4	19.261	4322.7	4631.0	240.632	.9242
12	2	.178	0.000	1.019	552.901	3613.4	0.003	3613.4	0.0	2.4412E-01	5445.7	0.000	0.0	4326.7	225.100	1
		.178	0.000	1.019	552.901	3613.4	0.003	3613.4	0.0	2.4412E-01	5445.7	0.000	0.0	4326.7	225.100	.9222
12	40	.113	1.352	2.421	75.458	6974.4	28.658	6120.0	3344.8	5.4137E-02	4022.0	19.261	4382.3	4701.2	244.078	2
		.113	1.352	2.421	75.458	6974.4	28.658	6120.0	3344.8	5.4137E-02	4022.0	19.261	4382.3	4701.2	244.078	.9214
13	3	.204	0.000	1.023	544.326	3660.4	0.000	3660.4	0.0	2.4036E-01	5421.6	0.000	0.0	4372.1	227.454	1
		.204	0.000	1.023	544.326	3660.4	0.000	3660.4	0.0	2.4036E-01	5421.6	0.000	0.0	4372.1	227.454	.9214
13	41	1.217	1.619	2.361	70.115	7051.3	28.464	6198.9	3360.7	4.5672E-02	3915.4	19.261	4431.5	4754.4	247.861	2
		1.217	1.619	2.361	70.115	7051.3	28.464	6198.9	3360.7	4.5672E-02	3915.4	19.261	4431.5	4754.4	247.861	.9214
14	4	.230	0.000	1.047	535.922	3704.6	0.000	3704.6	0.0	2.3785E-01	5407.6	0.000	0.0	4412.3	229.549	1
		.230	0.000	1.047	535.922	3704.6	0.000	3704.6	0.0	2.3785E-01	5407.6	0.000	0.0	4412.3	229.549	.9211
14	42	1.351	1.581	2.497	65.659	7120.2	28.283	6270.1	3373.7	4.1354E-02	3609.4	19.261	4475.1	4830.0	246.205	2
		1.351	1.581	2.497	65.659	7120.2	28.283	6270.1	3373.7	4.1354E-02	3609.4	19.261	4475.1	4830.0	246.205	.9211
15	5	.267	0.000	1.061	527.215	3750.4	0.000	3750.4	0.0	2.3463E-01	5392.8	0.000	0.0	4450.0	231.512	1
		.267	0.000	1.061	527.215	3750.4	0.000	3750.4	0.0	2.3463E-01	5392.8	0.000	0.0	4450.0	231.512	.9212
15	43	1.443	1.741	2.492	61.565	7145.3	28.106	6338.0	3385.0	3.2215E-02	3723.1	19.261	4516.4	4840.5	251.712	2
		1.443	1.741	2.492	61.565	7145.3	28.106	6338.0	3385.0	3.2215E-02	3723.1	19.261	4516.4	4840.5	251.712	.9212
16	6	.294	0.000	1.076	516.325	3767.2	0.000	3767.2	0.0	2.3133E-01	5377.6	0.000	0.0	4486.1	233.889	1
		.294	0.000	1.076	516.325	3767.2	0.000	3767.2	0.0	2.3133E-01	5377.6	0.000	0.0	4486.1	233.889	.9216
16	44	1.574	1.800	2.458	58.686	7245.1	27.928	6404.1	3394.8	3.7656E-02	3740.3	19.261	4556.2	4877.9	253.246	2
		1.574	1.800	2.458	58.686	7245.1	27.928	6404.1	3394.8	3.7656E-02	3740.3	19.261	4556.2	4877.9	253.246	.9216
17	7	.312	0.000	1.091	509.325	3844.6	0.000	3844.6	0.0	2.2798E-01	5341.9	0.000	0.0	4520.7	236.168	1
		.312	0.000	1.091	509.325	3844.6	0.000	3844.6	0.0	2.2798E-01	5341.9	0.000	0.0	4520.7	236.168	.9222
17	45	1.646	1.859	2.499	54.370	7309.2	27.750	6468.5	3403.2	3.4472E-02	3681.3	19.261	4594.6	4919.4	255.162	2
		1.646	1.859	2.499	54.370	7309.2	27.750	6468.5	3403.2	3.4472E-02	3681.3	19.261	4594.6	4919.4	255.162	.9222
18	8	.340	0.000	1.104	500.436	3891.8	0.000	3891.8	0.0	2.2465E-01	5346.2	0.000	0.0			1
		.340	0.000	1.104	500.436	3891.8	0.000	3891.8	0.0	2.2465E-01	5346.2	0.000	0.0			.9222

Figure F-1. Output for Sample Case 1 (Continued).

J	I	X	Y	M	P	C	TH	U	V	R	T	MUT/HC	F/LHC	THRUST	TSP	IC/IFF
18	46	1.796	1.917	2.532	51.207	7367.1	27.574	6530.3	3410.2	3.3644E-02	3655.0	19.231	4631.0	4553.3	236.485	1
		1.796	1.917	2.535	46.075	7406.9				3.6242E-02	3680.5	19.261		4541.9	256.460	.9229
19	9	.366	0.000	1.120	491.058	3337.3	0.000	3937.3	0.0	2.2144E-01	5330.8	0.000	0.0	4563.7	236.447	1
19	47	1.902	1.972	2.598	45.266	7484.4	27.402	6560.9	3415.7	3.5053E-02	3650.2	19.231	4655.2	4572.6	256.165	.9237
		1.902	1.972	2.598	45.266	7484.4				3.0330E-01	3561.9	19.261				
20	10	.362	0.000	1.154	481.769	3360.4	0.000	3960.4	0.0	2.1640E-01	5316.1	0.000	0.0	4611.7	236.423	1
20	48	2.005	2.025	2.592	45.196	7472.3	27.237	6643.8	3419.8	2.8505E-02	3587.6	19.231	4696.9	4998.2	259.498	.9246
		2.005	2.025	2.592	45.196	7472.3				2.8505E-02	3587.7	19.261				
21	11	.415	0.000	1.147	476.293	3402.5	0.000	4020.3	0.0	2.1559E-01	5302.3	0.000	0.0	4637.7	241.276	1
21	49	2.104	2.076	2.620	43.447	7520.7	27.076	6696.5	3423.2	2.9321E-02	3566.3	19.231	4726.6	5021.6	260.711	.9255
		2.104	2.076	2.620	43.447	7520.7				2.6901E-02	3497.0	19.261				
22	12	.545	0.000	1.245	421.426	3417.5	0.000	4317.5	0.0	1.9469E-01	5165.0	0.000	0.0	4766.1	247.959	2
22	50	2.658	2.354	2.860	27.719	7907.5	26.171	6964.3	3422.5	2.3355E-02	3396.2	19.231	4874.3	5129.3	264.300	.9311
		2.658	2.354	2.860	27.719	7907.5				2.0155E-02	3300.3	19.261				
23	13	.656	0.000	1.332	375.125	4577.3	0.000	4577.3	0.0	1.7670E-01	5095.0	0.000	0.0	4859.9	252.838	2
23	51	3.162	2.597	3.001	21.215	8115.5	25.534	7178.3	3398.4	1.6414E-02	3162.8	19.231	4966.9	5202.0	270.077	.9362
		3.162	2.597	3.001	21.215	8115.5				1.6128E-02	3166.9	19.261				
24	14	.761	0.000	1.420	332.285	4828.2	0.000	4828.2	0.0	1.5972E-01	4922.9	0.000	0.0	4937.1	256.853	2
24	52	3.674	2.835	3.125	16.771	8286.8	24.474	7370.2	3354.7	1.6414E-02	3162.8	19.231	5084.1	5259.1	272.688	.9403
		3.674	2.835	3.125	16.771	8286.8				1.3259E-02	3045.6	19.261				
25	15	.867	0.000	1.505	293.505	5046.6	0.000	5046.6	0.0	1.4408E-01	4800.7	0.000	0.0	5002.5	260.255	2
25	53	4.208	3.073	3.238	13.530	8434.7	23.562	7547.5	3291.5	1.4067E-02	3066.2	19.231	5171.4	5502.5	275.293	.9434
		4.208	3.073	3.238	13.530	8434.7				1.1087E-02	2998.9	19.261				
26	16	.976	0.000	1.593	247.266	5304.4	0.000	5304.4	0.0	1.2906E-01	4703.9	0.000	0.0	5059.7	263.233	2
26	54	4.789	3.320	3.346	11.025	8368.5	22.557	7718.4	3206.0	1.2147E-02	2977.0	19.231	5253.2	5338.2	277.150	.9478
		4.789	3.320	3.346	11.025	8368.5				9.2476E-03	2840.6	19.261				
27	17	1.061	0.000	1.686	223.023	5544.4	0.000	5544.4	0.0	1.1459E-01	4621.1	0.000	0.0	5109.9	265.844	2
27	55	5.433	3.560	3.271	12.734	8471.0	21.424	7855.6	3044.2	1.0559E-02	2804.3	19.231	5331.2	5366.3	278.407	.9512
		5.433	3.560	3.271	12.734	8471.0				7.9245E-03	2748.8	19.261				
28	18	1.214	0.000	1.782	191.257	5785.7	0.000	5785.7	0.0	1.0043E-01	4542.6	0.000	0.0	5153.1	268.080	2
28	56	6.149	3.852	3.352	10.870	8573.2	20.145	8048.8	2952.6	9.2552E-03	2618.7	19.231	5405.6	5386.7	279.465	.9556
		6.149	3.852	3.352	10.870	8573.2				6.7479E-03	2642.7	19.261				
29	19	1.350	0.000	1.884	161.715	6011.4	0.000	6011.4	0.0	8.7680E-02	4426.5	0.000	0.0	5189.7	269.994	2
29	57	6.950	4.137	3.433	9.377	8645.3	18.573	8209.2	2774.3	8.1836E-03	2750.0	19.231	5477.5	5390.6	280.134	.9611
		6.950	4.137	3.433	9.377	8645.3				5.7880E-03	2571.9	19.261				
30	20	1.501	0.000	1.993	134.388	6284.0	0.000	6284.0	0.0	7.5158E-02	4281.4	0.000	0.0	5220.0	271.574	2
30	58	7.883	4.434	3.504	8.196	8746.4	16.960	8366.0	2551.3	7.3153E-03	2688.8	19.231	5547.1	5404.9	280.410	.9678
		7.883	4.434	3.504	8.196	8746.4				4.9833E-03	2486.0	19.261				
31	21	1.672	0.000	2.112	109.417	6544.5	0.000	6544.5	0.0	6.3339E-02	4146.0	0.000	0.0	5244.0	272.822	2
31	59	8.945	4.738	3.567	7.287	8815.1	14.953	8516.6	2374.6	6.6334E-03	2646.5	19.231	5613.8	5402.7	280.499	.9726
		8.945	4.738	3.567	7.287	8815.1				4.3220E-03	2425.9	19.261				
32	22	1.871	0.000	2.242	86.929	6814.2	0.000	6814.2	0.0	5.2304E-02	3988.7	0.000	0.0	5260.1	273.659	2
32	60	10.000	5.000	3.609	6.727	8860.9	12.888	8636.5	1981.4	6.2058E-03	2601.6	19.231	5669.2	5395.3	280.114	.9770
		10.000	5.000	3.609	6.727	8860.9				3.6514E-03	2370.4	19.261				

0 CHARACTERISTICS CROSSED IN THE NOZZLE.

Figure F-1. Output for Sample Case 1 (Concluded).

## 2. Sample Case 2

Sample case 2 illustrates a boattail flow field analysis. Thus, the title cards contains 13 in the first two columns. A uniform flow initial-value line is specified by default (IVLB = 0). The wall geometry is specified with outer radius YTB = 8.0 in., initial expansion contour radius RDB = 5.0 in., attachment angle THETTB = 2.0 deg, exit radius YEB = 7.0 in., and length XEB = 10.0 in. The boattail wall is the second-order polynomial (IWALLB = 2). All of these parameters are the default values given in the program. For this sample case, KWRITB = 2 for abbreviated output. This option dictates that only wall points are printed out. The thrust values printed in the last column are obtained by integrating the pressure forces acting on the boattail contour. The following list presents the data deck for sample case 2.

```
13  SAMPLE CASE 2      BOATTAIL ANALYSIS
    $INFO KWRITB=2 $
```

Figure F-2 presents the output for sample case 2. The first page presents the program abstract and the job title. The second page presents boattail flow field analysis data and the initial-value line. The boattail geometric specification is given at the top of the third page. The third and fourth pages present the boattail flow field solution.

Sample case 2 required 4 seconds of central processor time on the CDC 6500 computer.

# ANALYSIS AND DESIGN OF SUPERSONIC NOZZLE-BASE-ROCKET COMBINATIONS

## ABSTRACT

THIS PROGRAM WAS PRODUCED AT THE PIQUETTE UNIVERSITY THERMAL SCIENCE AND PROPULSION CENTER BY J. G. ALLMAN AS A PART OF THE REQUIREMENTS OF AF CONTRACT NUMBER F33615-73-C-2010. THE CONTRACT WAS SPONSORED BY THE ARMY PROPULSION LABORATORY, WRIGHT PATTERSON AFB, OHIO. PRINCIPAL INVESTIGATION FOR PIQUETTE UNIVERSITY WAS PROFESSOR JOE V. HODPMAN.

THE EQUATIONS OF MOTION FOR AN AXISYMMETRIC SUPERSONIC FLOW ARE SOLVED USING A FINITE DIFFERENCE METHOD OF CHARACTERISTICS HAVING SECOND-ORDER ACCURACY. THE INITIAL FLOW VARIABLES FOR THE NOZZLE FLOW FIELD CAN BE SPECIFIED OR COMPUTED FROM KLIPFELS TRANSONIC FLOW ANALYSIS. THE INITIAL FLOW VARIABLES FOR THE ROCKET FLOW FIELD CAN BE SPECIFIED OR COMPUTED FROM A UNIFORM FLOW ANALYSIS. THE NOZZLE AND ROCKET GEOMETRIES CAN BE SPECIFIED AS CONICAL, SECOND-ORDER POLYNOMIAL OR TABULAR COORDINATE. THE ANALYSIS WAS BASED ON THE GOVERNING GAS DYNAMIC RELATIONS FOR A ROTATIONAL FLOW OF A FROZEN OR EQUILIBRIUM GAS MIXTURE.

## JOB TITLE:

SAMPLE CASE 2 ROCKET ANALYSIS

Figure F-2. Output for Sample Case 2.



BOATTAIL FLOW FIELD ANALYSIS

MP = 30  
IC = 2  
IUL = 0  
IMALL = 2  
DELTA = 1.00  
MORITE = 2

TO = 600.00 H  
PO = 12.00 PSIA  
PAMB = 0.00 PSIA

XE = 10.00 IN  
YT = 8.00 IN  
MO = 5.00 IN

G = 1.40  
NGAS = 53.50 (FT-LBF)/(LBM-H)  
TOL = .00100  
SPACE = .5

INITIAL-VALUE LINE  
THE INITIAL-VALUE LINE IS A UNIFORM FLOW WITH A MACH NUMBER OF 1.40

I	X	Y	M	P	U	TH	U	V	N	T
1	0.000	8.000	1.400	3.77	1424.2	0.000	1424.2	0.0	2.3636E-02	431.0
2	.167	8.170	1.400	3.77	1424.2	0.000	1424.2	0.0	2.3636E-02	431.0
3	.333	8.340	1.400	3.77	1424.2	0.000	1424.2	0.0	2.3636E-02	431.0
4	.500	8.510	1.400	3.77	1424.2	0.000	1424.2	0.0	2.3636E-02	431.0
5	.667	8.680	1.400	3.77	1424.2	0.000	1424.2	0.0	2.3636E-02	431.0
6	.833	8.851	1.400	3.77	1424.2	0.000	1424.2	0.0	2.3636E-02	431.0
7	1.000	9.021	1.400	3.77	1424.2	0.000	1424.2	0.0	2.3636E-02	431.0
8	1.167	9.191	1.400	3.77	1424.2	0.000	1424.2	0.0	2.3636E-02	431.0
9	1.333	9.361	1.400	3.77	1424.2	0.000	1424.2	0.0	2.3636E-02	431.0
10	1.500	9.531	1.400	3.77	1424.2	0.000	1424.2	0.0	2.3636E-02	431.0
11	1.667	9.701	1.400	3.77	1424.2	0.000	1424.2	0.0	2.3636E-02	431.0
12	1.833	9.871	1.400	3.77	1424.2	0.000	1424.2	0.0	2.3636E-02	431.0
13	2.000	10.041	1.400	3.77	1424.2	0.000	1424.2	0.0	2.3636E-02	431.0
14	2.167	10.211	1.400	3.77	1424.2	0.000	1424.2	0.0	2.3636E-02	431.0
15	2.333	10.381	1.400	3.77	1424.2	0.000	1424.2	0.0	2.3636E-02	431.0
16	2.500	10.552	1.400	3.77	1424.2	0.000	1424.2	0.0	2.3636E-02	431.0
17	2.667	10.722	1.400	3.77	1424.2	0.000	1424.2	0.0	2.3636E-02	431.0
18	2.833	10.892	1.400	3.77	1424.2	0.000	1424.2	0.0	2.3636E-02	431.0
19	3.000	11.062	1.400	3.77	1424.2	0.000	1424.2	0.0	2.3636E-02	431.0
20	3.167	11.232	1.400	3.77	1424.2	0.000	1424.2	0.0	2.3636E-02	431.0
21	3.333	11.402	1.400	3.77	1424.2	0.000	1424.2	0.0	2.3636E-02	431.0
22	3.500	11.572	1.400	3.77	1424.2	0.000	1424.2	0.0	2.3636E-02	431.0
23	3.667	11.742	1.400	3.77	1424.2	0.000	1424.2	0.0	2.3636E-02	431.0
24	3.833	11.912	1.400	3.77	1424.2	0.000	1424.2	0.0	2.3636E-02	431.0
25	4.000	12.082	1.400	3.77	1424.2	0.000	1424.2	0.0	2.3636E-02	431.0
26	4.167	12.253	1.400	3.77	1424.2	0.000	1424.2	0.0	2.3636E-02	431.0
27	4.333	12.423	1.400	3.77	1424.2	0.000	1424.2	0.0	2.3636E-02	431.0
28	4.500	12.593	1.400	3.77	1424.2	0.000	1424.2	0.0	2.3636E-02	431.0
29	4.667	12.763	1.400	3.77	1424.2	0.000	1424.2	0.0	2.3636E-02	431.0
30	4.833	12.933	1.400	3.77	1424.2	0.000	1424.2	0.0	2.3636E-02	431.0

BOATTAIL GEOMETRY

THE BOATTAIL LENGTH IS XE = 10.0000 IN.

THE THROAT WALL CONTOUR IS A CIRCULAR ARC WITH YT = 8.000 IN, THETAT = 2.000 DEGREES, RU = 5.000 IN.

Figure F-2. Output for Sample Case 2 (Continued).

THE SUPERSONIC WALL CONTOUR IS A SECOND-ORDER POLYNOMIAL WITH THETA = 2.000 DEGREES AND YL = 7.000 IN.

I	J	X	Y	M	P	Q	TH	U	V	R	T	IC/THRSIV
2	2	2.345	7.991	1.473	3.401	1474.0	-2.1318	1475.0	-54.9	2.1957E-02	416.5	1.7
3	3	2.696	7.977	1.480	3.354	1461.3	-2.4039	1460.0	-62.1	2.1785E-02	417.2	4.0
4	4	1.049	7.961	1.488	3.327	1484.6	-2.6772	1485.0	-69.4	2.1616E-02	415.9	6.6
5	5	1.403	7.944	1.495	3.292	1491.7	-2.9516	1491.8	-76.8	2.1450E-02	414.6	9.5
6	6	1.759	7.925	1.503	3.257	1496.4	-3.2273	1494.4	-84.3	2.1288E-02	413.3	12.7
7	7	2.117	7.904	1.510	3.223	1501.7	-3.5040	1498.9	-91.8	2.1130E-02	412.1	16.0
8	8	2.476	7.881	1.517	3.190	1506.6	-3.7818	1503.3	-99.4	2.0978E-02	410.9	19.7
9	9	2.837	7.856	1.524	3.158	1511.3	-4.0607	1507.5	-107.0	2.0823E-02	409.7	23.6
10	10	3.200	7.829	1.531	3.126	1515.9	-4.3406	1511.6	-114.7	2.0675E-02	408.5	27.7
11	11	3.564	7.801	1.537	3.096	1520.5	-4.6215	1515.5	-122.5	2.0530E-02	407.4	32.1
12	12	3.930	7.770	1.544	3.066	1524.9	-4.9034	1519.3	-130.3	2.0388E-02	406.3	36.6
13	13	4.297	7.738	1.551	3.037	1529.3	-5.1862	1523.0	-138.2	2.0249E-02	405.2	41.5
14	14	4.666	7.703	1.557	3.008	1533.5	-5.4699	1526.5	-146.2	2.0114E-02	404.1	46.5
15	15	5.036	7.667	1.563	2.981	1537.7	-5.7545	1529.9	-154.2	1.9982E-02	403.0	51.8
16	16	5.408	7.629	1.569	2.954	1541.7	-6.0400	1533.2	-162.2	1.9853E-02	402.0	57.2
17	17	5.781	7.588	1.575	2.928	1545.7	-6.3262	1536.3	-170.3	1.9727E-02	400.9	62.9
18	18	6.156	7.546	1.581	2.902	1549.6	-6.6133	1539.3	-178.5	1.9605E-02	400.0	68.8
19	19	6.532	7.501	1.587	2.878	1553.4	-6.9011	1542.1	-186.6	1.9485E-02	399.0	74.9
20	20	6.909	7.455	1.593	2.854	1557.0	-7.1897	1544.8	-194.9	1.9369E-02	398.0	81.2
21	21	7.288	7.406	1.598	2.830	1560.6	-7.4790	1547.3	-203.1	1.9257E-02	397.1	87.7
22	22	7.669	7.355	1.604	2.808	1564.1	-7.7689	1549.7	-211.4	1.9148E-02	396.2	94.3
23	23	8.050	7.302	1.609	2.786	1567.4	-8.0595	1551.9	-219.8	1.9042E-02	395.3	101.1
24	24	8.433	7.247	1.614	2.765	1570.7	-8.3508	1554.0	-228.1	1.8939E-02	394.5	108.1
25	25	8.818	7.189	1.619	2.745	1573.8	-8.6426	1556.0	-236.5	1.8840E-02	393.6	115.3
26	26	9.203	7.130	1.624	2.726	1576.9	-8.9350	1557.7	-244.9	1.8745E-02	392.8	122.7
27	27	9.590	7.068	1.628	2.707	1579.8	-9.2279	1559.4	-253.3	1.8653E-02	392.1	130.2
28	28	9.979	7.004	1.633	2.689	1582.6	-9.5212	1560.8	-261.8	1.8565E-02	391.3	137.8

Figure F-2. Output for Sample Case 2 (Continued).

I	J	X	Y	M	P	W	TH	U	V	R	T	IC/THSTV
29	29	10.000	7.000	1.633	2.687	15d2.9	-9.5373	1561.0	-262.3	1.6556E-02	391.3	13E+2

Figure F-2. Output for Sample Case 2 (Concluded).

### 3. Sample Case 3

Sample case 3 illustrates a complete nozzle-base-boattail flow field analysis for the combined nozzle and boattail contours specified in sample cases 1 and 2. Consequently, 11 is placed in the first two columns of the title card. The total thrust on the assembly is the sum of the thrusts acting on the nozzle, the boattail, and the base region. For this sample case, KWRITN = 2 and KWRITB = 2. This print option dictates that wall points only will be written out. The following list presents the data deck for sample case 3.

```
11  SAMPLE CASE 3    NOZZLE-BASE-BOATTAIL ANALYSIS
    $INFO KWRITN=2, KWRITB=2, YEB=5.2 $
```

Figure F-3 presents the output for sample case 3. The first page of the output lists the program abstract and the job title for the run. The second page presents the nozzle flow field analysis data and initial-value line. The third page presents the nozzle wall geometric specification, and the third and fourth pages present the nozzle flow field solution. At the end of the flow field data, -2 appears in the last column denoting the nozzle exit lip point. The number of internally crossing characteristics is zero.

The three pages following the nozzle flow field results present the boattail flow field results. The first page lists input variables, initial-value line data, and geometric parameters. The next page presents the boattail flow field solution. For this sample case, KWRITB = 2, thus, only wall point solutions are printed out. Each right-running characteristic begins on the initial-value line and extends to the boattail wall, where the thrust is computed. This procedure continues until a right-running characteristic passes the exit lip point. Then the inverse wall point routine computes the boattail exit lip point properties.

The base pressure and the contribution to the thrust from that pressure are then calculated. The exit lip point properties of the nozzle and the boattail, as well as the base region properties, are printed out on the last page. The total thrust, which is written out on the last line, is the sum of the nozzle, boattail, and base thrusts.

Sample case 3 required 13 seconds of central processor time on the CDC 6500 computer.

# ANALYSIS AND DESIGN OF SUPERSONIC NOZZLE-BASE-BOATTAIL COMBINATIONS

## ABSTRACT

THIS PROGRAM WAS CONDUCTED AT THE PURDUE UNIVERSITY THERMAL SCIENCE AND PROPULSION CENTER BY J. D. ALLAN AS PART OF THE REQUIREMENTS OF THE CONTRACT NUMBER 331-71-2-2010. THE CONTRACT WAS SPONSORED BY THE ARMY RESEARCH AND DEVELOPMENT PATTERSON AFB, OHIO. PRINCIPAL INVESTIGATOR FOR PURDUE UNIVERSITY WAS PROFESSOR JOE C. NORMAN.

THE EQUATIONS OF MOTION FOR AN AXISYMMETRIC SUPERSONIC FLOW ARE SOLVED USING A NUMERICAL METHOD OF CHARACTERISTICS HAVING SECOND-ORDER ACCURACY. THE INITIAL FLOW VARIABLES FOR THE NOZZLE FLOW FIELD CAN BE SPECIFIED OR COMPUTED FROM NOZZLE FLOW ANALYSIS. THE INITIAL FLOW VARIABLES FOR THE BOATTAIL FLOW FIELD CAN BE SPECIFIED OR COMPUTED FROM NOZZLE FLOW ANALYSIS. THE NOZZLE AND BOATTAIL GEOMETRIES CAN BE SPECIFIED IN SECTIONS USING POLYNOMIAL OR TABULAR CONTOURS. THE ANALYSIS WAS BASED ON THE GOVERNING GAS DYNAMIC RELATIONS FOR A STATIONARY FLOW OF A PERFECT GASEOUS MIXTURE.

## JCR TITLE

SAMPLE CASE NUMBER 3

NOZZLE-BASE-BOATTAIL ANALYSIS

Figure F-3. Output for Sample Case 3.



# NOZZLE FLOW FIELD ANALYSIS

MP = 11  
IC = 2  
IVL = 0  
ISALL = 2  
DPW = 22  
MWRITE = 2

TO = 4000.00 H  
PO = 1000.00 PSIA  
PAMB = 0.00 PSIA

ME = 10.000 IN  
VE = 3.000 IN  
MO = 3.000 IN  
RATIO = 2.00  
RATIO = 2.00  
TOL = .0010

G = 1.20  
GAS = 3  
RATIO = 2.00  
RATIO = 2.00  
TOL = .0010

## INITIAL-VALUE LINE

THE INITIAL-VALUE LINE IS A KILLER V=0 LINE

I	X	Y	Z	P	Q	TH	U	V	R	T	ALOT	THRUST	ISP
1	0.000	1.000	1.000	514.66	3616.6	-0.00	3616.6	-0.0	2.297E-01	5371.2	19.221	3696.821	202.733
2	.012	.961	1.075	519.00	3743.7	.004	3743.7	.3	2.3158E-01	5376.7	17.744	3596.924	202.708
3	.025	.914	1.067	523.76	3748.6	.010	3748.6	.7	2.3335E-01	5386.9	16.054	3253.909	202.684
4	.040	.857	1.058	528.90	3743.6	.019	3743.6	1.3	2.3525E-01	5395.7	14.143	2666.128	202.660
5	.057	.790	1.049	534.33	3713.0	.031	3713.0	2.0	2.3726E-01	5404.9	12.014	2434.523	202.637
6	.075	.710	1.040	539.92	3683.6	.043	3683.6	2.8	2.3933E-01	5414.3	9.496	1964.468	202.608
7	.094	.614	1.031	545.49	3644.3	.059	3644.3	3.4	2.4139E-01	5423.5	7.248	1468.370	202.584
8	.114	.499	1.022	550.76	3626.6	.084	3626.6	3.7	2.4333E-01	5432.2	4.766	969.851	202.564
9	.132	.361	1.015	555.39	3602.4	.084	3602.4	3.4	2.4503E-01	5439.8	2.511	508.367	202.541
10	.146	.197	1.009	558.62	3584.3	.034	3584.3	2.1	2.4629E-01	5445.4	.745	150.640	202.541
11	.161	.000	1.007	560.23	3577.0	0.000	3577.0	0.0	2.4681E-01	5447.7	0.000	0.000	0.000

## INITIAL-VALUE LINE PERFORMANCE PARAMETERS

THE NOZZLE MASS FLOW RATE IS 19.221 (LBM/SEC)  
THE START LINE THRUST IS 3696.8 LBF, AND THE START LINE ISP IS 202.733 (LBF-SEC/LBM)  
THE ONE-DIMENSIONAL MASS FLOW RATE IS 19.261 (LBM/SEC), AND THE DISCHARGE COEFFICIENT IS .9976  
THE ONE-DIMENSIONAL THRUST IS 3697.0 LBF, AND THE ONE-DIMENSIONAL SPECIFIC IMPULSE IS 202.323 (LBF-SEC/LBM)  
THE SPECIFIC IMPULSE EFFICIENCY IS 1.0020

Figure F-3. Output for Sample Case 3 (Continued).

THE SUPERSONIC WALL CONTOUR IS A SECOND-ORDER POLYNOMIAL WITH THEIAT = 30.000 DEGREES AND YE = 5.000 IN

J	I	X	Y	M	P	Q	TH	U	V	H	T	MDI/LRC	F/LRC	THRUST	ISP	IC/EF
1	12	.005	1.000	1.107	499.791	3695.2	.543	3895.0	36.9	2.2441E-01	5345.0	17.746	3596.9	3696.9	202.737	2
1	13	.010	1.000	1.132	485.317	3972.1	1.130	3971.3	78.3	2.1699E-01	5318.9	17.946	3697.1	3697.1	202.749	2
1	14	.015	1.000	1.156	470.917	4049.0	1.763	4047.1	124.6	2.1356E-01	5292.3	18.242	3696.0	3697.5	202.770	2
1	15	.021	1.000	1.182	456.380	4127.2	2.447	4123.4	176.2	2.0805E-01	5264.7	18.491	3748.9	3698.2	202.704	2
1	16	.026	1.001	1.208	441.520	4207.7	3.185	4201.2	233.6	2.0259E-01	5235.7	18.713	3794.5	3699.1	202.650	2
2	17	.035	1.001	1.236	426.189	4291.5	3.982	4281.1	298.0	1.9452E-01	5204.9	17.746	3609.5	3900.3	202.512	2
2	18	.042	1.002	1.264	410.783	4376.6	4.843	4361.0	369.5	1.8908E-01	5173.1	18.040	3660.0	3901.6	202.591	2
2	19	.050	1.003	1.294	394.877	4465.5	5.772	4442.8	449.1	1.8441E-01	5139.2	18.269	3708.0	3903.7	203.090	2
2	20	.059	1.003	1.326	378.368	4558.9	6.775	4527.1	537.6	1.7797E-01	5102.7	18.488	3753.9	3906.0	203.211	2
2	21	.066	1.005	1.360	361.185	4656.0	7.856	4613.3	636.8	1.7120E-01	5063.3	18.698	3798.3	3908.4	203.457	2
3	22	.076	1.006	1.397	343.203	4763.5	9.027	4704.5	747.4	1.6407E-01	5020.4	17.862	3637.5	3912.2	203.531	2
3	23	.089	1.008	1.434	325.382	4870.3	10.289	4792.0	869.9	1.5694E-01	4975.9	18.118	3689.2	3916.1	203.734	2
3	24	.101	1.010	1.475	306.916	4983.6	11.652	4880.9	1006.5	1.4948E-01	4927.7	18.345	3765.7	3920.6	203.980	2
3	25	.114	1.013	1.519	287.758	5104.5	13.123	4971.2	1159.0	1.4167E-01	4875.0	18.584	3820.6	3925.7	204.261	2
3	26	.127	1.016	1.567	267.788	5234.6	14.712	5063.0	1329.4	1.3392E-01	4816.9	18.774	3882.5	3931.7	204.548	2
4	27	.141	1.020	1.619	247.492	5371.9	16.427	5152.6	1513.2	1.2694E-01	4754.0	18.938	3938.3	3938.3	204.893	2
4	28	.157	1.025	1.673	227.484	5513.0	18.278	5238.4	1713.1	1.1947E-01	4687.6	19.293	3751.5	3945.7	205.275	2
4	29	.173	1.031	1.732	207.056	5663.8	20.276	5318.7	1933.0	1.1177E-01	4614.7	19.517	3803.0	3953.8	205.696	2
4	30	.191	1.038	1.797	186.404	5825.5	22.437	5388.5	2223.4	9.8663E-02	4534.3	18.729	3652.1	3962.5	206.152	2
5	31	.209	1.046	1.869	165.841	5998.5	24.767	5465.7	2513.0	8.9420E-02	4445.6	18.097	3743.2	3971.9	206.641	2
5	32	.229	1.056	1.946	143.637	6177.1	27.263	5590.4	2831.8	8.0339E-02	4351.3	18.329	3798.2	3981.8	207.156	2
5	33	.250	1.067	2.030	126.088	6368.3	30.000	5815.1	3194.2	7.1244E-02	4247.5	18.546	3850.0	3992.1	207.691	2
6	34	.274	1.092	2.046	122.846	6403.8	29.933	5849.6	3195.4	6.9619E-02	4226.0	19.225	4014.0	4013.5	208.462	1
7	35	.400	1.153	2.082	115.203	6482.7	29.769	5827.2	3216.7	6.6081E-02	4184.1	19.226	4065.4	4064.6	211.461	2
8	36	.521	1.222	2.123	107.223	6571.0	29.583	5714.4	3244.0	6.2244E-02	4134.3	19.227	4122.8	4121.8	214.435	2
9	37	.657	1.299	2.169	98.854	6668.3	29.372	5611.1	3270.6	5.8169E-02	4078.6	19.228	4185.6	4184.5	217.700	2
10	38	.807	1.383	2.220	90.367	6772.6	29.138	5515.5	3297.7	5.3977E-02	4018.0	19.228	4253.0	4251.5	221.186	2
11	39	.969	1.473	2.274	82.064	6881.2	28.885	6025.1	3324.0	4.9813E-02	3953.9	19.228	4321.0	4321.0	224.800	2
12	40	1.113	1.552	2.321	75.358	6974.4	28.658	6120.0	3344.4	4.6397E-02	3898.0	19.229	4382.3	4380.3	227.886	2
13	41	1.237	1.619	2.361	70.115	7051.3	28.464	6198.9	3360.7	4.3692E-02	3851.4	19.229	4431.3	4429.0	230.418	2
14	42	1.351	1.681	2.397	65.639	7120.2	28.283	6270.1	3373.7	4.1354E-02	3809.4	19.229	4475.1	4472.4	232.675	1
15	43	1.463	1.741	2.432	61.885	7185.3	28.106	6338.0	3385.0	3.9215E-02	3769.1	19.230	4516.4	4513.3	234.806	1
16	44	1.574	1.800	2.466	57.641	7248.2	27.928	6404.1	3394.8	3.7217E-02	3729.9	19.230	4556.2	4552.7	236.855	1
17	45	1.685	1.859	2.499	54.370	7309.2	27.750	6468.5	3403.2	3.5346E-02	3691.7	19.230	4594.6	4590.7	238.830	1
18	46	1.795	1.917	2.532	51.207	7367.1	27.574	6530.3	3410.2	3.3624E-02	3655.0	19.231	4631.0	4626.7	240.704	1
19	47	1.902	1.972	2.563	48.348	7421.6	27.402	6588.9	3415.7	3.2033E-02	3620.2	19.231	4665.2	4660.5	242.463	1

Figure F-3. Output for Sample Case 3 (Continued).

AD-A041 530

PURDUE UNIV LAFAYETTE IND THERMAL SCIENCES AND PROPU--ETC F/G 9/2  
PROPULSION NOZZLE STUDIES. VOLUME II. DESIGN OF MAXIMUM THRUST --ETC(U)  
MAR 77 J G ALLMAN, J D HOFFMAN F33615-73-C-2010

UNCLASSIFIED

AFAPL-TR-77-1-VOL-2

NL

2 OF 2

AD  
A041 530



END

DATE  
FILMED  
8-77

J	I	X	Y	M	P	Q	TH	U	V	R	T	MDT/LKC	F/LKC	THRUST	ISP	IC/IFF
20	48	2.005	2.025	2.592	45.796	7472.3	27.237	6643.8	3419.8	3.0636E-02	3587.4	19.231	4896.9	4691.8	244.091	1
21	49	2.104	2.076	2.620	43.447	7520.7	27.076	6696.5	3423.2	2.9321E-02	3546.3	19.231	4726.8	4721.1	245.616	1
22	50	2.458	2.354	2.767	33.084	7749.8	26.171	6964.3	3422.5	2.3365E-02	3396.2	19.232	4874.3	4868.9	253.304	2
23	51	3.162	2.597	2.885	26.457	7942.1	25.334	7178.3	3398.4	1.9409E-02	3271.5	19.232	4986.9	4981.6	259.168	2
24	52	3.674	2.835	2.992	21.631	8097.8	24.474	7370.2	3354.7	1.6414E-02	3162.8	19.231	5064.1	5079.0	264.236	2
25	53	4.206	3.073	3.070	17.972	8244.0	23.562	7547.5	3291.5	1.4067E-02	3066.2	19.230	5171.4	5166.5	268.788	2
26	54	4.789	3.320	3.183	15.067	8357.6	22.557	7718.4	3206.0	1.2147E-02	2977.0	19.228	5253.2	5248.6	273.058	2
27	55	5.433	3.580	3.271	12.734	8471.0	21.424	7885.6	3094.2	1.0559E-02	2894.3	19.226	5331.2	5326.9	277.135	2
28	56	6.149	3.852	3.355	10.870	8573.2	20.145	8048.8	2952.6	9.2552E-03	2818.7	19.224	5405.8	5401.8	281.031	2
29	57	6.959	4.137	3.433	9.377	8665.3	18.873	8209.2	2774.3	8.1836E-03	2750.0	19.220	5477.5	5474.3	284.803	2
30	58	7.883	4.434	3.505	8.196	8746.4	16.960	8366.0	2551.3	7.3153E-03	2688.8	19.216	5547.1	5544.6	288.461	2
31	59	8.945	4.738	3.567	7.287	8815.1	14.953	8516.6	2274.6	6.6334E-03	2636.5	19.211	5613.8	5612.4	291.885	2
32	60	10.000	5.000	3.609	6.727	8860.9	12.921	8636.5	1981.4	6.2058E-03	2601.6	19.206	5669.2	5668.5	294.806	-2

0 CHARACTERISTICS CROSSFED IN THE NOZZLE.

Figure F-3. Output for Sample Case 3 (Continued).

# HOATTAIL FLOW FIELD ANALYSIS

NP = 30  
 IC = 2  
 IVL = 0  
 IVAL = 2  
 DELTA = 1.00  
 MARITE = 2

TO = 600.00 M  
 PO = 12.00 PSIA  
 PAMB = 0.00 PSIA

XE = 10.00 IN  
 YT = 8.00 IN  
 HO = 5.00 IN

S = 1.40  
 K = 5.30 (FT-LBF)/(LBM-F)  
 LGAS = 1  
 TOL = .00100  
 SPACE = .5

## INITIAL-VALUE LINE

THE INITIAL-VALUE LINE IS A UNIFORM FLOW WITH A MACH NUMBER OF 1.40

I	X	Y	M	P	Q	TH	U	V	H	T
1	0.000	8.000	1.400	3.77	1424.2	0.000	1424.2	0.0	2.3636E-02	431.0
2	1.167	8.170	1.400	3.77	1424.2	0.000	1424.2	0.0	2.3636E-02	431.0
3	2.333	8.340	1.400	3.77	1424.2	0.000	1424.2	0.0	2.3636E-02	431.0
4	3.500	8.510	1.400	3.77	1424.2	0.000	1424.2	0.0	2.3636E-02	431.0
5	4.667	8.680	1.400	3.77	1424.2	0.000	1424.2	0.0	2.3636E-02	431.0
6	5.833	8.851	1.400	3.77	1424.2	0.000	1424.2	0.0	2.3636E-02	431.0
7	7.000	9.021	1.400	3.77	1424.2	0.000	1424.2	0.0	2.3636E-02	431.0
8	8.167	9.191	1.400	3.77	1424.2	0.000	1424.2	0.0	2.3636E-02	431.0
9	9.333	9.361	1.400	3.77	1424.2	0.000	1424.2	0.0	2.3636E-02	431.0
10	10.500	9.531	1.400	3.77	1424.2	0.000	1424.2	0.0	2.3636E-02	431.0
11	11.667	9.701	1.400	3.77	1424.2	0.000	1424.2	0.0	2.3636E-02	431.0
12	12.833	9.871	1.400	3.77	1424.2	0.000	1424.2	0.0	2.3636E-02	431.0
13	14.000	10.041	1.400	3.77	1424.2	0.000	1424.2	0.0	2.3636E-02	431.0
14	15.167	10.211	1.400	3.77	1424.2	0.000	1424.2	0.0	2.3636E-02	431.0
15	16.333	10.381	1.400	3.77	1424.2	0.000	1424.2	0.0	2.3636E-02	431.0
16	17.500	10.552	1.400	3.77	1424.2	0.000	1424.2	0.0	2.3636E-02	431.0
17	18.667	10.722	1.400	3.77	1424.2	0.000	1424.2	0.0	2.3636E-02	431.0
18	19.833	10.892	1.400	3.77	1424.2	0.000	1424.2	0.0	2.3636E-02	431.0
19	21.000	11.062	1.400	3.77	1424.2	0.000	1424.2	0.0	2.3636E-02	431.0
20	22.167	11.232	1.400	3.77	1424.2	0.000	1424.2	0.0	2.3636E-02	431.0
21	23.333	11.402	1.400	3.77	1424.2	0.000	1424.2	0.0	2.3636E-02	431.0
22	24.500	11.572	1.400	3.77	1424.2	0.000	1424.2	0.0	2.3636E-02	431.0
23	25.667	11.742	1.400	3.77	1424.2	0.000	1424.2	0.0	2.3636E-02	431.0
24	26.833	11.912	1.400	3.77	1424.2	0.000	1424.2	0.0	2.3636E-02	431.0
25	28.000	12.082	1.400	3.77	1424.2	0.000	1424.2	0.0	2.3636E-02	431.0
26	29.167	12.253	1.400	3.77	1424.2	0.000	1424.2	0.0	2.3636E-02	431.0
27	30.333	12.423	1.400	3.77	1424.2	0.000	1424.2	0.0	2.3636E-02	431.0
28	31.500	12.593	1.400	3.77	1424.2	0.000	1424.2	0.0	2.3636E-02	431.0
29	32.667	12.763	1.400	3.77	1424.2	0.000	1424.2	0.0	2.3636E-02	431.0
30	33.833	12.933	1.400	3.77	1424.2	0.000	1424.2	0.0	2.3636E-02	431.0

## HOATTAIL GEOMETRY

THE HOATTAIL LENGTH IS XE = 10.000 IN.

THE THROAT WALL CONTOUR IS A CIRCULAR ARC WITH YT = 8.000 IN., THETAT = 2.000 DEGREES, RU = 5.000 IN.

Figure F-3. Output for Sample Case 3 (Continued).



THE SUPERSONIC WALL CONTOUR IS A SECOND-ORDER POLYNOMIAL WITH THETAT = 2.000 DEGREES AND YE = 5.200 IN.

I	J	X	Y	M	P	Q	TH	U	V	R	T	IC/THRSIV
2	2	3.345	7.990	1.485	3.341	1484.6	-2.4970	1483.2	-64.7	2.1681E-02	416.4	1.7
3	3	7.02	7.971	1.518	3.185	1507.3	-3.5332	1504.4	-52.9	2.0952E-02	410.7	4.6
4	4	1.066	7.946	1.551	3.036	1529.4	-4.5886	1524.5	-122.4	2.0244E-02	405.1	8.6
5	5	1.438	7.912	1.584	2.893	1551.0	-5.6619	1543.5	-153.0	1.9559E-02	399.6	13.8
6	6	1.816	7.871	1.616	2.756	1572.1	-6.7518	1561.2	-184.8	1.8495E-02	394.1	19.5
7	7	2.202	7.822	1.649	2.626	1592.6	-7.8571	1577.7	-217.7	1.8253E-02	388.7	26.1
8	8	2.595	7.764	1.681	2.502	1612.6	-8.9768	1592.9	-251.6	1.7632E-02	383.3	33.4
9	9	2.995	7.696	1.713	2.384	1632.1	-10.1095	1606.7	-286.5	1.7034E-02	378.1	41.4
10	10	3.402	7.620	1.745	2.272	1651.0	-11.2538	1619.2	-322.2	1.6499E-02	372.9	50.0
11	11	3.816	7.533	1.776	2.166	1669.2	-12.4086	1630.2	-358.7	1.5906E-02	367.8	59.1
12	12	4.236	7.436	1.807	2.066	1686.9	-13.5722	1639.8	-395.9	1.5378E-02	362.9	68.8
13	13	4.664	7.328	1.838	1.972	1703.9	-14.7433	1647.8	-433.6	1.4875E-02	358.1	78.9
14	14	5.099	7.209	1.867	1.883	1720.2	-15.9202	1654.2	-471.8	1.4396E-02	353.4	89.4
15	15	5.540	7.078	1.896	1.801	1735.7	-17.1014	1659.0	-510.4	1.3945E-02	349.0	100.2
16	16	5.987	6.935	1.924	1.725	1750.5	-18.2850	1662.1	-549.2	1.3521E-02	344.7	111.3
17	17	6.442	6.780	1.951	1.655	1764.4	-19.4693	1663.5	-588.1	1.3125E-02	340.6	122.6
18	18	6.902	6.612	1.977	1.591	1777.4	-20.6524	1663.2	-626.9	1.2759E-02	336.8	134.0
19	19	7.368	6.430	2.001	1.533	1789.3	-21.8324	1661.0	-665.4	1.2425E-02	333.2	145.6
20	20	7.841	6.236	2.023	1.481	1800.2	-23.0073	1657.0	-703.6	1.2124E-02	330.0	157.3
21	21	8.318	6.027	2.042	1.436	1809.9	-24.1751	1651.1	-741.2	1.1859E-02	327.1	169.0
22	22	8.800	5.805	2.060	1.397	1818.2	-25.3337	1643.4	-778.0	1.1632E-02	324.5	180.8
23	23	9.287	5.568	2.074	1.366	1825.1	-26.4809	1633.6	-813.6	1.1445E-02	322.5	192.4
24	24	9.778	5.317	2.085	1.343	1830.3	-27.6145	1621.8	-848.4	1.1304E-02	320.9	204.0
25	25	10.000	5.200	2.090	1.334	1832.3	-28.1203	1616.0	-863.6	1.1253E-02	320.3	209.2

Figure F-3. Output for Sample Case 3 (Continued).

# NOZZLE AND BOATTAIL EXIT LIP POINT CONDITIONS

	X	Y	M	P	Q	TH	U	V	R	T	THRUST
NOZZLE	10.000	5.000	3.609	6.727	8660.9	12.9213	8636.5	1981.4	6.2056E-03	2601.6	5668.5
BOATTAIL	5.200	2.090	1.334	1832.3	-28.1203	1616.0	-863.6	1.1255E-02	320.3	209.2	

THE BASE PRESSURE IS .961 (LBF/IN<sup>2</sup>) AND THE BASE THRUST IS 6.16 (LBF)  
 THE TOTAL NOZZLE-BASE-BOATTAIL THRUST IS 5883.9 (LBF)

Figure F-3. Output for Sample Case 3 (Concluded).

#### 4. Sample Case 4

Sample case 4 illustrates a nozzle optimization using Newton's method. The nozzle gas dynamic model and geometry are specified by the program default values (see Sample Case 1). To reduce the output, KWRITN = 3. The locations of the initial-value points are specified by NPN = 9 and RATIØI = 4.0. The locations of the points on the initial expansion contour are specified by NPW = 12 and RATIØW = 3.0. The initial estimate for the throat attachment angle is ANSTRT(1) = 25.0. To minimize the flow field output during the optimization procedure, KWRITØ = 3. The nozzle attachment angle perturbation DA = 2.0. For a nozzle optimization, IØP = 1 specifies the geometric model and N = 2 specifies a two-dimensional optimization. The following list presents the data deck for sample case 4.

```
22  SAMPLE CASE 4    NOZZLE OPTIMIZATION
    $INFO  KWRITN=3, NPN=9, RATIØI=4.0, NPW=12, RATIØW=3.0,
        ANSTRT(1)=25.0, KWRITØ=3, DA=2.0 $
```

The first page of the output prints the program abstract and the job title. The second page presents the input data, the initial-value line, and the initial-value line performance parameters. For this sample case, KWRITN = 3 and KWRITØ = 3 to minimize output. A secondary-start line is computed at the minimum attachment angle, ANMIN(1) = 20.0, which is printed out on the next page (see the discussion in Section 11). The optimization parameters follow on the next page, which lists the type of geometry (IØP = 1), print option (KWRITØ = 3), convergence tolerance (TØLØ = 0.001), optimization variable space (N = 2), optimization method (IMETH = 3), and maximum number of base point moves (ITERØ = 10). The initial estimate for the throat attachment angle is 25.0 deg, and for the exit lip radius is 5.0 in. These values, and the minimum and maximum values of those variables, are listed for reference.

The next three pages present the results of the optimization. On the first of those three pages, a heading is printed out specifying the optimization method. The next three lines present the results of the nozzle flow field analysis for the initial nozzle contour. The output for each nozzle flow field analysis is reduced to three lines. The first line specifies the nozzle geometry, the second line presents the flow properties at the nozzle exit lip point, and the third line is the crossing characteristics count. After the analysis of the initial nozzle contour, an optimization base point data line is written out stating that for the base point (0 step), THETA = 25.0 deg, YE = 5.000 in., and the nozzle thrust is 5644.65 lbf.

Newton's method requires the values of the thrust for the base point and five neighboring points. The nozzles corresponding to these five points are analyzed, and the results presented in the next five groups of three lines each. From that data, Newton's method constructs the base point move and analyzes the corresponding new base point nozzle.

The next three lines present the results of that analysis. An optimization base point data line is then written out presenting the base point data for that step (1 step).

The above procedure is repeated for a total of three base point moves, at which time the optimization procedure has converged. The last line of output shows that the optimum nozzle contour has a throat attachment angle of 32.729 deg, an exit lip point radius of 5.244 in., and a thrust of 5679.81 lbf.

Sample case 4 required 80 seconds of central processor time on the CDC 6500 computer.

# ANALYSIS AND DESIGN OF SUPERSONIC NOZZLE-BASE-NOZTAIL COMBINATIONS

## ABSTRACT

THIS PROGRAM WAS PRODUCED AT THE PURDUE UNIVERSITY THERMAL SCIENCE AND PROPULSION CENTER BY J. G. ALLMAN AS A PART OF THE REQUIREMENTS OF AF CONTRACT NUMBER F33615-73-C-2010. THE CONTRACT WAS SPONSORED BY THE AERO PROPULSION LABORATORY, WRIGHT PATTERSON AFB, OHIO. PRINCIPAL INVESTIGATOR FOR PURDUE UNIVERSITY WAS PROFESSOR JOE U. HOFFMAN.

THE EQUATIONS OF MOTION FOR AN AXISYMMETRIC SUPERSONIC FLOW ARE SOLVED USING A NUMERICAL METHOD OF CHARACTERISTICS HAVING SECOND-ORDER ACCURACY. THE INITIAL FLOW VARIABLES FOR THE NOZZLE FLOW FIELD CAN BE SPECIFIED OR COMPUTED FROM KIEGELS TRANSONIC FLOW ANALYSIS. THE INITIAL FLOW VARIABLES FOR THE NOZTAIL FLOW CAN BE SPECIFIED OR COMPUTED FROM A UNIFORM FLOW ANALYSIS. THE NOZZLE AND NOZTAIL GEOMETRIES CAN BE SPECIFIED AS CONICAL, SECOND-ORDER POLYNOMIAL OR TABULAR COLOUR FLOW ANALYSIS. THE NOZZLE AND NOZTAIL GEOMETRIES CAN BE SPECIFIED AS CONICAL, SECOND-ORDER POLYNOMIAL OR TABULAR COLOUR FLOW ANALYSIS. THE ANALYSIS WAS BASED ON THE GOVERNING GAS DYNAMIC RELATIONS FOR A FROZEN OR EQUILIBRIUM GAS MIXTURE.

## JOB TITLE

SAMPLE CASE # NOZZLE OPTIMIZATION

Figure F-4. Output for Sample Case 4.



NOZZLE FLOW FIELD ANALYSIS

NP = 9  
IC = 2  
IVL = 0  
IWALL = 2  
NPM = 12  
WRITE = 3

TO = 6000.00 H  
PO = 1000.00 PSIA  
PAMB = 0.00 PSIA

XE = 10.000 IN  
YE = 5.000 IN  
RU = 5.000 IN  
RO = 5.000 IN  
YT = 1.000 IN

G = 1.20  
HG = 60.00 (FT-LBF)/(LBM-R)  
UGAS = 1  
RATIOI = 4.00  
RATIOW = 4.00  
TOL = .0010

INITIAL-VALUE LINE

THE INITIAL-VALUE LINE IS A KATIEGEL V=0 LINE

I	X	Y	M	P	Q	TH	U	V	N	T	WGT	THRUST	ISP
1	0.000	1.000	1.082	514.00	4616.6	-0.000	3816.6	-0.0	2.2997E-01	5371.2	19.221	3896.783	202.734
2	0.017	.943	1.072	520.79	3784.3	.006	3784.3	.4	2.3224E-01	5361.8	17.117	3896.783	202.701
3	0.036	.875	1.061	527.38	3749.5	.017	3749.5	1.1	2.3469E-01	5353.1	15.715	3896.783	202.668
4	0.057	.791	1.049	534.29	3713.2	.031	3713.2	2.0	2.3725E-01	5340.8	14.079	3896.783	202.636
5	0.080	.688	1.038	541.26	3676.5	.046	3676.5	2.9	2.3983E-01	5325.5	12.119	3896.783	202.604
6	0.103	.564	1.027	547.93	3641.4	.057	3641.4	3.6	2.4230E-01	5311.6	9.114	3896.783	202.574
7	0.126	.411	1.017	553.89	3610.2	.057	3610.2	3.6	2.4448E-01	5297.7	5.260	3896.783	202.543
8	0.144	.226	1.010	558.36	3586.7	.038	3586.7	2.4	2.4612E-01	5284.7	3.260	3896.783	202.512
9	0.151	0.000	1.007	560.23	3577.0	0.000	3577.0	0.0	2.4661E-01	5271.7	0.000	3896.783	202.481

INITIAL-VALUE LINE PERFORMANCE PARAMETERS

THE NOZZLE MASS FLOW RATE IS 19.221 (LBM/SEC)

THE START LINE THRUST IS 3896.8 LBF, AND THE START LINE ISP IS 202.734 (LBF-SEC)/LBM

THE ONE-DIMENSIONAL MASS FLOW RATE IS 19.261 (LBM/SEC), AND THE DISCHARGE COEFFICIENT IS .9979

THE ONE-DIMENSIONAL THRUST IS 3896.9 LBF, AND THE ONE-DIMENSIONAL SPECIFIC IMPULSE IS 202.322 (LBF-SEC)/LBM

THE SPECIFIC IMPULSE EFFICIENCY IS 1.0020

THE NOZZLE WALL CONTOUR IS A SECOND-ORDER POLYNOMIAL WITH THETA = 20.000 DEGREES, AND YE = 5.000 IN.

Figure F-4. Output for Sample Case 4 (Continued).

SECONDARY START LINE

J	I	X	Y	M	P	Q	TH	U	V	K	T	MDT/LRC	F/LRC	THRUST	ISP	IC/EF
21	1	.171	1.030	1.723	210.083	5640.6	20.000	5306.6	1929.3	1.0901E-01	4625.3	18.311	3755.7			
21	2	.190	1.025	1.729	206.190	5687.9	20.017	5316.1	1936.9	1.0894E-01	4620.6	18.311	3755.7			
21	3	.256	1.007	1.744	203.391	5696.1	20.034	5343.3	1978.9	1.0602E-01	4604.0	17.646	3695.3			
21	4	.331	.988	1.763	197.421	5743.2	20.471	5390.3	2008.5	1.0341E-01	4582.0	16.700	3479.9			
21	5	.416	.967	1.786	190.250	5800.3	20.946	5421.8	2025.2	1.0024E-01	4564.0	15.404	3251.6			
21	6	.504	.946	1.813	181.966	5867.3	20.946	5421.8	2025.2	9.6400E-02	4520.4	14.243	3018.0			
21	7	.600	.926	1.844	172.916	5942.3	20.715	5355.7	2110.1	9.2575E-02	4482.4	13.033	2788.9			
21	8	.681	.909	1.872	165.085	6010.6	20.715	5355.7	2110.1	8.9036E-02	4448.9	12.072	2606.1			
21	9	.747	.896	1.897	158.518	6060.3	20.715	5355.7	2110.1	8.6077E-02	4419.6	11.243	2462.7			
21	10	.808	.884	1.920	152.552	6124.3	20.635	5281.4	2158.3	8.3348E-02	4392.4	10.670	2337.0			
21	11	.860	.873	1.943	146.830	6179.6	20.522	5217.4	2166.4	8.0631E-02	4364.5	10.064	2219.6			
21	12	.927	.862	1.967	140.817	6235.4	20.345	5144.9	2172.0	7.7945E-02	4335.9	9.491	2106.0			
21	13	.985	.852	1.991	135.242	6290.7	20.231	5092.3	2175.2	7.5351E-02	4307.6	8.961	2006.0			
21	14	1.040	.842	2.015	129.762	6347.7	20.062	5056.8	2176.1	7.2876E-02	4279.9	8.478	1906.3			
21	15	1.093	.833	2.038	124.762	6397.5	19.848	6017.5	2172.1	7.0433E-02	4251.7	8.035	1820.3			
21	16	1.146	.826	2.062	119.762	6447.5	19.584	6326.0	2127.0	6.8263E-02	4223.9	7.641	1741.3			
21	17	1.199	.819	2.086	114.762	6497.5	19.298	6582.0	2049.8	6.6267E-02	4196.6	7.291	1667.7			
21	18	1.252	.812	2.110	109.762	6547.5	18.996	6816.7	1954.2	6.4482E-02	4172.2	6.985	1601.9			
21	19	1.305	.805	2.134	104.762	6597.5	18.665	7040.6	1842.5	6.2816E-02	4147.2	6.708	1542.2			
21	20	1.358	.798	2.158	99.762	6647.5	18.324	7264.4	1709.9	6.1266E-02	4122.7	6.459	1487.6			
21	21	1.411	.791	2.182	94.762	6697.5	17.976	7484.8	1558.5	5.9845E-02	4097.6	6.229	1437.6			
21	22	1.464	.784	2.206	89.762	6747.5	17.624	7707.6	1422.7	5.8530E-02	4072.1	6.015	1392.6			
21	23	1.517	.777	2.230	84.762	6797.5	17.272	7933.5	1278.5	5.7300E-02	4047.6	5.805	1352.9			
21	24	1.570	.770	2.254	79.762	6847.5	16.920	8162.8	1140.6	5.6160E-02	4022.1	5.605	1318.2			
21	25	1.623	.763	2.278	74.762	6897.5	16.568	8391.0	1008.6	5.5100E-02	3997.6	5.415	1288.6			
21	26	1.676	.756	2.302	69.762	6947.5	16.216	8620.0	882.7	5.4100E-02	3972.1	5.235	1264.6			
21	27	1.729	.749	2.326	64.762	6997.5	15.864	8847.3	767.3	5.3150E-02	3947.6	5.065	1240.6			

Figure F-4. Output for Sample Case 4 (Continued).

J	I	X	Y	M	P	Q	TH	U	V	R	T	MOT/LNC	F/LNC	THRUST	ISP	IC/IEF
OPTIMIZATION PARAMETERS																
ICP = 1																
N = 2																
ITERM = 3																
ITERO = 10																
TOLC = 0.00100																
NOZZLE ATTACHMENT ANGLE																
NOZZLE EXIT RADIUS																
START MINIMUM MAXIMUM																
1		25.00	20.00	42.00												
2		5.00	4.00	7.00												

Figure F-4. Output for Sample Case 4 (Continued).

# NOZZLE OPTIMIZATION IS BEING CARRIED OUT USING NEWTONS METHOD.

THE NOZZLE WALL CONTOUR IS A SECOND-ORDER POLYNOMIAL WITH THETAT = 25.000 DEGRFES AND YE = 5.000 IN  
 23 50 10.000 5.000 3.853 4.336 9083.5 18.845 8596.5 2354.7 4.358E-03 2398.8 19.237 5842.0 -2  
 0 CHARACTERISTICS CROSSED IN THE NOZZLE.

AT THE 0 STEP THETA = 25.000 YE = 5.000 THRUST = 5644.65

THE NOZZLE WALL CONTOUR IS A SECOND-ORDER POLYNOMIAL WITH THETAT = 27.000 DEGRFES AND YE = 5.000 IN  
 23 51 10.000 5.000 3.759 5.139 8498.8 16.509 8624.3 2569.2 4.985E-03 2473.9 19.219 5655.7 -2  
 0 CHARACTERISTICS CROSSED IN THE NOZZLE.

THE NOZZLE WALL CONTOUR IS A SECOND-ORDER POLYNOMIAL WITH THETAT = 25.000 DEGRFES AND YE = 5.200 IN  
 22 49 10.000 5.200 3.950 3.654 9169.1 20.920 8562.0 3722.6 3.771E-03 2355.1 19.250 5640.0 -2  
 0 CHARACTERISTICS CROSSED IN THE NOZZLE.

THE NOZZLE WALL CONTOUR IS A SECOND-ORDER POLYNOMIAL WITH THETAT = 27.000 DEGRFES AND YE = 5.200 IN  
 22 50 10.000 5.200 3.856 4.310 9048.1 18.718 8607.5 2916.5 4.313E-03 2398.3 19.225 5651.8 -2  
 0 CHARACTERISTICS CROSSED IN THE NOZZLE.

THE NOZZLE WALL CONTOUR IS A SECOND-ORDER POLYNOMIAL WITH THETAT = 23.000 DEGRFES AND YE = 5.000 IN  
 23 51 10.000 5.000 3.945 3.687 9160.4 20.975 8553.4 3779.0 3.402E-03 2371.2 19.252 5624.3 -2  
 0 CHARACTERISTICS CROSSED IN THE NOZZLE.

THE NOZZLE WALL CONTOUR IS A SECOND-ORDER POLYNOMIAL WITH THETAT = 25.000 DEGRFES AND YE = 4.800 IN  
 23 50 10.000 4.800 3.759 5.142 8987.2 18.727 8616.5 2889.5 4.930E-03 2472.8 19.234 5843.7 -2  
 0 CHARACTERISTICS CROSSED IN THE NOZZLE.

THE NOZZLE WALL CONTOUR IS A SECOND-ORDER POLYNOMIAL WITH THETAT = 34.864 DEGRFES AND YE = 4.877 IN  
 23 53 10.000 4.877 3.319 11.647 8526.8 4.745 8497.6 705.4 9.812E-03 2846.8 19.124 5645.3 -2  
 0 CHARACTERISTICS CROSSED IN THE NOZZLE.

AT THE 1 STEP THETA = 34.864 YE = 4.877 THRUST = 5657.79

THE NOZZLE WALL CONTOUR IS A SECOND-ORDER POLYNOMIAL WITH THETAT = 36.864 DEGRFES AND YE = 4.877 IN  
 23 54 10.000 4.877 3.218 14.106 8401.0 1.854 8397.5 242.5 1.150E-02 294.5 19.099 5619.3 -2  
 0 CHARACTERISTICS CROSSED IN THE NOZZLE.

THE NOZZLE WALL CONTOUR IS A SECOND-ORDER POLYNOMIAL WITH THETAT = 34.864 DEGRFES AND YE = 5.077 IN  
 23 53 10.000 5.077 3.402 9.971 8624.6 7.079 8558.8 1062.9 8.635E-03 2771.8 19.140 5654.1 -2  
 0 CHARACTERISTICS CROSSED IN THE NOZZLE.

THE NOZZLE WALL CONTOUR IS A SECOND-ORDER POLYNOMIAL WITH THETAT = 36.864 DEGRFES AND YE = 5.077 IN  
 23 54 10.000 5.077 3.296 12.167 8428.8 4.011 8476.0 594.4 1.017E-02 2870.1 19.095 5635.5 -2  
 0 CHARACTERISTICS CROSSED IN THE NOZZLE.

THE NOZZLE WALL CONTOUR IS A SECOND-ORDER POLYNOMIAL WITH THETAT = 32.864 DEGRFES AND YE = 4.877 IN  
 23 53 10.000 4.877 3.418 9.665 8644.0 7.659 8568.9 1152.1 8.403E-03 2760.4 19.156 5661.2 -2  
 0 CHARACTERISTICS CROSSED IN THE NOZZLE.

THE NOZZLE WALL CONTOUR IS A SECOND-ORDER POLYNOMIAL WITH THETAT = 34.864 DEGRFES AND YE = 4.677 IN  
 23 53 10.000 4.677 3.240 13.533 8428.6 2.395 8421.3 352.3 1.111E-02 2921.9 19.125 5628.2 -2  
 0 CHARACTERISTICS CROSSED IN THE NOZZLE.

THE NOZZLE WALL CONTOUR IS A SECOND-ORDER POLYNOMIAL WITH THETAT = 32.392 DEGRFES AND YE = 5.063 IN  
 23 53 10.000 5.063 3.522 7.958 8760.1 10.457 8614.7 1569.9 7.151E-03 2670.6 19.159 5666.2 -2  
 0 CHARACTERISTICS CROSSED IN THE NOZZLE.

AT THE 2 STEP THETA = 32.392 YE = 5.063 THRUST = 5678.41

THE NOZZLE WALL CONTOUR IS A SECOND-ORDER POLYNOMIAL WITH THETAT = 34.392 DEGRFES AND YE = 5.063 IN

Figure F-4. Output for Sample Case 4 (Continued).

```

23 53 10.000 5.063 3.420 9.631 8646.0 7.616 8569.7 1145.9 8.3788E-03 2759.6 19.128 5657.2 5671.9 295.846 -2
0 CHARACTERISTICS CROSSED IN THE NOZZLE.
THE NOZZLE WALL CONTOUR IS A SECOND-ORDER POLYNOMIAL WITH THETA = 32.392 DEGRS AND YE = 5.263 IN
22 52 10.000 5.263 3.404 6.430 8847.5 12.716 8630.5 1947.5 6.3007E-03 2611.6 19.169 5672.0 5670.7 295.493 -2
0 CHARACTERISTICS CROSSED IN THE NOZZLE.
THE NOZZLE WALL CONTOUR IS A SECOND-ORDER POLYNOMIAL WITH THETA = 34.392 DEGRS AND YE = 5.263 IN
22 52 10.000 5.263 3.499 8.308 8734.8 9.920 8604.2 1504.7 7.4116E-03 2690.2 19.168 5668.8 5677.1 295.455 -2
0 CHARACTERISTICS CROSSED IN THE NOZZLE.
THE NOZZLE WALL CONTOUR IS A SECOND-ORDER POLYNOMIAL WITH THETA = 30.392 DEGRS AND YE = 5.063 IN
23 52 10.000 5.063 3.623 6.595 8866.4 13.120 8635.0 2012.7 6.1220E-03 2365.8 19.162 5666.3 5675.9 295.292 -2
0 CHARACTERISTICS CROSSED IN THE NOZZLE.
THE NOZZLE WALL CONTOUR IS A SECOND-ORDER POLYNOMIAL WITH THETA = 32.392 DEGRS AND YE = 4.863 IN
23 53 10.000 4.863 3.436 9.355 8614.0 8.164 8576.2 1230.3 6.1785E-03 2745.1 19.162 5662.9 5672.3 295.109 -2
0 CHARACTERISTICS CROSSED IN THE NOZZLE.
THE NOZZLE WALL CONTOUR IS A SECOND-ORDER POLYNOMIAL WITH THETA = 32.729 DEGRS AND YE = 5.244 IN
22 52 10.000 5.244 3.578 7.164 8820.7 12.042 8626.6 1840.2 6.5545E-03 2623.1 19.186 5672.1 5679.6 295.492 -2
0 CHARACTERISTICS CROSSED IN THE NOZZLE.
AT THE 3 STEP THETA = 32.729 YE = 5.244 THRUST = 5679.81

```

Figure F-4. Output for Sample Case 4 (Concluded).



## 5. Sample Case 5

Sample case 5 illustrates a nozzle-base-boattail assembly optimization. The maximum thrust contour is approached in two steps. First, a two-dimensional optimization is performed. This is accomplished by requiring the width of the base region to be the minimum allowable value ( $y_{eb} = y_{en} + \Delta y_b$ ), which leaves two parameters ( $\theta_{an}$  and  $y_{en}$ ) unconstrained. This optimization converges quickly because of the relatively few function evaluations required for a base point move. After convergence, the optimization problem is redefined so that the boattail and nozzle exit lip points are independent, thus yielding a three-dimensional optimization problem. From the preliminary two-dimensional optimization, a good initial approximation to the maximum thrust nozzle-base-boattail contour is available, and the three-dimensional optimization converges in one pass.

The general operating conditions considered in sample case 5 are the same as those in sample case 3. The boattail outer radius  $YTB = 5.3$  in., the radius of curvature of the boattail initial expansion contour is the program default value  $RDB = 5.0$  in., and the boattail contour is conical ( $IWALLB = 1$ ). Output is minimized by setting  $KWRITN$ ,  $KWRITB$ , and  $KWRIT\emptyset$  equal to 3. Computation time for each analysis is kept small by setting  $NPN = 9$  and  $NPB = 40$ . The nozzle has 12 inverse wall points ( $NPW = 12$ ) spanning the minimum attachment angle [ $ANMIN(1) = 20.0$  deg.]. The initial-value line points and the wall points are spaced according to  $RATI\emptyset I = 3.0$ ,  $RATI\emptyset W = 3.0$ , and  $SPACE = 0.6$ .

Now the optimization employs Newton's method ( $IMETH = 3$ ) to calculate the maximum thrust contours to within a relative tolerance of  $T\emptyset L\emptyset = 0.0001$  or within a given number of iterations  $ITER\emptyset = 10$ . An initial estimate for the nozzle geometry is given by specifying  $ANSTRT(1) = 30.0$  deg and  $ANSTRT(2) = 4.0$  in. The maximum values of  $\theta_{an}$ ,  $y_{en}$ ,  $\theta_{ab}$ , and  $y_{eb}$  are specified as  $ANMAX(1) = 40.0$  deg, 5.0 in., 20.0 deg, and 5.0 in., respectively. The minimum values of those parameters are specified as the program default values. For a nozzle-base-boattail optimization,  $I\emptyset P = 3$  specifies the type of geometry, and  $N = 3$  specifies that a three-dimensional optimization is to be performed (i.e., the unconstrained geometric variables are the nozzle throat attachment angle  $\theta_{an}$ , the nozzle exit lip radius  $y_{en}$ , and the boattail exit lip radius  $y_{eb}$ . The  $\theta_{an}$  perturbation  $DA = 2.0$  deg, the  $y_{en}$  perturbation  $DB = 0.1 y_{tn}$ , and the  $y_{eb}$  perturbation  $DD = 0.2 y_{tn}$ . The minimum annular base width  $DBAS = 0.1$  in.

The following list presents the data deck for sample case 5.

```
21  SAMPLE CASE 5  NOZZLE-BASE-BOATTAIL OPTIMIZATION
$INFO  KWRITN=3, KWRITB=3, KWRIT\emptyset=3, YTB=5.3, IWALLB=1,
      NPN=9, NPW=12, NPB=40, RATI\emptyset I=3.0, RATI\emptyset W=3.0, SPACE=0.6,
      ANSTRT(1)=30.0, 4.0, ANMAX(1)=40.0, 5.0, 20.0, 5.0,
      IMETH=3, ITER\emptyset=10, T\emptyset L\emptyset=0.0001, I\emptyset P=3, N=3,
      DA=2.0, DB=0.1, DBAS=0.1 $
```

Figure F-5 presents the output for sample case 5. The first page presents the program abstract and the job title. The second page presents the nozzle flow field analysis data, the nozzle initial-value line, and the nozzle initial-value line performance parameters. The third page presents the nozzle secondary start line. The optimization parameters, the initial values of the nozzle geometric parameters, and the minimum and maximum values of the nozzle and boattail geometric parameters are presented on the fourth page. The fifth page presents the boattail flow field analysis data and the boattail initial-value line.

The results of the optimization procedure are presented on pages six to ten of Fig. F-5. The first line on page six identifies the optimization procedure as Newton's method. The next group of seven lines summarizes the results of the combined nozzle-base-boattail flow field analysis for the initial contour. The first line specifies the nozzle geometry, the second line presents the flow properties at the nozzle exit lip point, and the third line presents the crossing characteristics counter. The fourth line presents the boattail geometry, the fifth line presents the flow field properties at the boattail exit lip point, and the sixth line presents the base region pressure and thrust. Line seven presents the total nozzle-base-boattail thrust. Each flow field analysis for a particular nozzle-base-boattail configuration generates a corresponding set of seven lines of output.

After the analysis of the initial nozzle-base-boattail configuration, an optimization base point data line is written out summarizing the geometry and the corresponding thrust. The initial contour is designated the 0 step.

The two-dimensional optimization, in which the boattail exit lip point is constrained to be a fixed distance from the nozzle exit lip point, then commences. This procedure is analogous to the nozzle optimization discussed in sample case 4. Newton's method requires the values of thrust at the base point and five neighboring points. Those five points are the first five points after the 0 step data line. From that data, Newton's method constructs the base point move and analyzes the new base point configuration. The sixth set of data after the 0 step presents the results of that analysis. An optimization base point data line is then written out presenting the base point data for that step (1 step).

The above constrained boattail optimization is repeated for a total of three base point moves. The final results are printed out on the eighth page of Fig. F-7, as the seven lines immediately preceding the optimization data line for step 3. At this time, a full three-dimensional optimization is initiated in which the conical boattail moves independently of the nozzle exit lip point. The initial contour for the three-dimensional optimization is chosen to be the nozzle contour obtained in the constrained boattail optimization described above, and a boattail exit lip point moved outward from the nozzle exit lip point by

twice the minimum separation distance  $\Delta y_b$ . That contour is then analyzed and printed out as the next seven lines of output. The corresponding optimization base point data line is identified as step 0 for the three-dimensional optimization.

For the three-dimensional optimization, Newton's method requires the values of the thrust for the base point configuration and nine neighboring points. Those results are presented on the last three pages of Fig. F-5. From that data, Newton's method constructs the base point move and analyzes the corresponding new base point configuration. The final group of seven lines on the last page of Fig. F-5 presents the results of that analysis. The last line on Fig. F-5 presents the optimization base point data line for that step, step 1. For the present sample case, the results of step 1 satisfy the convergence criteria and the program stops.

Sample case 5 required 240 seconds of central processor time on the CDC 6500 computer.

ANALYSIS AND DESIGN OF SUPERSONIC NOZZLE-BASE-BOATTAIL COMBINATIONS

ABSTRACT

THIS PROGRAM WAS PROVIDED AT THE PURDUE UNIVERSITY THERMAL SCIENCE AND PROPULSION CENTER BY J. G. ALLMAN AS A PART OF THE REQUIREMENTS OF AF CONTRACT NUMBER F49615-73-C-2010. THE CONTRACT WAS SPONSORED BY THE AFRO PROPULSION LABORATORY, WRIGHT PATTERSON AFB, OHIO. PRINCIPAL INVESTIGATOR FOR PURDUE UNIVERSITY WAS PROFESSOR JOE U. MOFFAT.

THE EQUATIONS OF MOTION FOR AN AXISYMMETRIC SUPERSONIC FLOW ARE SOLVED USING A NUMERICAL METHOD OF CHARACTERISTICS HAVING SECOND-ORDER ACCURACY. THE INITIAL FLOW VARIABLES FOR THE NOZZLE FLOW FIELD CAN BE SPECIFIED OR COMPUTED FROM KIEFER'S TRANSONIC FLOW ANALYSIS. THE INITIAL FLOW VARIABLES FOR THE BOATTAIL FLOW CAN BE SPECIFIED OR COMPUTED FROM A LINEAR FLOW ANALYSIS. THE NOZZLE AND BOATTAIL GEOMETRIES CAN BE SPECIFIED AS CIRCULAR, ELLIPTICAL, POLYGONAL OR TABULAR. COORDINATE FLOW ANALYSIS WAS BASED ON THE GOVERNING GAS DYNAMIC RELATIONS FOR A ROTATIONAL FLOW OF A FROZEN OR EQUILIBRIUM GAS MIXTURE.

JOB TITLE

SAMPLE CASE 5 NOZZLE-BASE-BOATTAIL OPTIMIZATION

Figure F-5. Output for Sample Case 5.



# NOZZLE FLOW FIELD ANALYSIS

NP = 9  
IC = 2  
IUL = 0  
IHAL = 2  
NPW = 12  
KNRITE = 3

TO = 6000.00 H  
PO = 1000.00 PSIA  
PAMB = 0.00 PSIA

XE = 10.000 IN  
YE = 5.000 IN  
RU = 3.000 IN  
RD = .500 IN  
YT = 1.000 IN

G = 1.20  
KG = 60.00 (FT-LBF)/(LBM-R)  
NGAS = 1  
RATIO1 = 3.00  
RATIO2 = 3.00  
TOL = .0010

## INITIAL-VALUE LINE

THE INITIAL-VALUE LINE IS A KLEIGFL VEO LINE

I	X	Y	N	P	Q	TH	U	V	H	T	WDOT	THRUST	ISP
1	0.000	1.000	1.000	514.46	816.6	-0.00	3816.6	-0.0	2.2997E-01	5371.2	19.221	3896.780	202.734
2	.020	.932	1.070	521.92	878.3	.008	3778.3	1.5	2.3267E-01	5383.8	16.714	3387.868	202.406
3	.041	.853	1.038	529.27	879.6	.058	3759.6	1.3	2.3539E-01	5396.3	14.000	2837.272	202.459
4	.064	.760	1.046	536.50	870.3	.050	3703.5	2.3	2.3807E-01	5408.5	11.127	2254.750	202.429
5	.067	.652	1.034	543.40	864.3	.050	3663.3	3.2	2.4062E-01	5420.1	6.183	1857.871	202.404
6	.110	.521	1.024	549.67	862.3	.058	3632.4	3.7	2.4293E-01	5439.1	5.310	1075.667	202.584
7	.130	.377	1.016	554.74	864.7	.055	3604.7	3.4	2.4487E-01	5439.1	2.733	553.666	202.570
8	.145	.203	1.004	558.74	858.8	.035	3584.7	2.2	2.4624E-01	5445.2	.795	140.953	202.542
9	.151	0.000	1.007	560.23	8577.0	0.000	3577.0	0.0	2.4681E-01	5447.7	0.000	0.000	0.000

## INITIAL-VALUE LINE PERFORMANCE PARAMETERS

THE NOZZLE MASS FLOW RATE IS 19.221 (LRM/SEC)  
THE START LINE THRUST IS 3896.8 LBF, AND THE START LINE ISP IS 202.734 (LBF-SEC)/LRM  
THE ONE-DIMENSIONAL MASS FLOW RATE IS 19.261 (LRM/SEC), AND THE DISCHARGE COEFFICIENT IS .9979  
THE ONE-DIMENSIONAL THRUST IS 3896.9 LBF, AND THE ONE-DIMENSIONAL SPECIFIC IMPULSE IS 202.321 (LBF-SEC)/LRM  
THE SPECIFIC IMPULSE EFFICIENCY IS 1.0020  
THE NOZZLE WALL CONTOUR IS A SECOND-ORDER POLYNOMIAL WITH THETAT = 20.000 DEGR/FIN AND YF = 5.000 IN

Figure F-5. Output for Sample Case 5 (Continued).



SECONDARY START LINE

J	I	X	Y	Z	P	Q	TH	U	V	R	T	MDT/LRC	F/LRC	THRUST	ISP	IC/EF
21	1	1.71	1.030	1.724	209.919	5642.1	26.000	5301.8	1959.7	1.0894E-01	4924.7	17.927	8653.3			
21	2	1.210	1.019	1.734	206.708	5669.4	26.103	5325.0	1944.6	1.0749E-01	4915.1	18.562	8622.0			
21	3	1.274	1.001	1.750	201.576	5710.3	26.334	5355.4	1944.8	1.0523E-01	4912.3	17.550	8559.0			
21	4	1.353	.983	1.769	196.514	5768.4	26.532	5392.6	2013.6	1.0257E-01	4917.8	16.350	8458.4			
21	5	1.433	.963	1.791	186.558	5814.2	26.683	5433.4	2053.6	9.9508E-02	4917.8	15.203	8384.4			
21	6	1.514	.944	1.817	180.098	5876.8	26.778	5494.6	2084.6	9.8120E-02	4917.8	14.114	8322.5			
21	7	1.600	.926	1.846	172.020	5944.4	26.807	5565.7	2111.6	9.6350E-02	4917.8	13.053	8262.1			
21	8	1.678	.911	1.870	165.741	6005.7	26.786	5614.8	2111.6	9.4350E-02	4917.8	12.114	8204.1			
21	9	1.736	.894	1.898	158.676	6059.8	26.750	5664.2	2111.6	9.2050E-02	4917.8	11.445	8149.9			
21	10	1.792	.876	1.914	150.035	6111.4	26.683	5711.0	2111.6	8.9410E-02	4917.8	10.841	8092.3			
21	11	1.850	.858	1.937	140.356	6164.5	26.588	5755.0	2111.6	8.6430E-02	4917.8	10.244	8032.5			
21	12	1.909	.840	1.960	130.580	6218.2	26.458	5807.6	2111.6	8.3080E-02	4917.8	9.659	7970.9			
21	13	1.968	.822	1.986	120.719	6272.6	26.298	5857.6	2111.6	7.9380E-02	4917.8	9.104	7908.5			
21	14	2.027	.804	2.013	110.779	6327.6	26.101	5909.7	2111.6	7.5330E-02	4917.8	8.582	7845.3			
21	15	2.087	.786	2.040	100.769	6382.6	25.868	5961.7	2111.6	7.0930E-02	4917.8	8.088	7781.3			
21	16	2.147	.768	2.069	90.681	6437.9	25.598	6017.5	2111.6	6.6230E-02	4917.8	7.620	7716.3			
21	17	2.207	.750	2.098	80.513	6494.4	25.291	6075.6	2111.6	6.1130E-02	4917.8	7.174	7650.3			
21	18	2.267	.732	2.127	70.268	6552.0	24.948	6137.1	2111.6	5.5680E-02	4917.8	6.742	7583.3			
21	19	2.327	.714	2.156	60.049	6610.6	24.578	6200.6	2111.6	4.9880E-02	4917.8	6.332	7515.3			
21	20	2.387	.696	2.185	49.858	6670.2	24.181	6266.6	2111.6	4.3730E-02	4917.8	5.940	7446.3			
21	21	2.447	.678	2.214	39.697	6730.8	23.758	6335.6	2111.6	3.7230E-02	4917.8	5.570	7376.3			
21	22	2.507	.660	2.243	29.566	6792.4	23.308	6407.5	2111.6	3.0330E-02	4917.8	5.220	7305.3			
21	23	2.567	.642	2.272	19.465	6855.0	22.831	6482.1	2111.6	2.3030E-02	4917.8	4.880	7233.3			
21	24	2.627	.624	2.301	9.394	6918.6	22.328	6559.9	2111.6	1.5330E-02	4917.8	4.540	7160.3			
21	25	2.687	.606	2.330	0.000	6983.2	21.798	6640.9	2111.6	7.775E-03	4917.8	4.200	7086.3			
21	26	2.747	.588	2.359	0.000	7048.6	21.243	6724.8	2111.6	0.000	4917.8	3.860	7011.3			
21	27	2.807	.570	2.388	0.000	7115.0	20.668	6811.8	2111.6	0.000	4917.8	3.520	6936.3			

Figure F-5. Output for Sample Case 5 (Continued).

```

J I X Y W P Q R V TH U V R T MDT/LNC F/LNC THRUST ISP TC/FF
OPTIMIZATION PARAMETERS
ICP = 3
MPTO = 3
TOLC = 0.0010
DEAS = .10
IC = 3
IMETH = 3
ITERO = 10
NOZZLE ATTACHMENT ANGLE
NOZZLE EXIT RADIUS
BOATTAIL ATTACHMENT ANGLE
BOATTAIL EXIT RADIUS

```

```

START MINIMUM MAXIMUM
1 30.00 20.00 40.00
2 4.00 4.00 5.00
3 15.00 0.00 20.00
4 4.00 4.00 5.00

```

Figure F-5. Output for Sample Case 5 (Continued).

# BOATTAIL FLOW FIELD ANALYSIS

MP = 40  
IC = 7  
IUL = 0  
IALL = 2  
DELTA = 1.00  
KAPITE = 3

TO = 600.00 M  
PO = 12.00 PSIA  
PAMB = 0.00 PSIA

XE = 10.00 IN  
YT = 5.00 IN  
RU = 5.00 IN

G = 1.40  
PG = 53.30 (FT-LBF/(LEM-H))  
AGAS = 1  
TOL = .00100  
SPACF = .6

## INITIAL-VALUE LINE

THE INITIAL-VALUE LINE IS A UNIFORM FLOW WITH A MACH NUMBER OF 1.40

I	X	Y	M	P	Q	Th	U	V	R	T
1	0.000	5.500	1.400	3.77	1424.2	0.000	1424.2	0.0	2.5636E-02	431.0
2	.150	5.455	1.400	3.77	1424.2	0.000	1424.2	0.0	2.5636E-02	431.0
3	.300	5.406	1.400	3.77	1424.2	0.000	1424.2	0.0	2.5636E-02	431.0
4	.450	5.359	1.400	3.77	1424.2	0.000	1424.2	0.0	2.5636E-02	431.0
5	.600	5.312	1.400	3.77	1424.2	0.000	1424.2	0.0	2.5636E-02	431.0
6	.750	5.265	1.400	3.77	1424.2	0.000	1424.2	0.0	2.5636E-02	431.0
7	.900	5.219	1.400	3.77	1424.2	0.000	1424.2	0.0	2.5636E-02	431.0
8	1.050	5.172	1.400	3.77	1424.2	0.000	1424.2	0.0	2.5636E-02	431.0
9	1.200	5.125	1.400	3.77	1424.2	0.000	1424.2	0.0	2.5636E-02	431.0
10	1.350	5.078	1.400	3.77	1424.2	0.000	1424.2	0.0	2.5636E-02	431.0
11	1.500	5.031	1.400	3.77	1424.2	0.000	1424.2	0.0	2.5636E-02	431.0
12	1.650	4.984	1.400	3.77	1424.2	0.000	1424.2	0.0	2.5636E-02	431.0
13	1.800	4.937	1.400	3.77	1424.2	0.000	1424.2	0.0	2.5636E-02	431.0
14	1.950	4.890	1.400	3.77	1424.2	0.000	1424.2	0.0	2.5636E-02	431.0
15	2.100	4.843	1.400	3.77	1424.2	0.000	1424.2	0.0	2.5636E-02	431.0
16	2.250	4.796	1.400	3.77	1424.2	0.000	1424.2	0.0	2.5636E-02	431.0
17	2.400	4.749	1.400	3.77	1424.2	0.000	1424.2	0.0	2.5636E-02	431.0
18	2.550	4.702	1.400	3.77	1424.2	0.000	1424.2	0.0	2.5636E-02	431.0
19	2.700	4.655	1.400	3.77	1424.2	0.000	1424.2	0.0	2.5636E-02	431.0
20	2.850	4.608	1.400	3.77	1424.2	0.000	1424.2	0.0	2.5636E-02	431.0
21	3.000	4.561	1.400	3.77	1424.2	0.000	1424.2	0.0	2.5636E-02	431.0
22	3.150	4.514	1.400	3.77	1424.2	0.000	1424.2	0.0	2.5636E-02	431.0
23	3.300	4.467	1.400	3.77	1424.2	0.000	1424.2	0.0	2.5636E-02	431.0
24	3.450	4.420	1.400	3.77	1424.2	0.000	1424.2	0.0	2.5636E-02	431.0
25	3.600	4.373	1.400	3.77	1424.2	0.000	1424.2	0.0	2.5636E-02	431.0
26	3.750	4.326	1.400	3.77	1424.2	0.000	1424.2	0.0	2.5636E-02	431.0
27	3.900	4.279	1.400	3.77	1424.2	0.000	1424.2	0.0	2.5636E-02	431.0
28	4.050	4.232	1.400	3.77	1424.2	0.000	1424.2	0.0	2.5636E-02	431.0
29	4.200	4.185	1.400	3.77	1424.2	0.000	1424.2	0.0	2.5636E-02	431.0
30	4.350	4.138	1.400	3.77	1424.2	0.000	1424.2	0.0	2.5636E-02	431.0
31	4.500	4.091	1.400	3.77	1424.2	0.000	1424.2	0.0	2.5636E-02	431.0
32	4.650	4.044	1.400	3.77	1424.2	0.000	1424.2	0.0	2.5636E-02	431.0
33	4.800	4.000	1.400	3.77	1424.2	0.000	1424.2	0.0	2.5636E-02	431.0
34	4.950	3.956	1.400	3.77	1424.2	0.000	1424.2	0.0	2.5636E-02	431.0
35	5.100	3.912	1.400	3.77	1424.2	0.000	1424.2	0.0	2.5636E-02	431.0
36	5.250	3.868	1.400	3.77	1424.2	0.000	1424.2	0.0	2.5636E-02	431.0
37	5.400	3.824	1.400	3.77	1424.2	0.000	1424.2	0.0	2.5636E-02	431.0
38	5.550	3.780	1.400	3.77	1424.2	0.000	1424.2	0.0	2.5636E-02	431.0
39	5.700	3.736	1.400	3.77	1424.2	0.000	1424.2	0.0	2.5636E-02	431.0
40	5.850	3.692	1.400	3.77	1424.2	0.000	1424.2	0.0	2.5636E-02	431.0

Figure F-5. Output for Sample Case 5 (Continued).

A 3-DIMENSIONAL OPTIMIZATION IS BEING CARRIED OUT USING GEOMCON METHOD.

THE NOZZLE WALL CONTOUR IS A SECOND-ORDER POLYNOMIAL WITH THETA = 30.000 DEGREES AND YF = 4.000 IN.  
 23 52 10.000 4.000 3.196 14.92 473.6 1.392 6371.9 171.6 1.1001F-02 292.9 19.163 5597.7 291.294 -2  
 0 CHARACTERISTICS CROSSED IN THE NOZZLE.  
 THE BOATTAIL WALL CONTOUR IS A SECOND-ORDER POLYNOMIAL WITH THETA = 7.059 DEGREES AND YL = 4.100 IN.  
 31 31 10.000 4.100 1.402 3.258 1496.4 -7.0578 1485.1 -143.9 2.1302F-02 413.3 106.1  
 THE BASE PRESSURE IS 2.721 (LBF/IN<sup>2</sup>) AND THE BASE THRUST IS 6.92 (LBF)  
 THE TOTAL NOZZLE-BASE-BOATTAIL THRUST IS 5710.7 (LBF)  
 AT THE 0 STEP THETA = 30.000 YF = 4.000 THETA = 7.059 YL = 4.100 THRUST = 5710.71  
 THE NOZZLE WALL CONTOUR IS A SECOND-ORDER POLYNOMIAL WITH THETA = 32.000 DEGREES AND YF = 4.000 IN.  
 23 53 10.000 4.000 3.111 17.249 4242.5 -1.383 8259.9 -208.0 1.3594F-02 3044.3 19.144 5574.1 290.001 -2  
 0 CHARACTERISTICS CROSSED IN THE NOZZLE.  
 THE BOATTAIL WALL CONTOUR IS A SECOND-ORDER POLYNOMIAL WITH THETA = 7.059 DEGREES AND YL = 4.100 IN.  
 31 31 10.000 4.100 1.402 3.258 1496.4 -7.0578 1485.1 -143.9 2.1302F-02 413.3 106.1  
 THE BASE PRESSURE IS 2.736 (LBF/IN<sup>2</sup>) AND THE BASE THRUST IS 6.96 (LBF)  
 THE TOTAL NOZZLE-BASE-BOATTAIL THRUST IS 5697.2 (LBF)  
 THE NOZZLE WALL CONTOUR IS A SECOND-ORDER POLYNOMIAL WITH THETA = 30.000 DEGREES AND YF = 4.100 IN.  
 23 52 10.000 4.100 3.232 17.738 4418.8 2.565 8410.4 376.8 1.1255E-02 2959.4 19.180 5613.3 292.034 -2  
 0 CHARACTERISTICS CROSSED IN THE NOZZLE.  
 THE BOATTAIL WALL CONTOUR IS A SECOND-ORDER POLYNOMIAL WITH THETA = 6.459 DEGREES AND YL = 4.200 IN.  
 32 32 10.000 4.200 1.491 3.313 1444.4 -6.4574 1479.1 -167.4 2.1555F-02 415.3 100.3  
 THE BASE PRESSURE IS 2.763 (LBF/IN<sup>2</sup>) AND THE BASE THRUST IS 7.20 (LBF)  
 THE TOTAL NOZZLE-BASE-BOATTAIL THRUST IS 5720.8 (LBF)  
 THE NOZZLE WALL CONTOUR IS A SECOND-ORDER POLYNOMIAL WITH THETA = 32.000 DEGREES AND YF = 4.100 IN.  
 23 53 10.000 4.100 3.144 16.101 4310.9 -2.206 8310.8 -29.9 1.2841F-02 3009.2 19.149 5586.0 291.003 -2  
 0 CHARACTERISTICS CROSSED IN THE NOZZLE.  
 THE BOATTAIL WALL CONTOUR IS A SECOND-ORDER POLYNOMIAL WITH THETA = 6.459 DEGREES AND YL = 4.200 IN.  
 32 32 10.000 4.200 1.491 3.313 1444.4 -6.4574 1479.1 -167.4 2.1555F-02 415.3 100.3  
 THE BASE PRESSURE IS 2.783 (LBF/IN<sup>2</sup>) AND THE BASE THRUST IS 7.26 (LBF)  
 THE TOTAL NOZZLE-BASE-BOATTAIL THRUST IS 5700.3 (LBF)  
 THE NOZZLE WALL CONTOUR IS A SECOND-ORDER POLYNOMIAL WITH THETA = 28.000 DEGREES AND YF = 4.000 IN.  
 23 52 10.000 4.000 3.274 12.664 4472.2 4.046 8451.1 597.7 1.0521F-02 2849.0 19.200 5608.8 291.674 -2  
 0 CHARACTERISTICS CROSSED IN THE NOZZLE.  
 THE BOATTAIL WALL CONTOUR IS A SECOND-ORDER POLYNOMIAL WITH THETA = 7.059 DEGREES AND YL = 4.100 IN.  
 31 31 10.000 4.100 1.402 3.258 1496.4 -7.0578 1485.1 -143.9 2.1302F-02 413.3 106.1  
 THE BASE PRESSURE IS 2.699 (LBF/IN<sup>2</sup>) AND THE BASE THRUST IS 6.87 (LBF)  
 THE TOTAL NOZZLE-BASE-BOATTAIL THRUST IS 5721.8 (LBF)  
 THE NOZZLE WALL CONTOUR IS A SECOND-ORDER POLYNOMIAL WITH THETA = 30.000 DEGREES AND YF = 4.900 IN.  
 24 53 10.000 4.900 3.156 15.655 4321.4 2.217 8321.3 31.5 1.2679E-02 3011.2 19.136 5570.4 290.707 -2  
 0 CHARACTERISTICS CROSSED IN THE NOZZLE.  
 THE BOATTAIL WALL CONTOUR IS A SECOND-ORDER POLYNOMIAL WITH THETA = 8.264 DEGREES AND YL = 3.900 IN.  
 31 31 10.000 3.900 1.512 3.211 1503.3 -8.2648 1487.7 -216.1 2.1083F-02 411.5 115.6  
 THE BASE PRESSURE IS 2.693 (LBF/IN<sup>2</sup>) AND THE BASE THRUST IS 0.00 (LBF)  
 THE TOTAL NOZZLE-BASE-BOATTAIL THRUST IS 5696.6 (LBF)  
 THIS ASSEMBLY IS A PHYSICAL IMPOSSIBILITY  
 THE NOZZLE WALL CONTOUR IS A SECOND-ORDER POLYNOMIAL WITH THETA = 28.597 DEGREES AND YF = 4.235 IN.  
 23 52 10.000 4.235 3.346 11.072 4459.0 6.000 8512.1 496.7 9.4091F-03 2824.2 19.203 5625.9 293.214 -2  
 0 CHARACTERISTICS CROSSED IN THE NOZZLE.  
 THE BOATTAIL WALL CONTOUR IS A SECOND-ORDER POLYNOMIAL WITH THETA = 5.653 DEGREES AND YL = 4.336 IN.  
 32 32 10.000 4.335 1.483 3.351 1483.2 -5.6540 1476.0 -146.1 2.1727E-02 416.6 91.6  
 THE BASE PRESSURE IS 2.729 (LBF/IN<sup>2</sup>) AND THE BASE THRUST IS 7.35 (LBF)  
 THE TOTAL NOZZLE-BASE-BOATTAIL THRUST IS 5754.9 (LBF)

Figure F-5. Output for Sample Case 5 (Continued).



AT THE 1 STEP THETA = 28.597 YE = 4.235 THEIA = 5.653 YE = 4.335 THRUST = 5734.89

THE NOZZLE WALL CONTOUR IS A SECOND-ORDER POLYNOMIAL WITH THETA = 30.597 DEGREES AND YE = 4.235 IN  
 23 52 10.000 4.235 31.80 1.027 84.0 2.627 1479.7 -5.0571 1472.9 -130.3 2.1873E-02 2903.2 19.174 5624.5 -2  
 0 CHARACTERISTICS CROSSED IN THE NOZZLE

THE ROCKET WALL CONTOUR IS A SECOND-ORDER POLYNOMIAL WITH THETA = 5.653 DEGREES AND YE = 4.335 IN  
 32 32 10.000 4.335 1.463 1.451 1493.2 -5.6549 1476.0 -146.1 2.1727E-02 416.6 91.0  
 THE BASE PRESSURE IS 2.779 (LBF/IN<sup>2</sup>) AND THE BASE THRUST IS 7.44 (LBF)

THE TOTAL NOZZLE-BASE-ROCKET THRUST IS 5724.3 (LBF)

THE NOZZLE WALL CONTOUR IS A SECOND-ORDER POLYNOMIAL WITH THETA = 28.597 DEGREES AND YE = 4.335 IN  
 23 52 10.000 4.335 31.80 1.027 84.0 2.627 1479.7 -5.0571 1472.9 -130.3 2.1873E-02 2903.2 19.174 5624.5 -2  
 0 CHARACTERISTICS CROSSED IN THE NOZZLE

THE ROCKET WALL CONTOUR IS A SECOND-ORDER POLYNOMIAL WITH THETA = 5.653 DEGREES AND YE = 4.335 IN  
 32 32 10.000 4.335 1.476 1.482 1479.7 -5.0571 1472.9 -130.3 2.1873E-02 417.4 84.6  
 THE BASE PRESSURE IS 2.721 (LBF/IN<sup>2</sup>) AND THE BASE THRUST IS 7.50 (LBF)

THE TOTAL NOZZLE-BASE-ROCKET THRUST IS 5737.1 (LBF)

THE NOZZLE WALL CONTOUR IS A SECOND-ORDER POLYNOMIAL WITH THETA = 30.597 DEGREES AND YE = 4.335 IN  
 23 52 10.000 4.335 31.80 1.027 84.0 2.627 1479.7 -5.0571 1472.9 -130.3 2.1873E-02 2903.2 19.174 5624.5 -2  
 0 CHARACTERISTICS CROSSED IN THE NOZZLE

THE ROCKET WALL CONTOUR IS A SECOND-ORDER POLYNOMIAL WITH THETA = 5.653 DEGREES AND YE = 4.335 IN  
 32 32 10.000 4.335 1.476 1.482 1479.7 -5.0571 1472.9 -130.3 2.1873E-02 417.4 84.6  
 THE BASE PRESSURE IS 2.762 (LBF/IN<sup>2</sup>) AND THE BASE THRUST IS 7.66 (LBF)

THE TOTAL NOZZLE-BASE-ROCKET THRUST IS 5731.2 (LBF)

THE NOZZLE WALL CONTOUR IS A SECOND-ORDER POLYNOMIAL WITH THETA = 28.597 DEGREES AND YE = 4.335 IN  
 23 52 10.000 4.235 31.80 1.027 84.0 2.627 1479.7 -5.0571 1472.9 -130.3 2.1873E-02 2903.2 19.174 5624.5 -2  
 0 CHARACTERISTICS CROSSED IN THE NOZZLE

THE ROCKET WALL CONTOUR IS A SECOND-ORDER POLYNOMIAL WITH THETA = 5.653 DEGREES AND YE = 4.335 IN  
 32 32 10.000 4.335 1.483 1.483 1493.2 -5.6549 1476.0 -146.1 2.1727E-02 416.6 91.0  
 THE BASE PRESSURE IS 2.661 (LBF/IN<sup>2</sup>) AND THE BASE THRUST IS 7.16 (LBF)

THE TOTAL NOZZLE-BASE-ROCKET THRUST IS 5732.8 (LBF)

THE NOZZLE WALL CONTOUR IS A SECOND-ORDER POLYNOMIAL WITH THETA = 28.597 DEGREES AND YE = 4.335 IN  
 23 52 10.000 4.235 31.80 1.027 84.0 2.627 1479.7 -5.0571 1472.9 -130.3 2.1873E-02 2903.2 19.174 5624.5 -2  
 0 CHARACTERISTICS CROSSED IN THE NOZZLE

THE ROCKET WALL CONTOUR IS A SECOND-ORDER POLYNOMIAL WITH THETA = 5.653 DEGREES AND YE = 4.335 IN  
 32 32 10.000 4.335 1.490 1.490 1504.2 -5.6549 1476.0 -146.1 2.1727E-02 416.6 91.0  
 THE BASE PRESSURE IS 2.685 (LBF/IN<sup>2</sup>) AND THE BASE THRUST IS 7.16 (LBF)

THE TOTAL NOZZLE-BASE-ROCKET THRUST IS 5729.2 (LBF)

THIS ASSEMBLY IS A PHYSICAL IMPOSSIBILITY

THE NOZZLE WALL CONTOUR IS A SECOND-ORDER POLYNOMIAL WITH THETA = 28.597 DEGREES AND YE = 4.335 IN  
 23 52 10.000 4.335 31.80 1.027 84.0 2.627 1479.7 -5.0571 1472.9 -130.3 2.1873E-02 2903.2 19.174 5624.5 -2  
 0 CHARACTERISTICS CROSSED IN THE NOZZLE

THE ROCKET WALL CONTOUR IS A SECOND-ORDER POLYNOMIAL WITH THETA = 5.653 DEGREES AND YE = 4.335 IN  
 32 32 10.000 4.335 1.490 1.490 1504.2 -5.6549 1476.0 -146.1 2.1727E-02 416.6 91.0  
 THE BASE PRESSURE IS 2.685 (LBF/IN<sup>2</sup>) AND THE BASE THRUST IS 7.16 (LBF)

THE TOTAL NOZZLE-BASE-ROCKET THRUST IS 5729.2 (LBF)

THE NOZZLE WALL CONTOUR IS A SECOND-ORDER POLYNOMIAL WITH THETA = 28.597 DEGREES AND YE = 4.335 IN  
 23 52 10.000 4.335 31.80 1.027 84.0 2.627 1479.7 -5.0571 1472.9 -130.3 2.1873E-02 2903.2 19.174 5624.5 -2  
 0 CHARACTERISTICS CROSSED IN THE NOZZLE

THE ROCKET WALL CONTOUR IS A SECOND-ORDER POLYNOMIAL WITH THETA = 5.653 DEGREES AND YE = 4.335 IN  
 32 32 10.000 4.335 1.476 1.476 1479.7 -5.0571 1472.9 -130.3 2.1873E-02 417.4 84.6  
 THE BASE PRESSURE IS 2.718 (LBF/IN<sup>2</sup>) AND THE BASE THRUST IS 7.51 (LBF)

THE TOTAL NOZZLE-BASE-ROCKET THRUST IS 5737.3 (LBF)

AT THE 2 STEP THETA = 28.552 YE = 4.349 THEIA = 4.974 YE = 4.449 THRUST = 5737.30

THE NOZZLE WALL CONTOUR IS A SECOND-ORDER POLYNOMIAL WITH THETA = 30.552 DEGREES AND YE = 4.349 IN  
 23 52 10.000 4.349 31.80 1.027 84.0 2.627 1479.7 -5.0571 1472.9 -130.3 2.1873E-02 2903.2 19.174 5624.5 -2  
 0 CHARACTERISTICS CROSSED IN THE NOZZLE

THE ROCKET WALL CONTOUR IS A SECOND-ORDER POLYNOMIAL WITH THETA = 4.974 DEGREES AND YE = 4.449 IN  
 32 32 10.000 4.449 1.476 1.476 1479.7 -4.9731 1472.4 -128.1 2.1894E-02 417.9 83.6  
 THE BASE PRESSURE IS 2.718 (LBF/IN<sup>2</sup>) AND THE BASE THRUST IS 7.51 (LBF)

THE TOTAL NOZZLE-BASE-ROCKET THRUST IS 5737.3 (LBF)

THE NOZZLE WALL CONTOUR IS A SECOND-ORDER POLYNOMIAL WITH THETA = 28.552 DEGREES AND YE = 4.349 IN  
 23 52 10.000 4.349 31.80 1.027 84.0 2.627 1479.7 -5.0571 1472.9 -130.3 2.1873E-02 2903.2 19.174 5624.5 -2  
 0 CHARACTERISTICS CROSSED IN THE NOZZLE

THE ROCKET WALL CONTOUR IS A SECOND-ORDER POLYNOMIAL WITH THETA = 4.974 DEGREES AND YE = 4.449 IN  
 32 32 10.000 4.449 1.476 1.476 1479.7 -4.9731 1472.4 -128.1 2.1894E-02 417.9 83.6  
 THE BASE PRESSURE IS 2.761 (LBF/IN<sup>2</sup>) AND THE BASE THRUST IS 7.69 (LBF)

THE TOTAL NOZZLE-BASE-ROCKET THRUST IS 5731.9 (LBF)

Figure F-5. Output for Sample Case 5 (Continued).



THE NOZZLE WALL CONTOUR IS A SECOND-ORDER POLYNOMIAL WITH THETA = 28.582 DEGREES AND YE = 4.449 IN  
 23 52 10.000 4.449 3.439 9.294 8667.2 8.532 8571.3 1965.9 8.1372E-03 2741.3 19.205 5652.2 -2  
 0 CHARACTERISTICS CROSSED IN THE NOZZLE  
 THE BOATTAIL WALL CONTOUR IS A SECOND-ORDER POLYNOMIAL WITH THETA = 4.581 DEGREES AND YL = 4.549 IN  
 33 33 10.000 4.549 1.461 3.456 1467.8 4.4798 1466.0 -112.3 2.2144E-02 419.8 76.0  
 THE BASE PRESSURE IS 2.725 (LBF/IN<sup>2</sup>) AND THE BASE THRUST IS 7.70 (LBF)  
 THE TOTAL NOZZLE-BASE-BOATTAIL THRUST IS 5737.1 (LBF)

THE NOZZLE WALL CONTOUR IS A SECOND-ORDER POLYNOMIAL WITH THETA = 30.552 DEGREES AND YE = 4.449 IN  
 23 52 10.000 4.449 3.439 11.007 8562.9 5.892 8517.6 1799.1 9.5622E-03 2821.5 19.183 5647.2 -2  
 0 CHARACTERISTICS CROSSED IN THE NOZZLE  
 THE BOATTAIL WALL CONTOUR IS A SECOND-ORDER POLYNOMIAL WITH THETA = 4.361 DEGREES AND YL = 4.544 IN  
 33 33 10.000 4.549 1.464 3.441 1470.3 4.4798 1466.0 -112.3 2.2144E-02 419.8 76.0  
 THE BASE PRESSURE IS 2.798 (LBF/IN<sup>2</sup>) AND THE BASE THRUST IS 7.81 (LBF)  
 THE TOTAL NOZZLE-BASE-BOATTAIL THRUST IS 5734.1 (LBF)

THE NOZZLE WALL CONTOUR IS A SECOND-ORDER POLYNOMIAL WITH THETA = 26.552 DEGREES AND YE = 4.349 IN  
 23 52 10.000 4.349 3.434 10.409 8564.4 6.223 8517.9 1498.8 7.5894E-03 2701.4 19.222 5643.2 -2  
 0 CHARACTERISTICS CROSSED IN THE NOZZLE  
 THE BOATTAIL WALL CONTOUR IS A SECOND-ORDER POLYNOMIAL WITH THETA = 4.374 DEGREES AND YL = 4.449 IN  
 33 33 10.000 4.449 1.476 3.387 1478.0 4.4751 1472.4 -128.1 2.1894E-02 417.9 83.4  
 THE BASE PRESSURE IS 2.640 (LBF/IN<sup>2</sup>) AND THE BASE THRUST IS 7.30 (LBF)  
 THE TOTAL NOZZLE-BASE-BOATTAIL THRUST IS 5732.8 (LBF)

THE NOZZLE WALL CONTOUR IS A SECOND-ORDER POLYNOMIAL WITH THETA = 28.552 DEGREES AND YE = 4.249 IN  
 23 52 10.000 4.249 3.454 10.409 8564.4 6.223 8517.9 1498.8 7.5894E-03 2701.4 19.204 5637.3 -2  
 0 CHARACTERISTICS CROSSED IN THE NOZZLE  
 THE BOATTAIL WALL CONTOUR IS A SECOND-ORDER POLYNOMIAL WITH THETA = 6.167 DEGREES AND YL = 4.249 IN  
 33 33 10.000 4.249 1.488 3.326 1466.7 -6.1661 1478.1 -159.7 2.1615E-02 415.7 97.2  
 THE BASE PRESSURE IS 2.700 (LBF/IN<sup>2</sup>) AND THE BASE THRUST IS 0.00 (LBF)  
 THE TOTAL NOZZLE-BASE-BOATTAIL THRUST IS 5734.6 (LBF)  
 THIS ASSEMBLY IS A PHYSICAL IMPOSSIBILITY

THE NOZZLE WALL CONTOUR IS A SECOND-ORDER POLYNOMIAL WITH THETA = 28.710 DEGREES AND YE = 4.399 IN  
 23 52 10.000 4.399 3.411 9.802 8634.9 7.749 8555.8 1165.7 8.5041E-03 2746.3 19.203 5649.1 -2  
 0 CHARACTERISTICS CROSSED IN THE NOZZLE  
 THE BOATTAIL WALL CONTOUR IS A SECOND-ORDER POLYNOMIAL WITH THETA = 4.674 DEGREES AND YL = 4.499 IN  
 33 33 10.000 4.499 1.472 3.404 1478.6 4.4732 1470.7 -120.2 2.1973E-02 418.5 79.8  
 THE BASE PRESSURE IS 2.719 (LBF/IN<sup>2</sup>) AND THE BASE THRUST IS 7.60 (LBF)  
 THE TOTAL NOZZLE-BASE-BOATTAIL THRUST IS 5737.5 (LBF)  
 AT THE 3 STEP THETA = 28.710 YE = 4.399 THETA = 4.674 YE = 4.499 THRUST = 5737.47

THE NOZZLE WALL CONTOUR IS A SECOND-ORDER POLYNOMIAL WITH THETA = 28.710 DEGREES AND YE = 4.399 IN  
 23 52 10.000 4.399 3.411 9.802 8634.9 7.749 8555.8 1165.7 8.5041E-03 2746.3 19.203 5649.1 -2  
 0 CHARACTERISTICS CROSSED IN THE NOZZLE  
 THE BOATTAIL WALL CONTOUR IS A SECOND-ORDER POLYNOMIAL WITH THETA = 4.082 DEGREES AND YE = 4.599 IN  
 33 33 10.000 4.599 1.461 3.458 1467.8 4.4810 1464.1 -104.5 2.2224E-02 420.4 71.9  
 THE BASE PRESSURE IS 2.767 (LBF/IN<sup>2</sup>) AND THE BASE THRUST IS 15.65 (LBF)  
 THE TOTAL NOZZLE-BASE-BOATTAIL THRUST IS 5737.6 (LBF)  
 AT THE 0 STEP THETA = 28.710 YE = 4.399 THETA = 4.082 YE = 4.599 THRUST = 5737.64

THE NOZZLE WALL CONTOUR IS A SECOND-ORDER POLYNOMIAL WITH THETA = 30.710 DEGREES AND YE = 4.399 IN  
 23 52 10.000 4.399 3.422 11.593 8524.8 5.100 8496.0 758.3 9.7749E-03 2846.5 19.160 5641.9 -2  
 0 CHARACTERISTICS CROSSED IN THE NOZZLE  
 THE BOATTAIL WALL CONTOUR IS A SECOND-ORDER POLYNOMIAL WITH THETA = 4.082 DEGREES AND YL = 4.599 IN  
 33 33 10.000 4.599 1.461 3.458 1467.8 4.4810 1464.1 -104.5 2.2224E-02 420.4 71.9  
 THE BASE PRESSURE IS 2.836 (LBF/IN<sup>2</sup>) AND THE BASE THRUST IS 16.03 (LBF)  
 THE TOTAL NOZZLE-BASE-BOATTAIL THRUST IS 5732.9 (LBF)

Figure F-5. Output for Sample Case 5 (Continued).

23 52 10.000 4.499 3.424 9.041 8493.9 6.908 6579.1 1444.7 7.9530E-03 2728.5 19.204 5654.9 5656.7 294.297 -2  
 0 CHARACTERISTICS CROSSED IN THE NOZZLE.  
 THE BOATTAIL WALL CONTOUR IS A SECOND-ORDER POLYNOMIAL WITH THETA = 28.710 DEGREES AND YE = 4.499 IN  
 33 33 10.000 4.499 3.458 1467.8 -4.0810 1464.1 -104.5 2.2224E-02 420.4 71.9  
 THE BASE PRESSURE IS 2.724 (LBF/IN<sup>2</sup>) AND THE BASE THRUST IS 7.79 (LBF)  
 THE TOTAL NOZZLE-BASE-BOATTAIL THRUST IS 5736.4 (LBF)

23 52 10.000 4.399 3.411 9.402 8444.9 7.759 8555.8 1165.7 8.5041E-03 2746.3 19.203 5649.1 5650.1 293.952 -2  
 0 CHARACTERISTICS CROSSED IN THE NOZZLE.  
 THE BOATTAIL WALL CONTOUR IS A SECOND-ORDER POLYNOMIAL WITH THETA = 2.905 DEGREES AND YE = 4.799 IN  
 33 33 10.000 4.799 1.446 3.533 1457.3 -2.9035 1455.4 -73.8 2.2563E-02 423.0 54.5  
 THE BASE PRESSURE IS 2.814 (LBF/IN<sup>2</sup>) AND THE BASE THRUST IS 32.76 (LBF)  
 THE TOTAL NOZZLE-BASE-BOATTAIL THRUST IS 5737.3 (LBF)

23 52 10.000 4.499 3.363 10.723 8579.3 6.265 8528.1 936.2 9.1614E-03 2809.1 19.161 5650.3 5653.9 294.150 -2  
 0 CHARACTERISTICS CROSSED IN THE NOZZLE.  
 THE BOATTAIL WALL CONTOUR IS A SECOND-ORDER POLYNOMIAL WITH THETA = 4.082 DEGREES AND YE = 4.599 IN  
 33 33 10.000 4.599 1.461 3.458 1467.8 -4.0810 1464.1 -104.5 2.2224E-02 420.4 71.9  
 THE BASE PRESSURE IS 2.802 (LBF/IN<sup>2</sup>) AND THE BASE THRUST IS 6.01 (LBF)  
 THE TOTAL NOZZLE-BASE-BOATTAIL THRUST IS 5733.6 (LBF)

23 52 10.000 4.399 3.450 8.300 8744.0 10.280 8593.8 1556.7 7.4102E-03 2648.1 19.220 5646.3 5645.5 293.712 -2  
 0 CHARACTERISTICS CROSSED IN THE NOZZLE.  
 THE BOATTAIL WALL CONTOUR IS A SECOND-ORDER POLYNOMIAL WITH THETA = 4.082 DEGREES AND YE = 4.599 IN  
 33 33 10.000 4.599 1.461 3.458 1467.8 -4.0810 1464.1 -104.5 2.2224E-02 420.4 71.9  
 THE BASE PRESSURE IS 2.465 (LBF/IN<sup>2</sup>) AND THE BASE THRUST IS 15.18 (LBF)  
 THE TOTAL NOZZLE-BASE-BOATTAIL THRUST IS 5732.6 (LBF)

23 52 10.000 4.299 3.386 10.817 8545.4 6.603 8528.5 987.2 9.0871E-03 2649.2 19.202 5641.5 5641.9 293.524 -2  
 0 CHARACTERISTICS CROSSED IN THE NOZZLE.  
 THE BOATTAIL WALL CONTOUR IS A SECOND-ORDER POLYNOMIAL WITH THETA = 4.082 DEGREES AND YE = 4.599 IN  
 33 33 10.000 4.599 1.461 3.458 1467.8 -4.0810 1464.1 -104.5 2.2224E-02 420.4 71.9  
 THE BASE PRESSURE IS 2.487 (LBF/IN<sup>2</sup>) AND THE BASE THRUST IS 23.54 (LBF)  
 THE TOTAL NOZZLE-BASE-BOATTAIL THRUST IS 5737.4 (LBF)

23 52 10.000 4.399 3.411 9.402 8444.9 7.759 8555.8 1165.7 8.5041E-03 2746.3 19.203 5649.1 5650.1 293.952 -2  
 0 CHARACTERISTICS CROSSED IN THE NOZZLE.  
 THE BOATTAIL WALL CONTOUR IS A SECOND-ORDER POLYNOMIAL WITH THETA = 5.269 DEGREES AND YE = 4.399 IN  
 33 33 10.000 4.399 1.479 3.371 1440.3 -5.2676 1474.1 -135.9 2.1820E-02 417.3 87.1  
 THE BASE PRESSURE IS 2.669 (LBF/IN<sup>2</sup>) AND THE BASE THRUST IS 5.00 (LBF)  
 THE TOTAL NOZZLE-BASE-BOATTAIL THRUST IS 5737.2 (LBF)  
 THIS ASSEMBLY IS A PHYSICAL IMPOSSIBILITY

23 52 10.000 4.399 3.422 11.593 8529.8 5.100 8496.0 756.3 9.7749E-03 2846.5 19.160 5641.9 5645.0 293.686 -2  
 0 CHARACTERISTICS CROSSED IN THE NOZZLE.  
 THE BOATTAIL WALL CONTOUR IS A SECOND-ORDER POLYNOMIAL WITH THETA = 2.905 DEGREES AND YE = 4.799 IN  
 33 33 10.000 4.799 1.446 3.533 1457.3 -2.9035 1455.4 -73.8 2.2563E-02 423.0 54.5  
 THE BASE PRESSURE IS 2.905 (LBF/IN<sup>2</sup>) AND THE BASE THRUST IS 33.58 (LBF)  
 THE TOTAL NOZZLE-BASE-BOATTAIL THRUST IS 5733.0 (LBF)

23 52 10.000 4.499 3.454 9.041 8493.9 6.908 6579.1 1444.7 7.9530E-03 2728.5 19.204 5654.9 5656.7 294.297 -2  
 0 CHARACTERISTICS CROSSED IN THE NOZZLE.  
 THE BOATTAIL WALL CONTOUR IS A SECOND-ORDER POLYNOMIAL WITH THETA = 2.905 DEGREES AND YE = 4.799 IN

Figure F-5. Output for Sample Case 5 (Continued).

```

33 33 10.000 4.799 1.446 3.533 1457.3 -2.9045 1465.4 -73.4 2.2563E-02 423.0 54.5
THE BASE PRESSURE IS 2.790 (LBF/IN2) AND THE BASE THRUST IS 24.45 (LBF)
THE TOTAL NOZZLE-BASE-ROATTAIL THRUST IS 5735.7 (LBF)

23 52 10.000 4.347 3.196 10.090 4617.0 7.358 4545.1 1103.5 8.711E-03 2740.0 19.204 5645.5 -2
THE NOZZLE WALL CONTOUR IS A SECOND-ORDER POLYNOMIAL WITH THETA = 28.561 DEGREES AND YE = 4.347 IN
0 CHARACTERISTICS CROSSED IN THE NOZZLE.
THE ROATTAIL WALL CONTOUR IS A SECOND-ORDER POLYNOMIAL WITH THETA = 3.661 DEGREES AND YL = 4.670 IN
33 33 10.000 4.670 1.456 3.484 1464.2 -3.6602 1461.2 -92.5 2.2341E-02 421.3 66.0
THE BASE PRESSURE IS 2.406 (LBF/IN2) AND THE BASE THRUST IS 25.75 (LBF)
THE TOTAL NOZZLE-BASE-ROATTAIL THRUST IS 5737.8 (LBF)

AT THE 1 STEP THETA = 28.561 YE = 4.347 THETA = 3.661 YE = 4.670 THRUST = 5737.76

```

Figure F-5. Output for Sample Case 5 (Concluded).

## REFERENCES

1. C.M. Byington, Jr. and J.D. Hoffman, "Effects of Base Pressure on Conical Thrust Nozzle Optimization," AIAA Journal, Vol. 7, No. 3, March 1970, pp. 380-382.
2. D.M. Himmelblau, Applied Nonlinear Programming, McGraw-Hill Book Co., New York, 1972.
3. M.J. Zucrow and J.D. Hoffman, Gas Dynamics, Vol. I, John Wiley and Sons, New York, 1976, pp. 549.
4. M.J. Zucrow and J.D. Hoffman, Gas Dynamics, Vol. I, John Wiley and Sons, New York, 1976, Chapter 12.
5. J.R. Kliegel and J.N. Levine, "Transonic Flow in Small Radius of Curvature Nozzles," AIAA Journal, Vol. 7, No. 7, July 1969, pp. 1375-1378.
6. I.M. Hall, "Transonic Flow in Two-Dimensional and Axially-Symmetric Nozzles," Quarterly Journal of Mechanics and Applied Mathematics, Vol. XV, Pt. 4, 1962, pp. 487-508.
7. S.A. Pasley and J.D. Hoffman, "Flow Field Analysis of a Nozzle-Boattail System", Air Force Aero Propulsion Laboratory, AFAPL-TR-74-38, 1974.
8. A.L. Addy, "Analysis of the Axisymmetric Base-Pressure and Base-Temperature Problem with Supersonic Interacting Freestream-Nozzle Flows Based on the Flow Model of Korst, et al., Part I: A Computer Program and Representative Results for Cylindrical Afterbodies," Advanced Systems Laboratory, Redstone Arsenal, Alabama, Report No. RD-TR-69-12, July 1969.
9. Y. Bard, Nonlinear Parameter Estimation, Academic Press, New York, 1974.
10. G.V.R. Rao, "Exhaust Nozzle Contour For Optimum Thrust," Jet Propulsion, Vol. 28, 1958, pp. 377-382.